KERNFORSCHUNGSANLAGE JÜLICH GmbH

Institut für Reaktorwerkstoffe

FISSION PRODUCT RELEASE PROFILES FROM SPHERICAL HTR FUEL ELEMENTS AT ACCIDENT TEMPERATURES

by

Werner Schenk
Dieter Pitzer
Heinz Nabielek

Jül-2234
September 1988
ISSN 0366-0885

FISSION PRODUCT RELEASE PROFILES FROM SPHERICAL HTR FUEL ELEMENTS AT ACCIDENT TEMPERATURES

by

Werner Schenk
Dieter Pitzer
Heinz Nabielek

Kernforschungsanlage Jülich GmbH
Institut für Reaktorwerkstoffe
Jül-2234 September 1988

FISSION PRODUCT RELEASE PROFILES FROM SPHERICAL HTR FUEL ELEMENTS AT ACCIDENT TEMPERATURES

by
W. Schenk, D. Pitzer, H. Nabielek

SUMMARY

With the construction of the cold finger apparatus, a new method has been developed to determine fission product release profiles during heating tests of irradiated spherical fuel elements. It is shown that this equipment works with high sensitivity and great precision for all important fission product nuclides up to 1800 °C.

Together with the existing equipment, a total of 22 fuel elements with modern TRISO particles has been tested in the temperature range of 1500-2500 °C. In addition, experiments were done on seven UO_2 samples at 1400 to 1800 °C.

For heating times up to 100 hours at the maximum temperature, the following results were obtained: silver is the only fission product to be released at 1200-1600 °C by diffusion through intact SiC, but is of low significance in accident scenarios; caesium, iodine, strontium and noble gas releases up to 1600 °C are solely due to various forms of contamination. At 1700-1800 °C, corrosion-induced SiC defects cause the release of Cs, Sr, I/Xe/Kr. Above 2000 °C, thermal decomposition of the silicon carbide layer sets in, while pyrocarbons still remain intact.

Around 1600 °C, the accident specific contribution of caesium, strontium, iodine and noble gas release is negligible.

This report is a translation of Jül-2091 published October 1986 in German.

Index of abbreviations used

AVR-Jülich	Arbeitsgemeinschaft Versuchsreaktor - Jülich
THTR 300	Thorium High Temperature Reactor with electrical output of 300 MW
HOBEG/NUKEM	German fuel manufacturer
HRB	Reactor design company in Mannheim, FRG
INTERATOM	Reactor design company in Bensberg, FRG
KFA Jülich	National nuclear research centre, Jülich
ÖFZS	Austrian Research Centre, Seibersdorf, Austria
A.E.R.E.	Atomic Energy Research Establishment, Harwell
GA	General Atomics, San Diego

Descriptions of particles

PyC layer	Particle coating of pyrocarbon
BISO coating	Particle coating of several different pyrocarbon layers
TRISO coating	Particle coating of pyrocarbon layers with an additional SiC intermediate layer
HTI	High temperature isotropic (PyC from methane)
LTI	Low temperature isotropic (PyC from propene or propene/ethine)
HEU	High enriched uranium
LEU	Low enriched uranium

Designations of fuel elements

GO	Fuel elements with $(Th,U)O_2$ BISO particles
GK	Fuel elements with $(Th,U)C_2$ BISO particles
GFB	Fuel elements with UO_2 TRISO fissile and ThO_2 BISO fertile particles
GLE	Fuel elements with low enriched UO_2 particles (low enriched)
DR-K	Fuel elements irradiated in the Dragon Reactor, Britain
FRJ2-K	Fuel elements irradiated in the Jülich Dido reactor
R2-K	Fuel elements irradiated in material test reactor R2 in Studsvik, Sweden
HFR-K	Fuel elements irradiated in material test reactor HFR in Petten, the Netherlands

Index

1. Introduction

During an accident, the temperatures in the core of a pebble bed HTR, which are normally around 800° to 900 °C, may increase. For the extreme case of pressure loss in the core with failure of all heat sinks, temperatures of more than 2000 °C are reached in medium size HTR's /1/. With the rise of the core temperatures above normal operating temperatures, fission products may be released to an increased extent from fuel elements into the primary circuit and into the environment.

For a realistic assessment of fission product release, accident simulation tests with spherical fuel elements have been carried out since 1977 in the hot cells of the Institute for Reactor Materials at KFA Jülich /3/. Data for the analysis of hypothetical accidents have been determined in experiments up to temperatures of 2500 °C /4/. The most extensive tests were on fuel elements with $(Th,U)O_2$ BISO particles (the fuel kernel is surrounded by layers of pyrocarbons), as used in the 300 MWe THTR at Schmehausen, at temperatures between 1600 and 2500 °C /5/. The experiments showed that Cs 137 diffuses through the particle coating within 100 hours at 1600 °C and is released from the fuel element, but that the outer very dense pyrocarbon coating of the particle remains intact up to 2500 °C, and that fission gases are well retained.

With interest in small HTR's, such as the HTR 100 and the MODUL /6/ growing, and with regard to the lower temperature range of hypothetical accidents in the HTR 500, relatively low accident temperatures between 1400 and 1800 °C have become important (Fig. 1), where generally only very low quantities of radio-activity are released from spherical fuel elements.

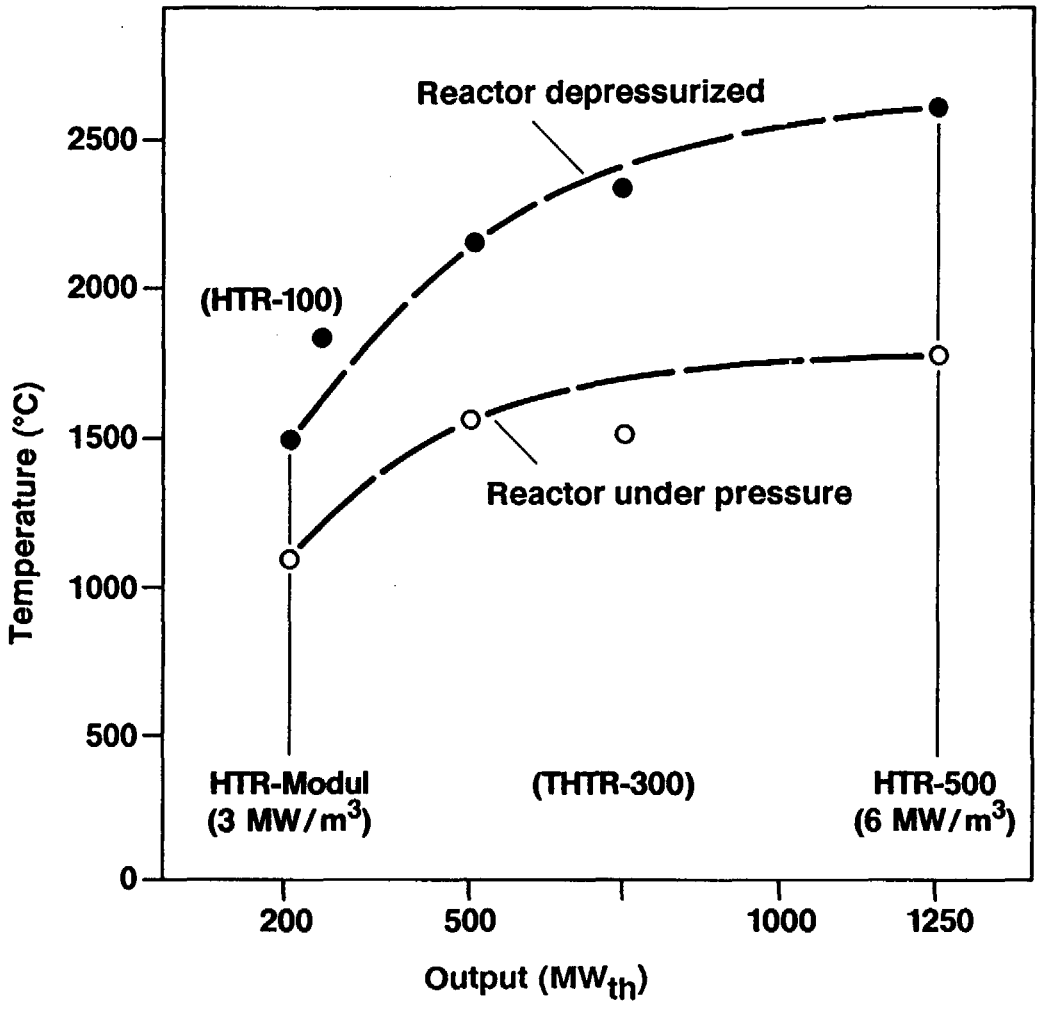

Fig. 1: Accident temperatures for pebble bed HTR's /2/

The fuel elements provided for new HTR's do not contain $(Th,U)O_2$ BISO particles, but UO_2 TRISO particles, which have an additional intermediate SiC layer /7/.

The existing heating equipment was not sufficient for testing TRISO fuel elements at temperatures up to 1800 °C. A new process had to be developed, by which the release of all relevant fission products could be measured more accurately and with much higher sensitivity.

The important fission products in accidents are given in the risk analyses, e.g. of the HTR 500 /8/. In case of depressurization there are no early

health effects, later health effects are due to Cs 137, followed by Sr 90 and I 131 /8/.

The very high iodine activity a few days after an accident together with its high volatility makes radio-iodine the most important early source of radio activity. The knowledge of iodine release is therefore necessary for the licensing of small and medium sized HTR's. On the other hand, Ag 110m is the only fission product which may be released after a long time at about 1200 °C from intact TRISO particles. Silver release behaviour is of great interest with regard to reactor operation and maintenance. The measurement of Kr 85 gives information on particle defects and the release behaviour of the other fission gas nuclides.

In the past, a large variety of experiments have been performed with individual particles /9/ or small numbers of particles /10,11,12,13/ at accident temperatures. The test rigs have the advantage that they are simpler, cheaper and more accessible, as they only need light shielding. However, particularly in measurements on TRISO particles, there was a great deal of scatter in the results. Also, loose individual particles became defective at relatively low temperatures, although the same fuel particles embedded in the matrix graphite of a spherical fuel element can withstand considerably higher temperatures without damage /14/. These are not the only reasons which led to accident simulation tests being done in the Hot Cells of KFA on whole spherical fuel elements and not on loose particles /14/:

- the release from heavy metal contamination in the fuel elements is measured
- realistic information can be obtained on very small fractions of particle defects
- in fission product release, the retention of the matrix is considered
- mean values are obtained from a large number of particles, which differ from each other (there are about 16400 UO_2 TRISO particles in the spherical fuel element)

2. Process

In the old heating equipment used since 1977, with two resistance furnaces with graphite components inside, experiments are done at temperatures up to 1900 to 2500 °C, these temperatures could occur in hypothetical accidents on medium-sized and large HTR's /15/.
In the newly developed cold finger apparatus, which has been working since 1984, experiments are possible up to 1800 °C, which covers the range of design accidents of the smaller HTR's. In contrast to the old system, the cold finger apparatus (KÜFA = Kühlfingerapparatur) can detect and measure very small releases of radioactivity of all fission products relevant to accidents. The release profile of the fission products can be determined from the results. Characteristics of each apparatus are compared in Table 1.

	New equipment (KÜFA)	Old equipment (A. Test)
Technical data		
Number of resistance furnaces	1	2
Heater body material	tantalum	graphite
Guide tube material	tantalum	graphite
Max. temperature	1800 °C	2500 °C
Sweep gas pressure (He)	1100 mbar	1070-1200 mbar
Quantity of flow (He)	20-30 l/h	20-30 l/hour
Temperature measurement	W/Re thermocouple Pyrometer	Pyrometer
Experimental range	Design accidents	Hypothetical accidents
Fission gas	Continuous fission gas measurement during the whole test (Kr 85, Xe 133)	
Solid fission products	Regular extraction of cold finger samples and measurement of condensed fission products Cs 134, Cs 137, I 131, Sr 90, Ag 110m	Inventary before and after test (Cs 134, Cs 137)

Table 1: Accident simulation equipment compared

2.1 Cold finger apparatus

The furnace of the cold finger apparatus is part of a helium sweep gas circuit.

2.1.1 Cold finger furnace

Fission products released from fuel samples in heating experiments can either be caught in filters or they are deposited at cold positions, e.g. a cold finger, which can be measured after insertion. Such cold finger devices have already been successfully used in furnaces for single particles or small particle samples /12,17/. In order to obtain not just one, but several measuring points for an experiment on a fuel element, a furnace had to be developed which had condensate plates which could be replaced during heating. Preliminary tests were done for the cold finger assembly and dimensioning, and the choice of materials for the furnace.

a) Preliminary experiments

A cold finger prototype with an electromagnetically held replaceable condensate plate was developed and built at KFA. Preliminary experiments in a graphite furnace of the existing apparatus showed that the condensate plate could be cooled sufficiently and that with remote release of the plate, handling of the condensate plate without contamination was possible.

The second part of the design tests was concerned with the problem of choice of material for the heating chamber of the furnace. In the existing apparatus, the spherical fuel elements were heated in graphite pans above graphite heaters. In the planned system, it was important that fission products did not diffuse into the pan walls, as is the case with graphite crucibles.The spherical elements were therefore to be heated in a metal crucible, the gas pipe, open upwards for the cold finger.

As at the intended temperatures of 1600 to 1800 °C, metals resistant to high temperatures could be corroded by carbon and impurities in the helium sweep gas so preliminary tests were again done in a graphite furnace of the

existing apparatus with sheets of niobium, tantalum and molybdenum. All three materials were satisfactory at 1600 °C, as long as the sheets only supported their own weight on the graphite. During tests to find the most suitable material for the spherical fuel elements to rest on, tantalum proved superior to niobium and molybdenum, where great carburization occurred on the contact surfaces with the graphite sphere. Experiments with beryllium oxide and aluminium oxide ceramics were also less satisfactory in their results than those with tantalum.

Although during the initial phase, molybdenum components were used in the cold finger furnace up to a maximum of 1600 °C for cost reasons, after this, because of the longer life and higher temperature resistance, only tantalum parts were used.

b) Design

Based on the preliminary tests, the furnace of the cold finger apparatus was developed with the firm of Degussa at Hanau/Wolfgang (Fig. 2).

The recipient is built into the floor of the gastight hot cell box. The hood can be opened to load it, using a hydropneumatic device. The spherical fuel element is placed by a suction device on the thre-point support made of small tantalum tubes in the tantalum gas pipe.
During the experiment, the fuel element is swept from the bottom upwards with helium (about 30 l/hour). The gas pressure in the furnace is held at 1100 millibar by automatic filling or release. The gas pipe and sphere are heated by the tantalum heater carrying a maximum current of 2400 A.

The cold finger, with the replaceable condensate plate at its end, projects into the gas pipe. The finger can be taken out of the furnace at a certain point of the heating test, when the pneumatic slide valve is closed. The used condensate plate falls into a holder after remote unlatching a new condensate plate can then be taken out of another holder. The condensate plates already used in the furnace are locked out of the hot cell and are measured by gamma and beta spectrometry at two low activity measuring positions.

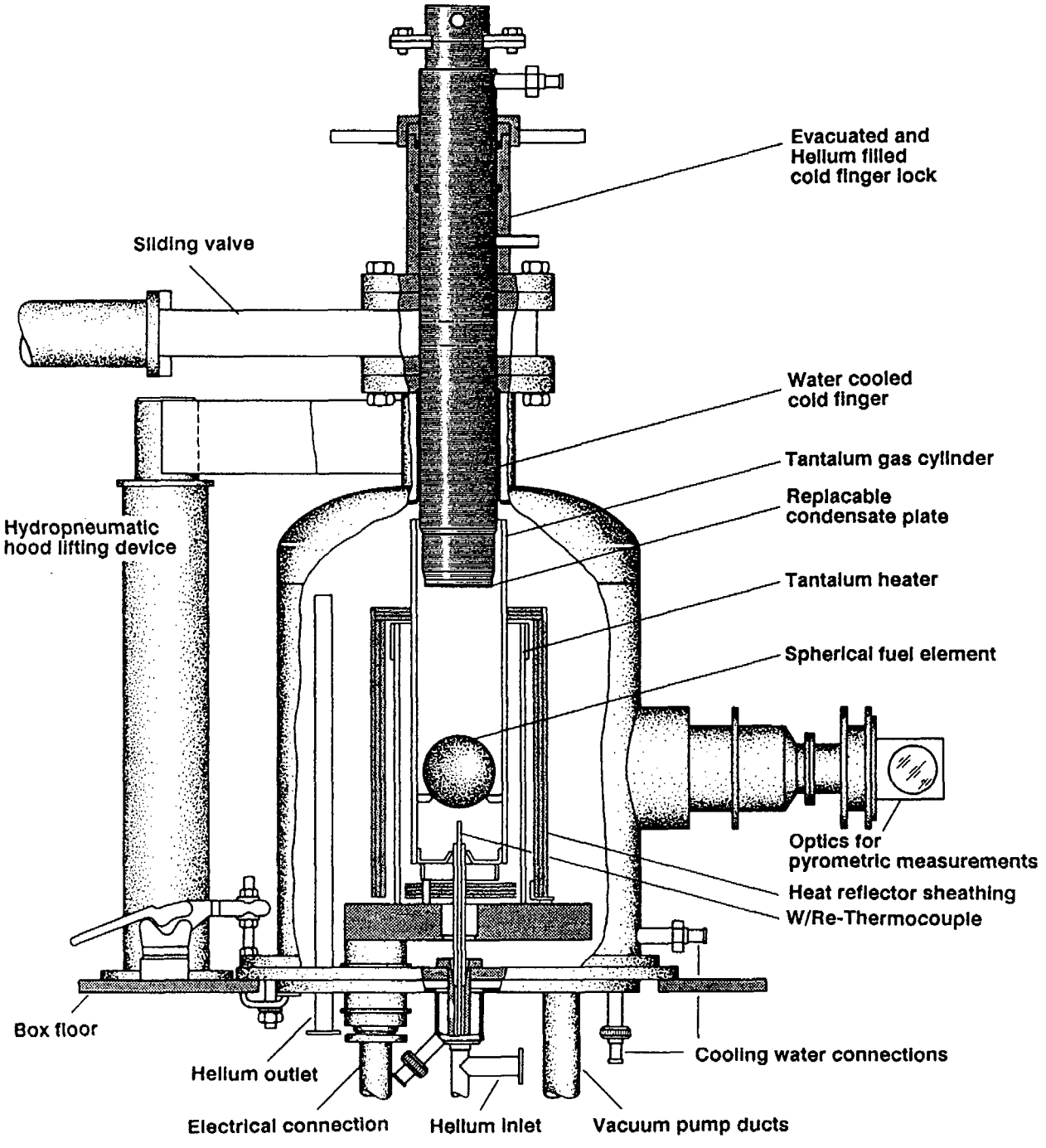

Fig. 2: Heating furnace used in accident simulation tests with irradiated spherical fuel elements (KÜFA)

When the coldd finger is reinserted in the furnace, the cold finger lock is evacuated and flooded with helium before the pneumatic slide valve is opened, in order to be able to lower the cold finger to the selected test position. In the orginal design, the condensate plate was held electro-magnetically. When there was a fault in the coil, the plate consisting of stainless steel and soft iron, fell on a hot spherical fuel element at 1600 °C and melted (Fig. 3).

Although the fuel element was undamaged (apart from molten pearls, one can see a groove, where a sample had been extracted from the fuel-free zone (left of picture)), the gas pipe and heater (right of picture) were destroyed.

In order to prevent faults of this kind, a new cold finger was developed and has been used with success since the beginning of 1986. In this cold finger, the condensate plate is held by springs and can be remotely unlatched pneumatically (Fig. 4). The temperature of the cold finger is measured with a Pt 100 thermometer, and that of the sphere by a W/Re double thermocouple. Both temperatures are continuously recorded. When measuring the sphere temperature, one must consider that the W/Re thermocouples will measure 10 to 20 °C too low, depending on the temperature. As a check and in case of failure of the W/Re double thermocouple, it is possible to measure the temperature of the gas cylinder by pyrometry. The temperature profile of a heating test is controlled via the thermocouple voltage or if there is a thermocouple defect via the furnace power, according to a program.

Heater faults were the most frequent cause of premature ending of experiments. The lives at similar temperatures were very different, varying from 20 to 1500 hours. It was found that it was not corrosion causing faults, as was feared, but distortions of the heater and steel sheets led to shortcircuits. The design of the heaters and steel sheets was therefore changed, in collaboration with the firms of Degussa and Plansee.
To cool the furnace, cold finger and slide valve, five closed cooling circuits are necessary, which can in turn be cooled via a heat exchanger, which is connected to an open water circuit /18/.

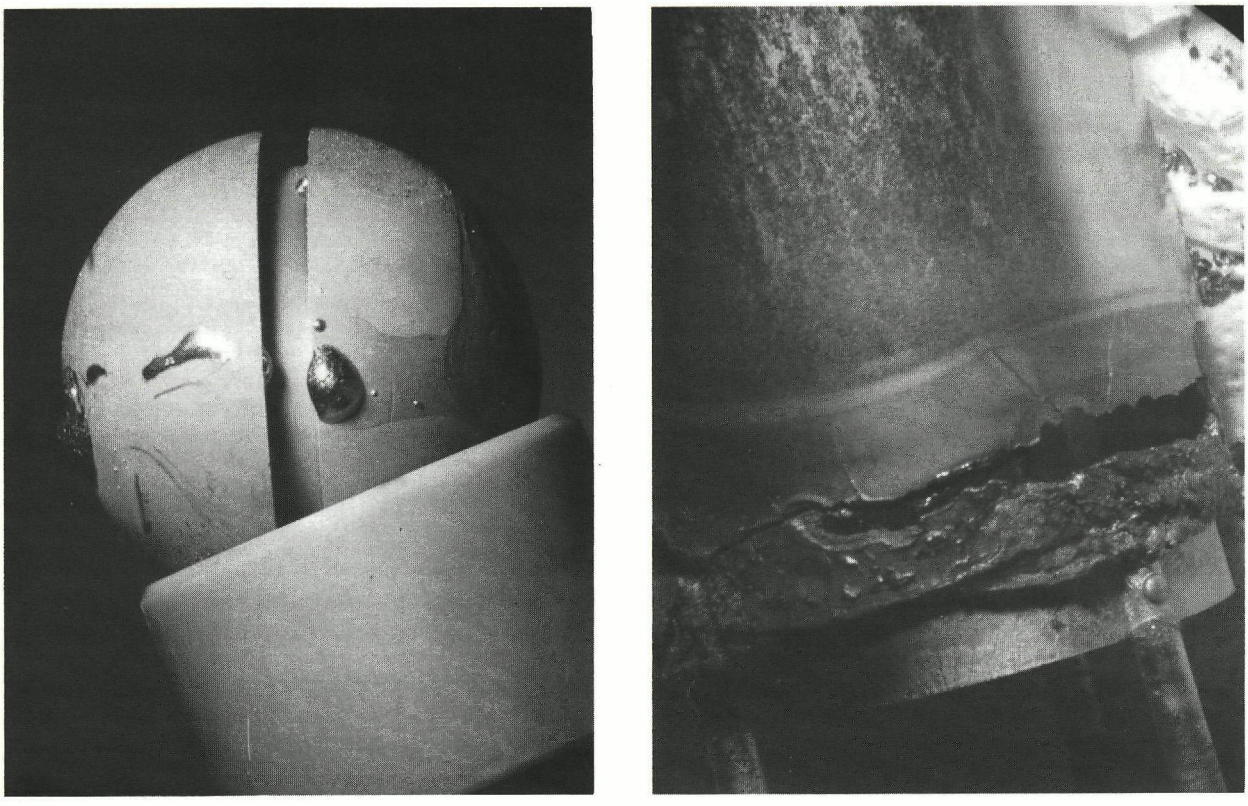

Fig. 3: KÜFA accident at 1600 °C

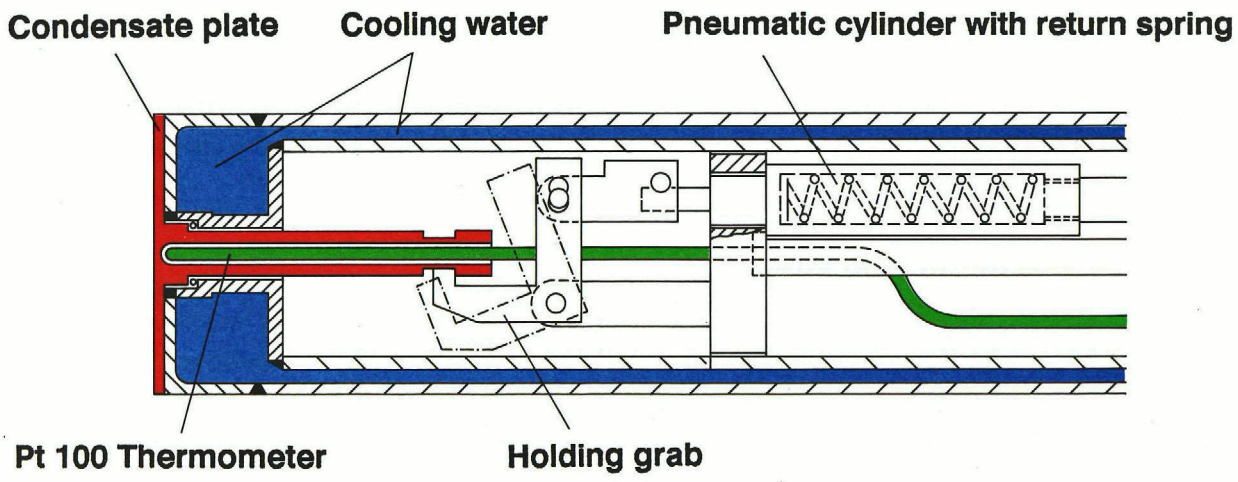

Fig. 4: Section through lower part of cold finger

With failure of cooling, flow and temperature sensors in each circuit shut off the heating. For a small leak in the closed cooling system, the heating is stopped via a cooling water level control.

2.1.2 Sweep gas circuit

The cold finger furnace is integrated in a helium sweep gas circuit, the main task of which is to make measurement of fission gases possible (Fig. 5).

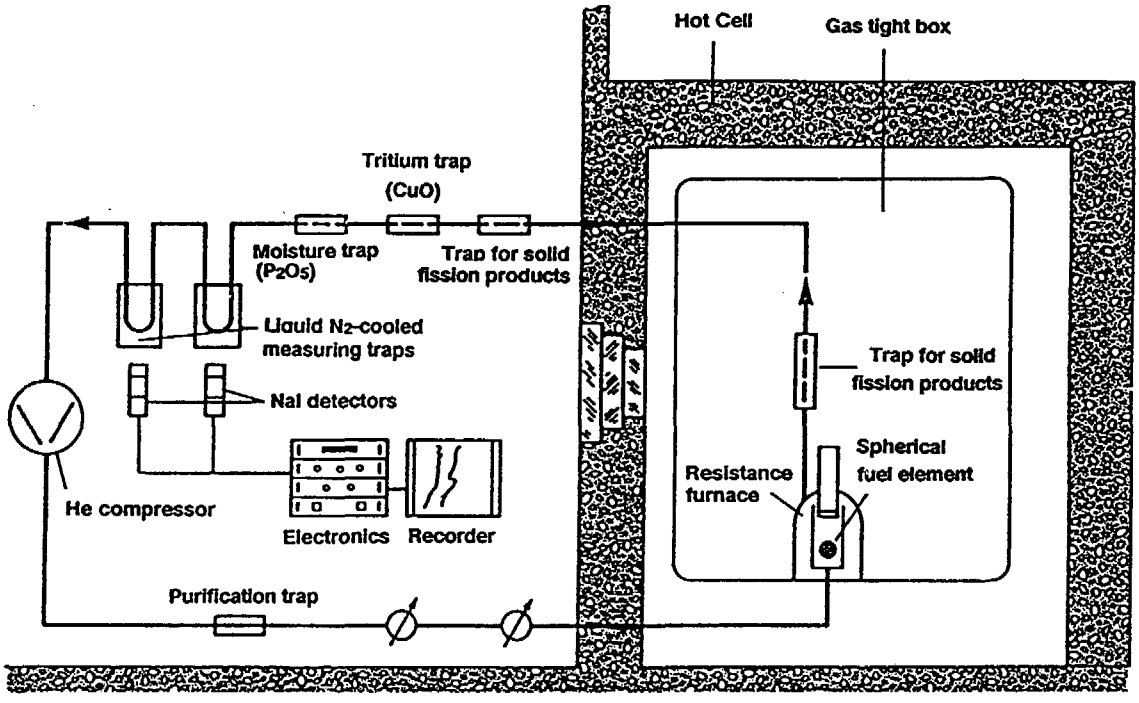

Fig. 5: Sweep gas circuit of cold finger apparatus (KÜFA)

While the solid fission products released from a fuel element during a heating test mostly settle out on the cold finger or in the gas pipe, and only small quantities reach the traps for solid fission products, the fission gases Kr 85 and possibly Xe 133 are carried over to the measuring trap by the sweep gas. The released fission noble gases are collected in this active carbon tray cooled by liquid nitrogen. The second trap is only intended to check the fission gas retention of the first one. The activity in both measuring traps is measured and recorded during the entire test by NaI (sodium iodide) detectors.

CuO (copper oxide) and P_2O_5 (phosphorus pentoxide) traps are intended to oxidize heated tritium from the fuel element and furnace, or to filter water vapor from the measuring trap, respectively. There are two parallel pairs of cleaning traps after the He compressor in the circuit, which can be heated alternately during an experiment. A pair of traps consists of a zeolith trap and an active carbon trap cooled with liquid nitrogen. Details on the construction and methods of operation of the traps have already been given.

Next, after the cleaning traps, and before the sweep gas reaches the furnace, the H_2O and O_2 in the helium are measured and recorded by a printer. The sweep gas circuit is cleaned before a heating test, until the measured values are less than 10 ppm. Small impurities in the furnace are a precondition for a long life of the valuable tantalum parts. Apart from the fuel element and cold finger temperature, release of fission gas and impurities in the helium are also constantly recorded from the sweep gas flow (in general about 30 l/hour).

Fig. 6 shows the main features of the controls of the cold finger apparatus in the fuel cell laboratory of KFA. Fig. 7 shows the cold finger furnace with a cold finger taken out of the furnace by a cell crane.

2.2 Execution of experiments

The accident situation in the reactor core is to be simulated by the heating experiments. The fuel elements would be heated by the operating temperature in an accident in an HTR. In an experiment, one must avoid additional effects caused by fast heating from room temperature or by impurities in the sweep gas circuit damaging particles and fuel elements, which would not occur in the reactor in the conditions existing there during an accident. The following test programme was developed during a series of tests /14/ (Fig. 8).

Fig. 6:
Operating controls of cold finger apparatus with (from the left) fission gas electronic cubicle, operating cubicle for He sweep gas circuit. Operating desk for cold finger furnace with temperature programmer, pyrometer in front of cell window.

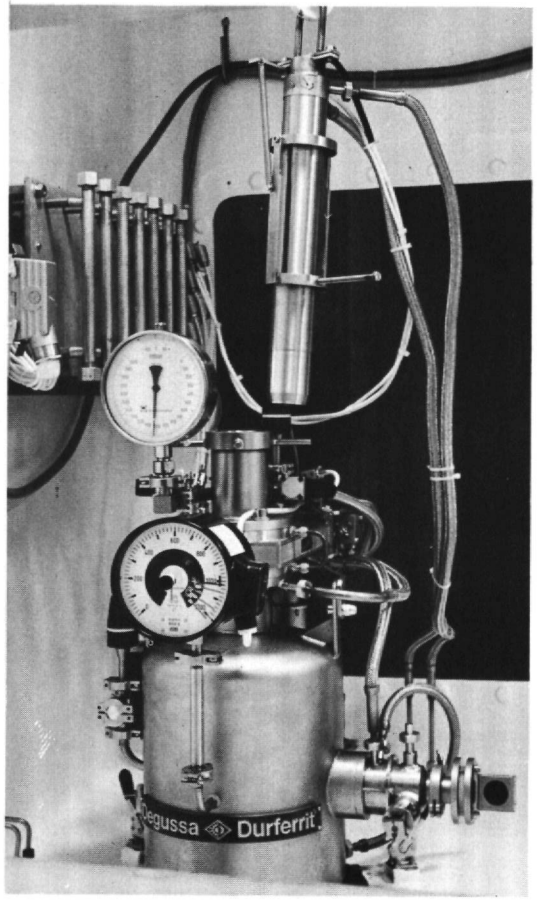

Fig. 7:
Furnace with cold finger pulled out

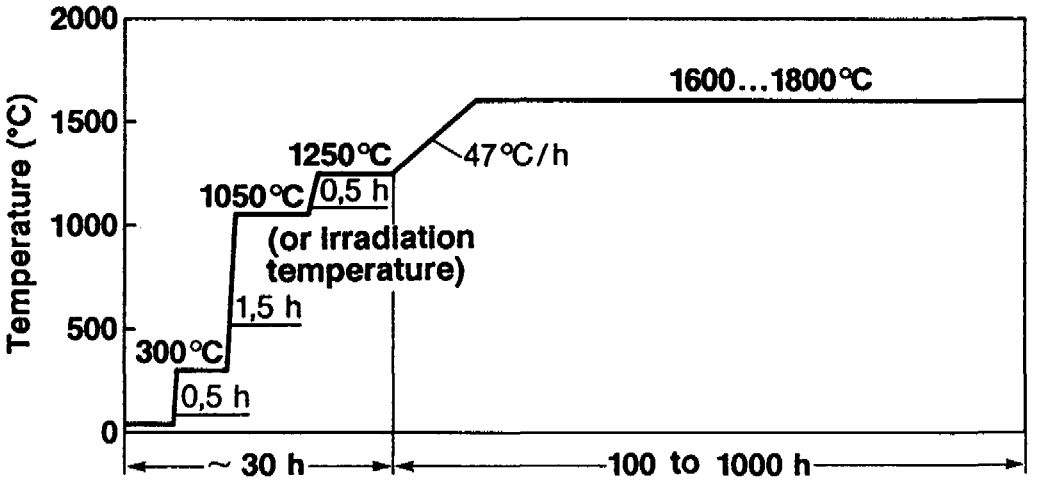

Fig. 8: Standard experiment in the cold finger apparatus

a) Cleaning of sweep gas and measurement of fission gas emission at room temperature

b) Heating for cleaning at 300 °C, in order to drive out water vapour absorbed by fuel element

c) Simulating reactor operation
In this section of the experiment, a steady state for diffusion processes should be reached at irradiation temperatures in the particles, such as would occur at the start of an accident.

Also, in the context of testing, fission gas equilibrium releases should be determined for 1050 °C (mean working temperature) and 1250 °C (maximum working temperature) for AVR fuel elements.

d) Simulating an accident
The heating rate for simulating an accident should be close to circumstances in the reactor, on the one hand, i.e. close to the calculated transients, which are different, depending on the type of accident and

the type of reactor, but on the other hand, the tests should be comparable with each other.

With few exceptions, heating was done at a standard rate of about 47 °C per hour, i.e. from 1100 to 2500 °C in 30 hours. This transient represents the calculated one for the case of the HTR 500 core heating accident (Fig. 9), and is used for accident simulation tests on fuel element particles at GA, San Diego, USA /19/.

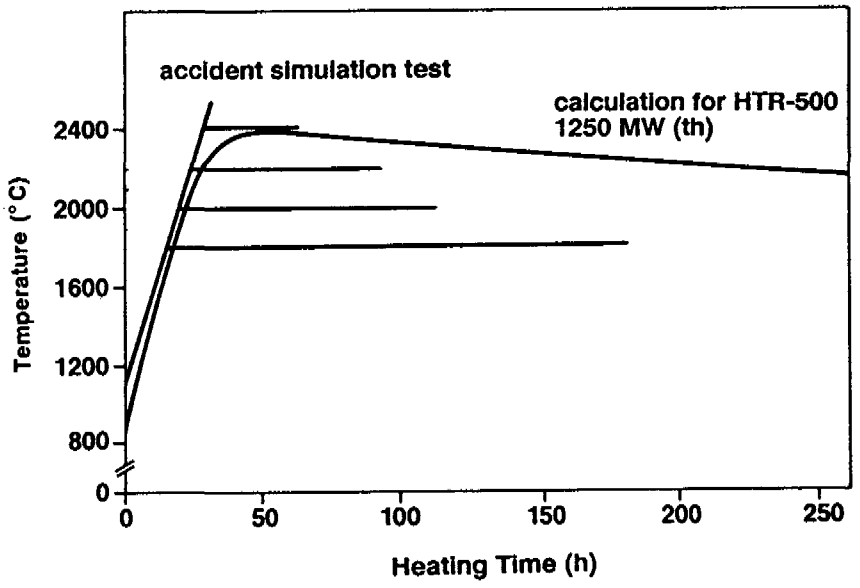

Fig. 9: Simulation of hypothetical accidents up to a maximum of 2500 °C

In some cases, heating was done more slowly, i.e. from the irradiation temperature to the maximum accident temperature of 1400 to 1800 °C in 30 hours, which simulates the calculated accident transients more accurately in this temperature range.

The isothermal temperature period following the heating is generally longer (500 or 1000 hours) at 1600 °C than at 1800 °C (100 hours) (Fig. 10). The reason for this is that at 1600 °C, only small quantities of fission products are released from the fuel elements after a long time, while the release at 1800 °C can be measured within 100 hours.

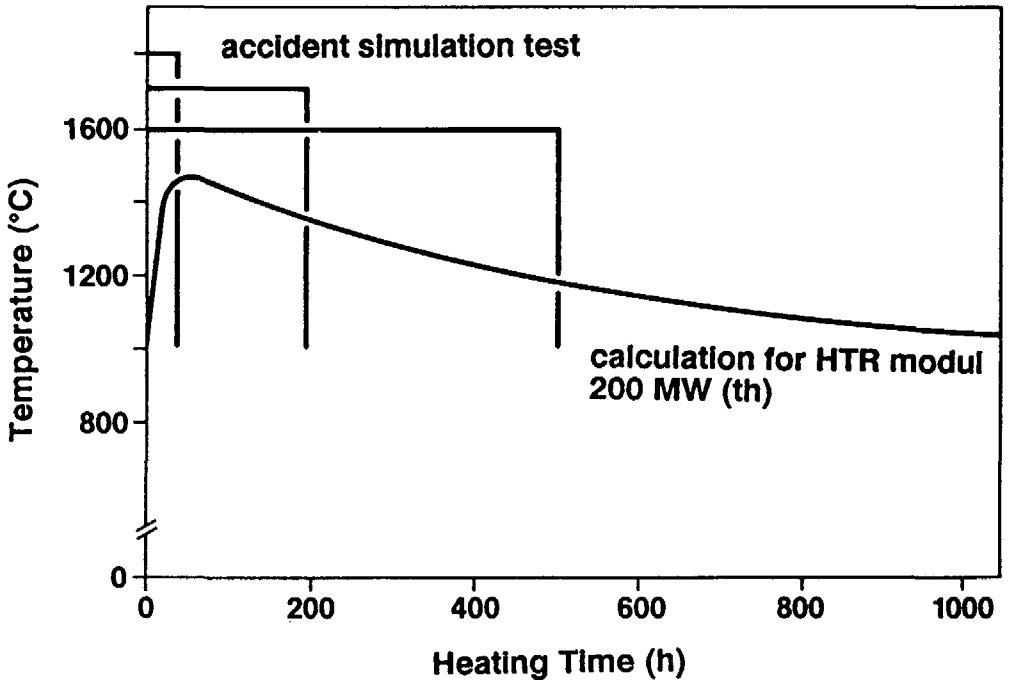

Fig. 10: Accident simulation tests at 1600 to 1800 °C

Table 2 shows the agreement and differences between an accident in the reactor core and the heating test:

	Reactor core	Heating furnace
Sample	pebble bed	single spherical fuel element
Accidents without pressure loss in the core	high pressure and high cooling gas speed, good removal of released fission products, even temperature distribution in fuel elements	low pressure and low sweep gas speed, good removal of released fission products, even temperature distribution in fuel element
Accidents with pressure loss in the core	low pressure and low cooling gas speed, obstruction to release of solid fission products from spherical fuel elements by partial pressure building up in cooling gas /20/, even temperature distribution in fuel elements	

Table 2: Comparison of conditions for accidents in reactor and accident simulation tests

2.3 Measurement and calibration of fission products

The noble fission gases are collected in a trap during the whole experiment and are continuously measured, while the condensate plates have to be taken from the furnace and then measured at intervals of several hours a day. The measurement is established by calibration in both cases.

Also, the inventory of fission products is measured in the fuel element before and after a test.

2.3.1 Measurement and calibration of fission gases

The Kr 85 and Xe 133 radioactivity in the measuring traps is measured by NaI detectors. The measuring pulses reach two single channel discriminators, which are set to characteristic Kr 85 (515 KeV) and Xe 133 (81 KeV) energies, respectively. The signals reach a printer via counters (rateme-ters), on which the measured share of the activity of the two fission gas nuclides in the measuring trap is printed in pulses/sec for the whole experiment. The exact setting of the discriminators on the width of photographic line can be controlled via a coincidence circuit using a multichannel analyser. The measurement of the whole spectrum with the multichannel analyser is important for checking the content of the traps and the background radiation at the measuring position. Furthermore, for superimposed energy lines, gross and net peak areas can be printed where one can correct the pulse rates. To determine the complete fission gas activity in the measuring trap, the set-up must be calibrated.

In order to calibrate, once or twice a year glass ampoules with different calibrated Kr 85 or Xe 133 radioactivity must be heated to destruction in the furnace, with the test rig remaining the same. The released fission gas is adsorbed completely in measuring traps filled with active carbon, as in the heating test with fuel elements. The calibration factor can then be calculated from the known and measured activity.

Gamma emitting nuclides are used for calibration for intermediate tests, where the gamma emission lines are close to the used emission lines of Xe 133 (81 KeV) and Kr 85 (515 KeV). Ba 133 (79 KeV) was used in calibration for Xe 133 and Ru 106 (511 KeV) for Kr 85. During calibration after evaporating a weighed quantity of the calibration solution on a plate, the solution is placed on a plate in an empty Dewar flask, which has the same dimensions and configuration as the floor of the measuring trap. In this way the same counting geometry and radiation absorption is obtained for calibration solutions and the fission gases trapped during the test. The cali-

bration factor f_E is the ratio of the measured fission gas pulse rate Ip (pulses/sec) to the actual fission gas rate R (decays/sec) accumulated in the trap.

The calibration factor for calibrating with Ba 133 and Ru 106 can be calculated from the following equation:

$$f_E = \frac{I_P}{A_P \cdot e^{-\lambda_P \cdot t_P}} \cdot \frac{\gamma_{SP}}{\gamma_P}$$

where Ip (pulses/sec) = measured pulse rate for solution used
Ap (Bq) = activity of solution at time of manufacture
λp (per sec) = decay constant of solution
tp (sec) = decay time of solution since manufacture
Yp = gamma yield of solution for the appropriate energy
Ysp = gamma yield of fission gas nuclide (Xe, Kr) for the appropriate energy

The gamma yield, half life and decomposition constants of the abovementioned nuclides are given in the following table /21/:

Nuclide	γ(%)	$T_{1/2}$(d)	λ (1/d)
Kr 85	0,427 (515 keV)	3927	$1,77 \times 10^{-4}$
Ru 106	20,6 (511 keV)	368,8	$1,88 \times 10^{-3}$
Xe 133	36,6 (81 keV)	5,27	$1,32 \times 10^{-1}$
Ba 133	29,0 (79 keV)	3835	$1,81 \times 10^{-4}$

Table 3: Data of measured fission gas nuclides and associated calibration solution

The accuracy of the measured release values, taking into account the systematic calibration and measuring errors, is about 15 %.

2.3.2 Measurement of solid fission products

The condensate plates taken from the furnace and locked out of the hot cell can be measured very accurately at shielded measuring positions by gamma and beta spectrometry. The germanium-lithium detector for gamma spectrometry measurement is connected to a computer via a multi-channel analyser, which determines the Cs, I and Ag fission product activity on the condensate plate.

The deposited Sr 90, which does not emit gamma radiation, is measured by beta spectrometry with a scintillation detector connected to the multi-channel analyser. This makes use of the fact that the decay product of Sr 90, Y 90 with 2.3 MeV, has the highest beta energy of the fission products deposited on the condensate plate, with negligible exceptions. The beta spectrum measured from a condensate plate is used to determine the Sr 90 activity originating from high energy Sr beta radiation (Fig. 11, black area) by calibration with Cs 137, Ag 110m, Sr 89 and Sr 90 preparations. Comparative measurements with calibration preparations of similar activity are done for different active condensation plates, in order to be able to exclude superposition in the evaluated energy range with competing beta radiation.

If calibration and measurement errors are taken into account in the fission product release values, the accuracy of the values for Cs 134, Cs 137 and I 131 is $\pm$13 %, that for Ag 110m is $\pm$30 % and that for Sr 90 is $\pm$50 %. The caesium release values are controlled by gamma spectrometry inventory measurements of fuel samples before and after a test, where the caesium loss can only be found in $\pm$1 % of the total inventory. In order to reach the high accuracy required for this, a fuel element must be measured three to five times alternately with a comparative element.

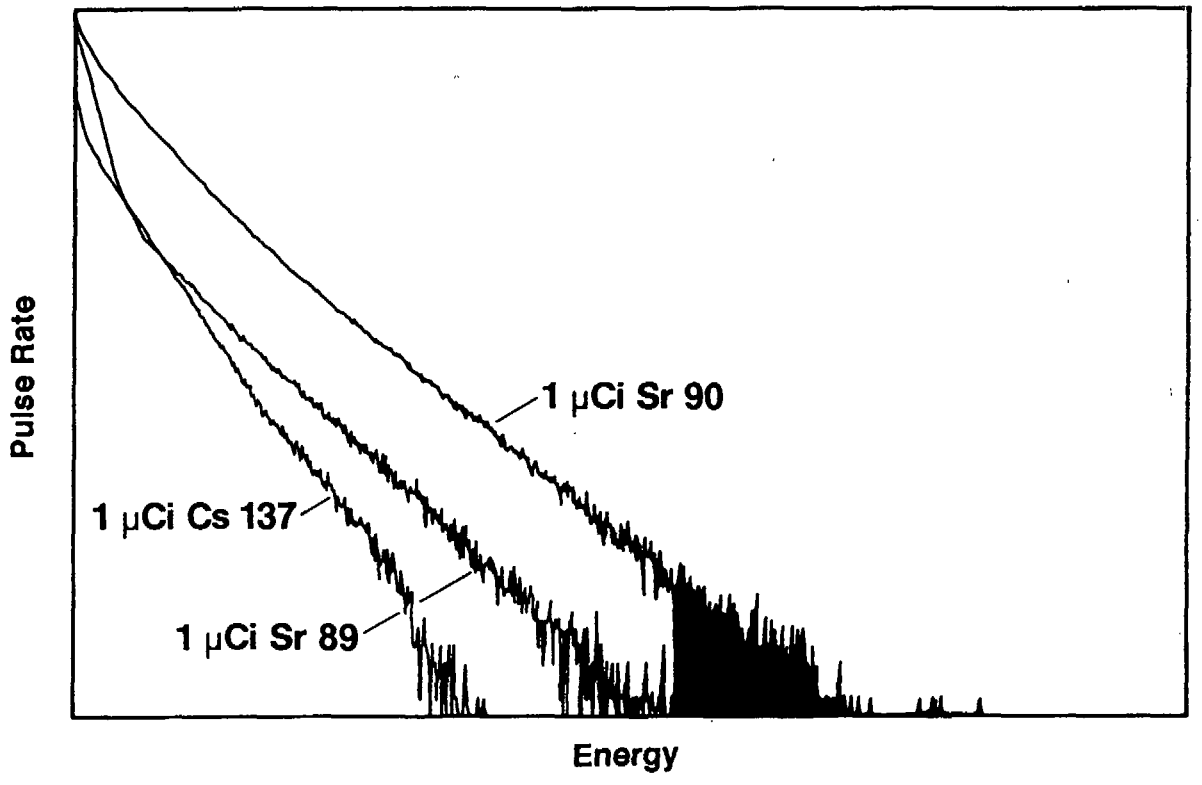

Fig. 11: Beta spectra of fission products deposited on condensation plate

2.3.3 Calibration of the condensate plates

The fraction deposited on the condensate plate must be known for the quantitative determination of the fission product activity released from a fuel sample. Experiments are done with calibration preparations and the experimental results obtained are used, as far as possible.

a) Caesium, strontium

Different quantities of Cs 137 and Sr 90 are evaporated on to several tantalum sheets with a diameter of 6 cm. Some sheets are placed in the cold finger furnace with the deposited surface on top and others with it at the bottom, and are heated. It was found that the Cs 137 activity deposited on the condensate plate was about 70 % on average, and only about 2-5 % less with the sheet facing downwards, than with the deposited surface on top.

Only very small quantities were found in the tantalum gas pipe. About 30 % of the quantity of caesium released is deposited on the outside wall of the cold finger, or on the furnace wall which is also cooled.

The behaviour of strontium is quite different. With the sheet facing downwards, nearly the whole of the strontium is deposited on the hot inside surfaces of the tantalum tube, below and at the height of the sheet. With the sheet turned upwards, more than 30 % is deposited on the condensate plate, however.

In order to approximate to the release conditions in heating tests with spherical fuel elements, a total of 10 graphite spheres were previously heated at 1600 to 1800 °C, which had different amounts of activity of Cs 137 and Sr 85 applied to them. Sr 85 radiates gamma radiation, in contrast to Sr 90, so that the proportion of Sr 85 remaining in a graphite shpere after the heating test can be measured. The results were confirmed with tantalum sheets in these tests. The measured proportion of Sr 85 of 20 % at the condensate plate corresponds roughly to the mean value of plate activity of sheets placed in different positions. The calibration tests showed that caesium diffuses much more quickly through the graphite matrix than strontium. While caesium was released 100 % from a graphite sphere after 20 hours at 1700 °C, only 70 % of the strontium preparation was released after 120 hours at 1700 °C.

b) Iodine, silver

Similar to caesium, iodine and silver deposit 70 % of their activity on the condensate plate in the heating test.

The I 131 fraction on the condensate plate could be determined by heating experiments at 1400 to 1800 °C on 5 fuel samples with 5 UO_2 kernels each (FRJ2-P28 Coupons), where the I 131 inventory was measured before and after a test. In the same way, the caesium deposition behaviour could again be checked in these experiments.
The calculated silver inventory was completely heated from some samples, so that in these cases, the release could be determined at the condensate plate.

The fission product distribution in the cold finger furnace is shown in Fig. 12.

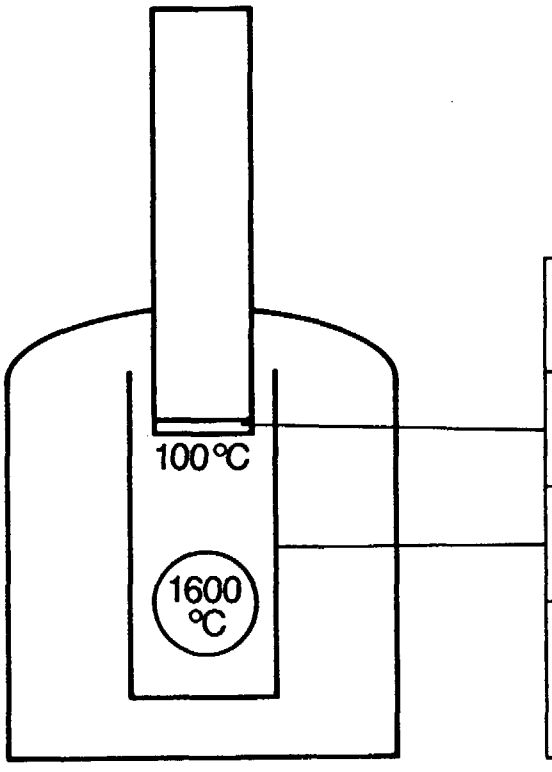

	Released portion	
	Cs, J, Ag	Sr
plate	0,7	0,2
Ta-tube	0,02	0,8
furnace	0,3	–

Fig. 12: Fission product distribution in KÜFA furnace

2.4 Evaluation of measurements

The fission gas release curves, the condensate plate measurements and the inventory measurements must be evaluated before and after a heating test.

2.4.1 Evaluation of fission gas release

In the tested temperature range 1400 to 1800 °C, the release of fission gas from fuel elements with TRISO particles remains very small, even after a longer period of heating (Fig. 13). Any Kr 85 activity due to contamination is heated and driven off during heating up. When defects occur in the coating, fission gases are released from the fuel particles.

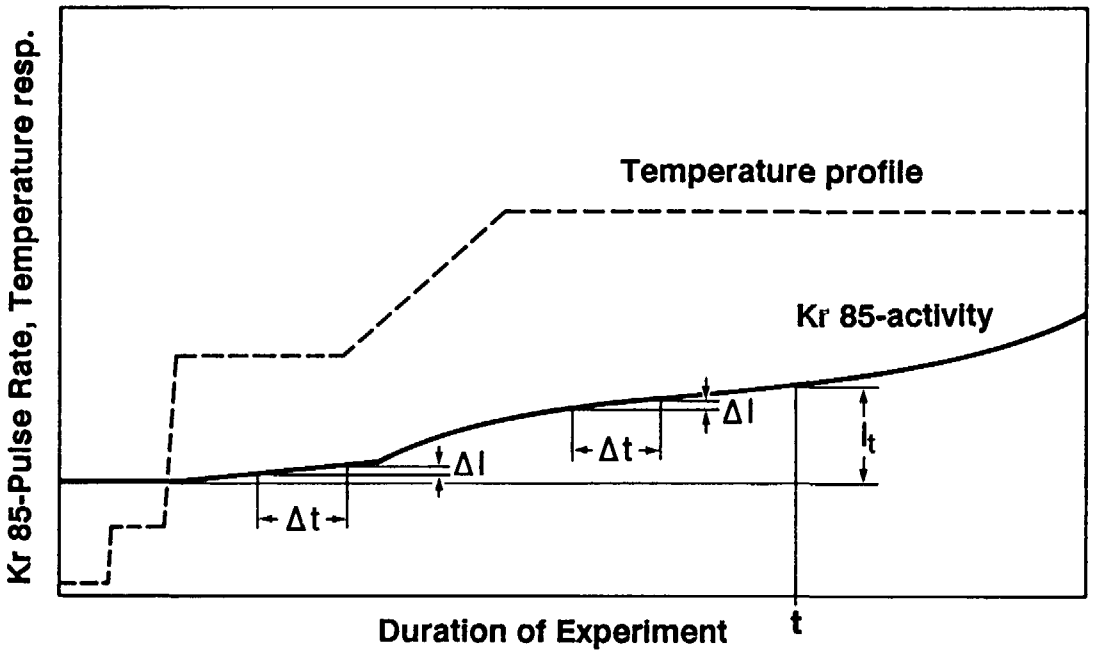

Fig. 13: Schematic diagram of release profile from Kr 85 from a fuel element with TRISO particles at 1600 °C

There are jumps in releases in exceptional cases, which are caused by a simultaneous defect of the SiC and pyrolitic carbon layers of a particle. About 50 % of the fission gas inventory of a particle is released spontaneously at 1600 to 1800 °C. The release fraction shown in the diagrams of results is determined as follows:

$$\text{Release fraction} = \frac{\text{release activity } A_t \text{ calculated from measurements (Bq)}}{\text{inventory A (Bq)}}$$

$$A_t = \frac{I_t \cdot e^{\lambda \cdot t}}{f_E}$$

where A_t (Bq) = activity released at time t calculated at end of irradiation

I_t (1/s) = measured pulse rate from released activity at time t (Fig. 13)

λ (1/s) = decay constant

t (s) = time from end of irradiation to test

f_E = calibration factor

The inventory values A can be calculated from the irradiation data /18,22/. The burnup is determined by gamma spectrometry inventory measurements for AVR fuel elements /23/ and the associated gas inventories are calculated from average irradiation data /24,25/ and confirmed by measurements.

Equilibrium release is of particular interest with regard to testing the AVR fuel elements. The measurement of relatively short lived Xe 133 gives better information on release during use in the reactor than the long lived Kr 85 /14/.

For nuclides with a short half-life, where the rate of birth and rate of decay during irradiation are equal (birth/decay equilibrium), the relative release is defined as the quotient of the release and birth rate:

$$\frac{R}{B} = \frac{\text{release rate}}{\text{birth rate}}$$

For the long lived Kr 85, no R/B equilibrium is established during irradiation. In this case, the measured release rate is therefore related to the inventory N (atoms at the end of irradiation). The release rate R for Xe 133 or Kr 85, referred back to the end of irradiation, is determined as follows from the release diagram:

$$R = \frac{\Delta I}{\Delta t} \cdot \frac{e^{\lambda \cdot t}}{\lambda \cdot f_E}$$

where

$\frac{\Delta I}{\Delta t}$ = slope in release curve in area of equilibrium release (Fig. 13)

2.4.2 Evaluation of solid fission product release

The gammaspectrometrie measurements of the fission products of interest, i.e. Cs 134, Cs 137, I 131 and Ag 110m, deposited on the condensate plate are evaluated directly by a computer connected to the test rig. Using a special program, radioactivity from superimposed energy lines, such as in the case of Cs 137 and Ag 110m at 660 KeV, can be calculated.

The Sr 90 activity is calculated from the beta spectrometer condensate plate and Sr 90 calibration measurements.

The inventories required for calculating the release proportions are measured in the case of Cs 134, Cs 137 and I 131. Ag 110m and Sr 90 have to be calculated, similarly to the fission gas nuclides /22,25/.

2.5 Post heating examinations

In order to obtain additional information on fission product distribution and defects in particle coatings in the heated fuel elements, other tests are done on the spheres, which are of particular importance for constructing a model of heating results.

2.5.1 Fission product distribution in fuel elements

Different work is necessary in order to determine the fission product distribution in the fuel free zone, in the matrix graphite and in the particles of a spherical fuel element.

a) Fission product distribution in the fuel free zone.
Fission product concentration profiles in the outer sphere shell can be determined in several ways, i.e. before and after one heating experiment or after several heating tests. In general, 8 rotating samples are taken step by step from the fuel free spherical shell, which is at least 5 mm thick, so that a 4.6 mm deep groove is formed. The samples are then measured by gamma spectrometry.

The fission product concentrations per gram of matrix graphite are obtained from the measurements. In order to be able to compare the fission product profiles with profiles from different fuel elements, relative parts in the matrix graphite are calculated and shown graphically:

$$\text{Relative part in graphite: } \frac{\text{measured concentration (Bq/g) x matrix weight (g)}}{\text{inventory (Bq)}}$$

The total weight of the matrix graphite in the fuel free zone is about 100 g.

b) Fission product distribution in matrix graphite.
The fission product concentration profiles in the matrix graphite can be determined by the profile deconsolidation of fuel element and the subsequent measurement of the graphite matrix samples. Fuel particles can be obtained simultaneously for individual examination.

In the profile deconsolidation process /26/, the rotating fuel element is gradually immersed in an electrolyte. The material is removed in annular layers from the sphere, so that a cylinder of about 20 mm diameter remains. This cylinder is now immersed in the electrolyte in a vertical position (in general in 5 mm steps), where a new electrolyte is used after every step (Fig. 14). After separating the particles from the fraction obtained, electrolyte and matrix samples are left over for gamma spectrometer measurements. The relative fission product proportions in the matrix graphite of the fuel zone are also calculated in the same way as the profiles in the fuel free zone.

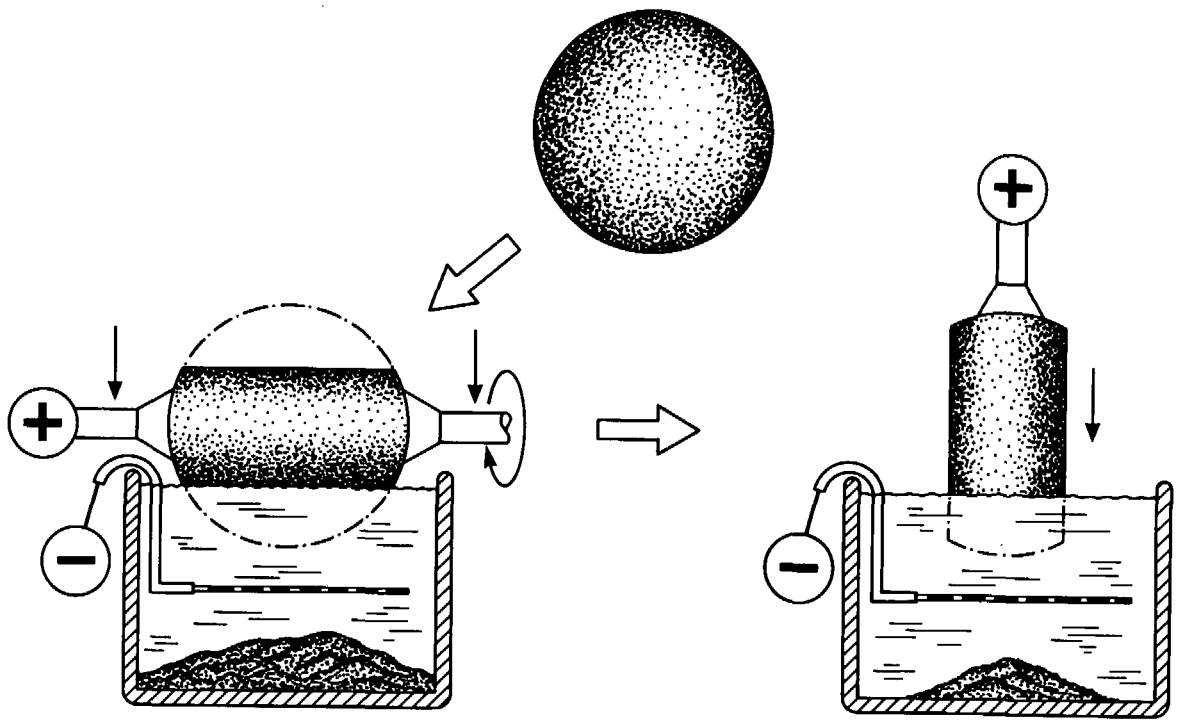

Fig. 14: Electrolytic profile deconsolidation of spherical fuel elements

The profile deconsolidation process was developed at A.E.R.E. Harwell, and has been used for fuel elements heated to high temperatures at KFA /5, 27/. After completion of this work at Harwell, a similar device was built in the hot cells at KFA and developed further.

c) Fission product distribution in fuel particles.
Individual fuel particles obtained during deconsolidation are measured by gamma spectrometry and are then crushed, so that the kernel and coating are separated. These components are then measured separately, so that fission product proportions in the kernel and coating can be determined.

2.5.2 Ceramography of particles /28/

Ceramographic examination is intended to make changes in the fuel particles, particularly of the SiC coating, visible. The start of corrosion of

the SiC is of particular interest in connection with the start of fission product release from fuel particles.
Ceramographic work is therefore done on two to three times 50 particles each from various fractions obtained during profile deconsolidation. Drilled samples can also be taken from fuel elements which were not deconsolidated and can be polished in one or more planes.

The samples embedded in liquid plastic are first vacuum impregnated, in order to close pores and cracks on the sample surface and to avoid air bubbles.

After polishing, the polished plane is thinly covered with the embedding material and again vacuum impregnated. To produce the sample surface, one polishes it with four different, ever finer diamond pastes, where the speed of the polishing equipment, sample load and polishing times have to be adapted to the size of the sample and the material being examined.

3. Results

The results obtained from the cold finger apparatus are in the forefront in this chapter, but the results obtained in experiments up to 2500 °C in the heating test apparatus are also given.

The most important results in accident simulation tests are the fission product release values from the spherical fuel elements. The following sources and release mechanisms are important:

1. Fission products present at start of test from uncoated fuel
   - contamination and defective particles due to manufacture
   - particle failure due to irradiation
   - contamination in the AVR reactor
   - contamination in the hot cell laboratory

2. Release from intact particles (diffusion through coating)

3. Release from particle defects during test
   - SiC damage: corrosion
     decomposition
   - complete particle defect (SiC and PyC layers)

3.1 Fuel elements with TRISO mixed oxide particles

The further development of the THTR fuel element with high enriched $(Th,U)O_2$-BISO particles resulted in the fuel element with $(Th,U)O_2$-TRISO particles. Fuel with a 7-11 % FIMA burnup was available from the AVR 15 spheres (Type GO2 with $(Th,U)O_2$-TRISO) used since 1981.

3.1.1 Fuel and irradiation data

The particle data are given in Table 4 below and the loading data of the fuel elements with mixed oxide TRISO particles in Table 5 below. Several spherical fuel elements of charge AVR 15 (AVR-GO2) used in the AVR were

heated. A fuel element irradiated in an R2-K13 experiment (material test reactor R2 at Studsvik, Sweden) was also examined, which differed from the AVR 15 fuel elements due to a higher heavy metal content, i.e. twice the amount of thorium.

Table 5 also shows the very small proportion of free heavy metal in the fuel element including contamination from particles with manufacturing defects. For manufacture 6×10^{-5} was specified /29/.

Experiment Type of particle	AVR 15 HT 150-160 162-167	R2-K13 EO 1674
kernel composition	$(Th,U)O_2$	$(Th,U)O_2$
kernel diameter (µm)	500 ±2 %	496 ±3 %
kernel density (g/cm^3)	10.08	10.10
Thickness of coating (µm)		
Buffer layer	90 ±11 %	89 ±13 %
inner PyC layer	43 ± 9 %	37 ± 8 %
SiC layer	34 ± 7 %	33 ± 5 %
outer PyC layer	41 ± 9 %	39 ± 8 %
Density of coating (g/cm^3)		
Buffer layer	1.11	1.06
inner PyC layer	1.90	1.90
SiC layer	3.20	3.19
outer PyC layer	1.91	1.90

Table 4: Particle data of mixed oxide TRISO particles

In 1980, the first fuel element with mixed oxide TRISO particles, which had been irradiated in experiment FRJ2-K11 at Jülich was tested at 1600 °C. The particles from the adjacent deconsolidated spheres were also heated /30/.

Experiment		AVR 15	R2-K13
Type of sphere		AVR-G02	R2-K13
Type of graphite		N U K E M	A3-27
Charge			
U 235	(g/FE)	1	1
Th/U 235		5	10
heavy metal	(g/FE)	6	11
U 235 enrichment	(%)	92,5	89,0
Particles in FE		10 000	20 000
Proportion of free heavy metal (Burn-Leach results)			
Particles		$<2 \times 10^{-6}$	$<2 \times 10^{-6}$
Fuel element		4×10^{-5}	1×10^{-5}
Year of manufacture		1978	1979

Table 5: Data of fuel elements with high enriched mixed oxide TRISO particles

The results of these experiments /5/ do not agree with the later accident simulation tests on a total of 22 fuel elements with TRISO coated particles (including UO_2-TRISO). The large release of caesium in the heating test on FRJ2-K11/3 sphere (fuel element 19) is traced back to considerably higher temperatures than the 1600 °C measured by pyrometer.

Possibly because of a dirty furnace window (the furnace later had to be shut down and dismantled because of defects), temperatures of up to 1800 °C were reached.

Table 6 shows the irradiation ddata of the fuel elements with mixed oxide TRISO particles examined in the accident simulation test. The burnup was determined for all fuel elements by measuring the Cs 137 /23/. As no

Fuel element	Burnup (% FIMA)	Fluence [a] $x10^{25}$ m^{-2} E>0,1 MeV	Full [a] power days	Mean [b] irradiation temperature (°C)
R2-K13/1	10,3	8,3	517	1000 - 1200
AVR 69/28	6,8	1,0	510	~700
AVR 70/15	7,1	1,0	510	~700
AVR 70/18	7,1	1,0	510	~700
AVR 70/7	7,3	1,0	520	~700
AVR 70/26	8,2	1,2	590	~700
AVR 69/13	8,6	1,2	610	~700
AVR 74/17	10,3	1,5	730	~700
AVR 74/24	11,2	1,7	780	~700

a) AVR values from interpolation in calculated data

b) AVR temperatures of 700 °C are a rough estimate, max. surface temperatures of 1000 to 1300 °C were measured.

Table 6: Irradiation data of fuel elements tested, using mixed oxide TRISO particles

precise irradiation data are known for the AVR fuel elements in the pebble bed core, fast neutron flux and full power days were interpolated from average values. The irradiation temperature of about 700 °C given for the AVR fuel elements is only a rough estimate. The spherical fuel elements reach max. surface temperatures of 1000 °C to 1300 °C during irradiation in the AVR.

The R2-K13/1 fuel element was subjected to a much higher fast neutron fluence and irradiation temperature than is intended in the planned HTR (see Table 12).

3.1.2 Fission product release profiles at 1600 °C

Two of the 9 fuel elements with mixed oxide TRISO particles tested so far, were examined in the cold finger apparatus. Both spheres were heated to 1600 °C, for 312 hours in AVR 70/26 and 1000 hours in R2-K13/1. The fission product release during the heating phase from 1250 to 1600 °C is shown in Fig. 15 and that during isothermal treatment at 1600 °C in Fig. 16.

When comparing the release curves of the two fuel elements, there is a clear difference, which is traced back to the comparatively high stress in the R2-K13/1 sphere during irradiation.

The Ag 110m release from the R2-K13/1 fuel element, which was 2.2 % during irradiation /22/ is nearly completed during the heating up phase. By contrast, 1.8 % of Ag 110m was released from the AVR fuel element 70/26 during this heating up phase and there was no additional amount during the rest of the test. The release of silver during irradiation in the AVR is not known.

Although the release of Cs 137 from the R2-K13/1 fuel element is very small during heating up (Fig. 15) and at the start of the 1600 °C phase, because the Cs 137 produced by heavy metal contamination was partly (i.e. 1.3×10^{-6}) released during irradiation /22/, it rises during the whole heating period at 1600 °C, to a final value of 1.5 % after 1000 hours (Fig. 16). The inventory loss measurements of the sphere before and after the heating test show satisfactory agreement with a release of Cs 137 of 2.1 %. The profile and amount of release prove that caesium and to a lesser extent, strontium and krypton, are released from the fuel particles. The Sr 90 profile is similar to that of Cs 137, but at a lower level, because strontium is retained better in the fuel kernel and matrix graphite than caesium. In contrast to caesium, krypton is well retained at 1600 °C not only by SiC, but also by pyrolytic carbon layers, which is why the release starts at a very low rate and only increases after a delay period of 175 hours, where it remains two orders of magnitude below the caesium release.

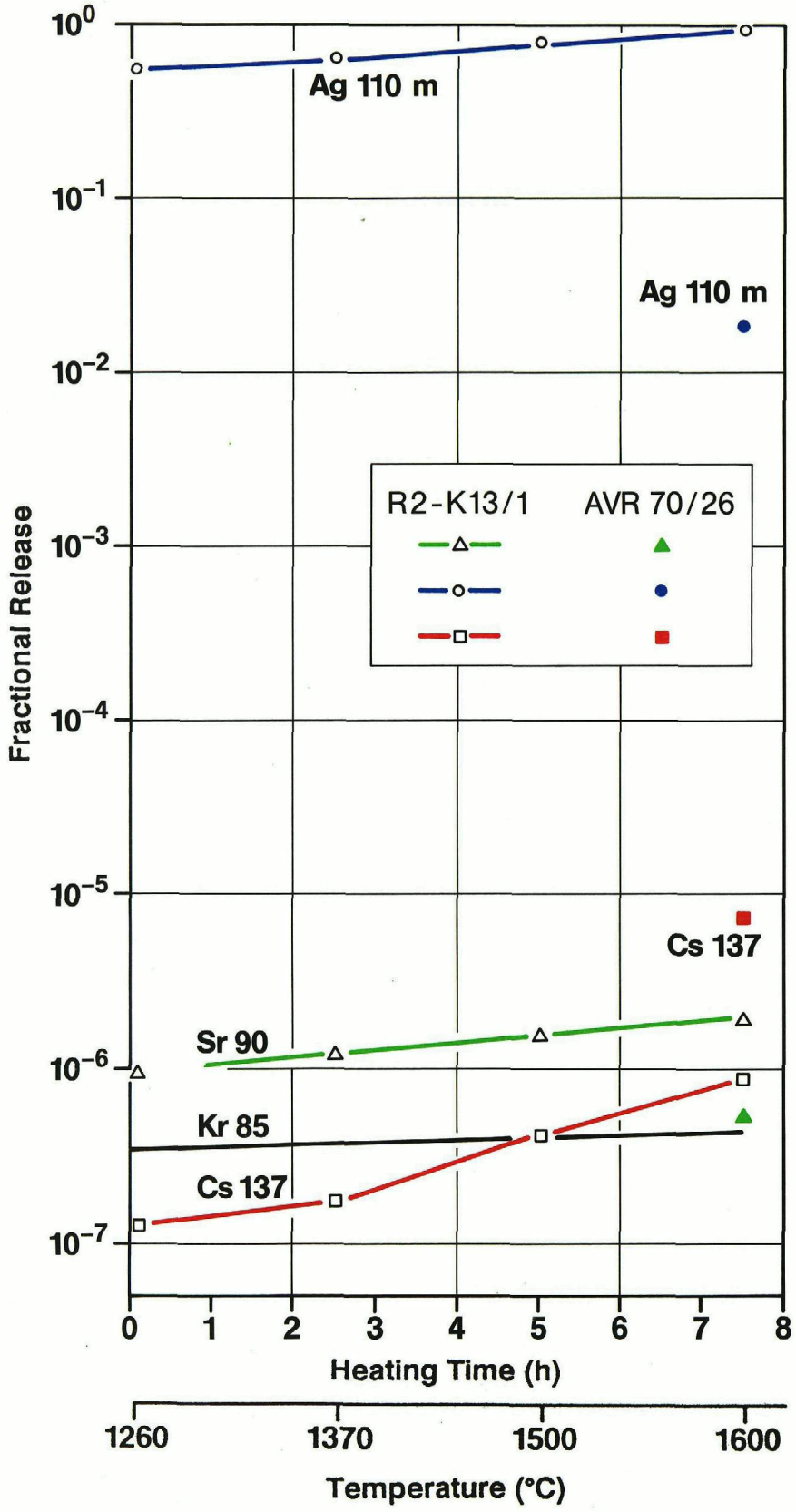

Fig. 15: Fission product release during heating from 1250 to 1600 °C from two fuel elements with TRISO mixed oxide particles

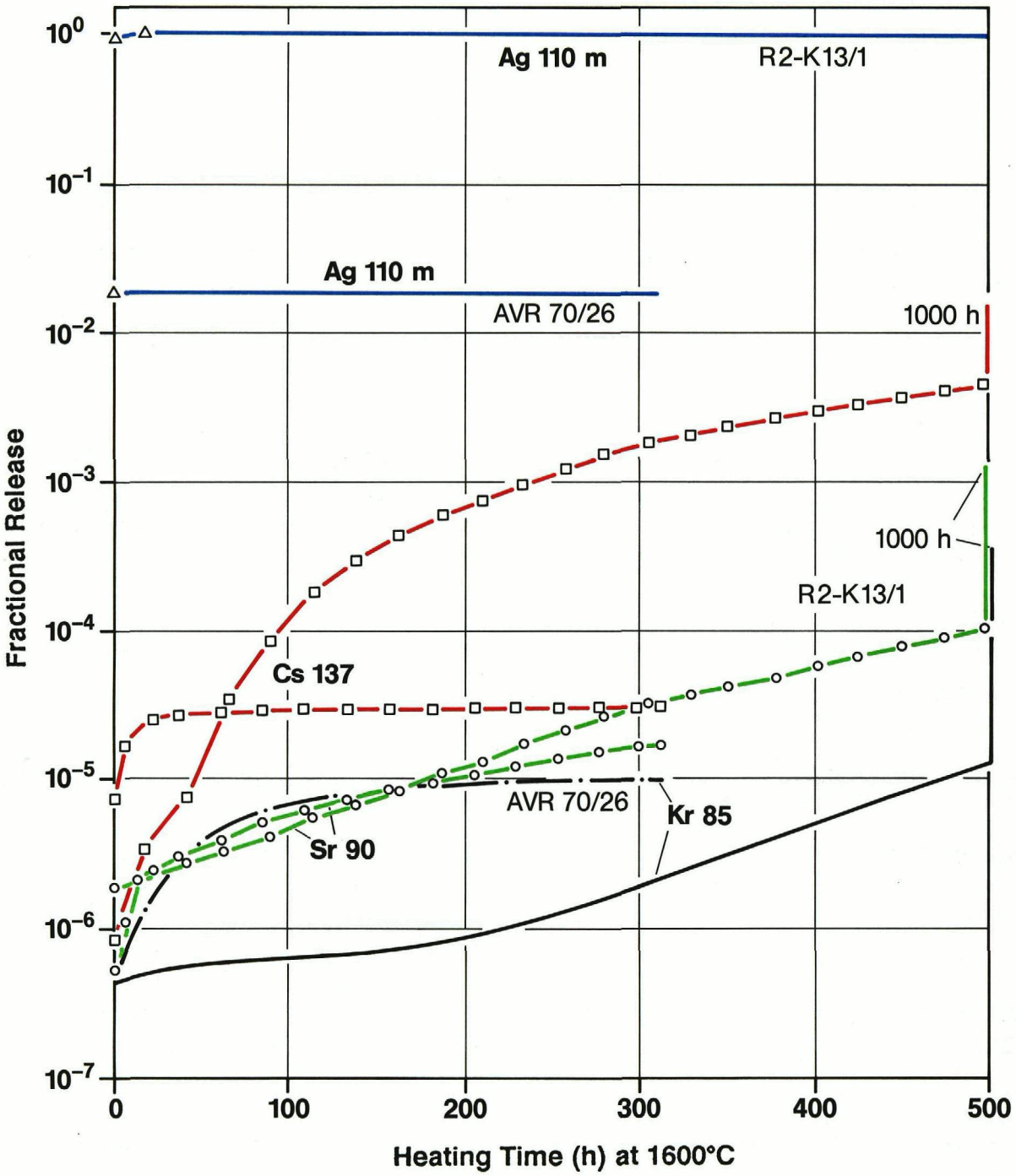

Fig. 16: Fission product release during 1000 h (R2-K13/1) and 312 h (AVR 70/26) at 1600 °C from fuel elements with mixed oxide TRISO particles

By contrast, the release of Cs 137 from sphere 70/26 during heating up and at the start of the 1600 °C treatment is higher than that from the R2-K13/1 fuel element. The reason for the relatively high release of caesium from AVR fuel elements at 1600 °C is contamination in the AVR core. Caesium is released from old fuel element sorts with high burnup used in the AVR reactor with comparatively high heavy metal contamination /24/ and particle defects due to irradiation, and penetrates into the modern fuel elements with TRISO particles. This effect is confirmed by measurements of fission product profiles in the fuel-free zone of AVR fuel elements. The high Cs 137 concentrations in old sorts of fuel elements are measured and low concentrations in fuel elements with $(Th,U)O_2$ and UO_2 TRISO particles, which rise towards the sphere surface are found (see chapter 3.2.7).

After heating the Cs 137 out of the AVR fuel element 70/26 the release rate decreases steadily during the whole period of heating, while for the R2-K13/1 sphere it rises (Fig. 17). This shows that in the heating test on fuel element 70/26, no caesium release took place from the fuel kernels, but only caesium from contamination was released.

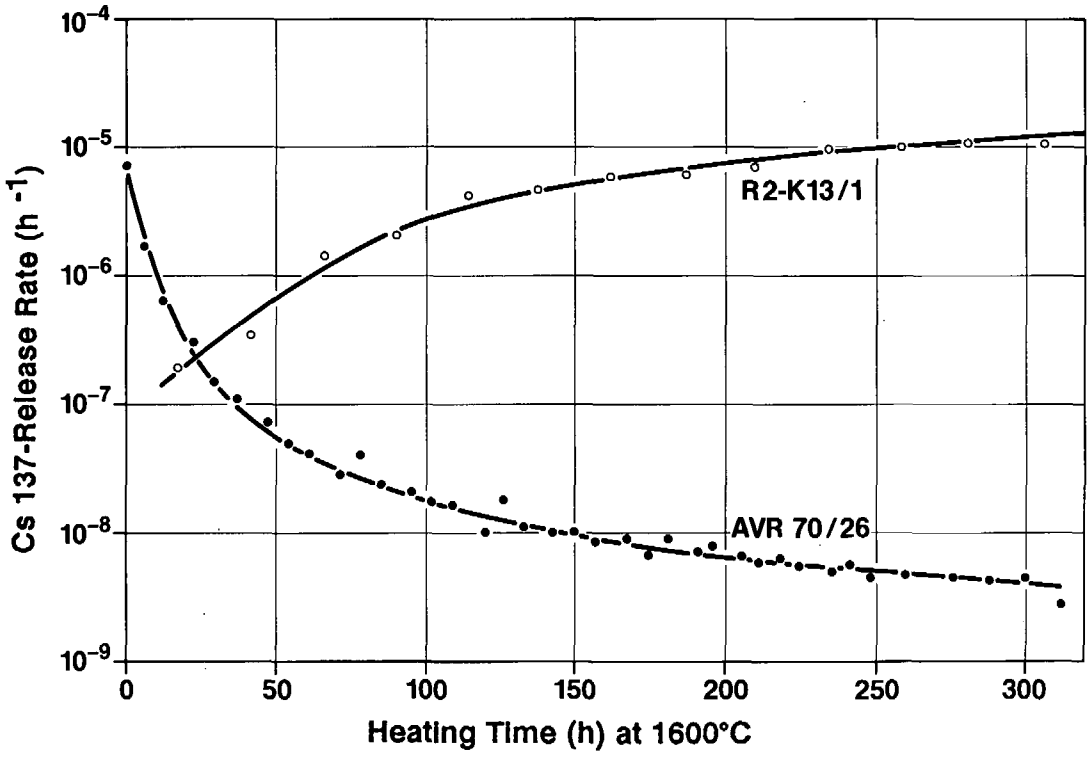

Fig. 17: Relative Cs 137 release rate per hour from two fuel elements with TRISO mixed oxide particles

The Sr 90 release rate from sphere 70/26 is similar, but with a considerable delay as compared to Cs 137. The Kr 85 release rate could not be measured, because at this time the detection limit of the measuring equipment was relatively high (Fig. 16).

Corrosion in the SiC coating is regarded as the cause for the fission product release from the fuel particles in sphere R2-K13/1. At the beginning, this could be grain boundary corrosion by fission products, which leads to increased permeability of the SiC layer. As no fission product release from the fuel particles was measured in the AVR fuel element in the same experimental conditions, it is concluded that the higher irradiation of R2-K13/1 sphere (particularly the fast neutron fluence of 8×10^{25} m^{-2} and irradiation temperatures up to 1200 °C) leads to SiC corrosion already at 1600 °C.

3.1.3 Release of caesium

The release of Cs 137 for fuel elements with TRISO mixed oxide particles is shown in Fig. 18.

Except for the two fuel elements AVR 70/26 and R2-K13/1 heated at 1600 °C in the cold finger apparatus, for which the profile of the low caesium release was measured, the loss of caesium could only be determined by gamma spectrometry measurement of the spherical fuel elements before and after a test. In order to obtain several measured points, three fuel elements were heated several times. The gamma spectrometry detection limit of 2 or 1 % respectively was not exceeded after the heating tests at 1500 °C and 1800 °C. At 2100 °C, when the SiC layer becomes defective after a short time, the caesium release occurs relatively quickly, so that the proportion of 50 % release is reached after 30 hours. The caesium release from the three fuel elements, which were heated to 2150, 2400 and 2500 °C was 22, 82 and 83 % respectively (see chapter 3.1.7).

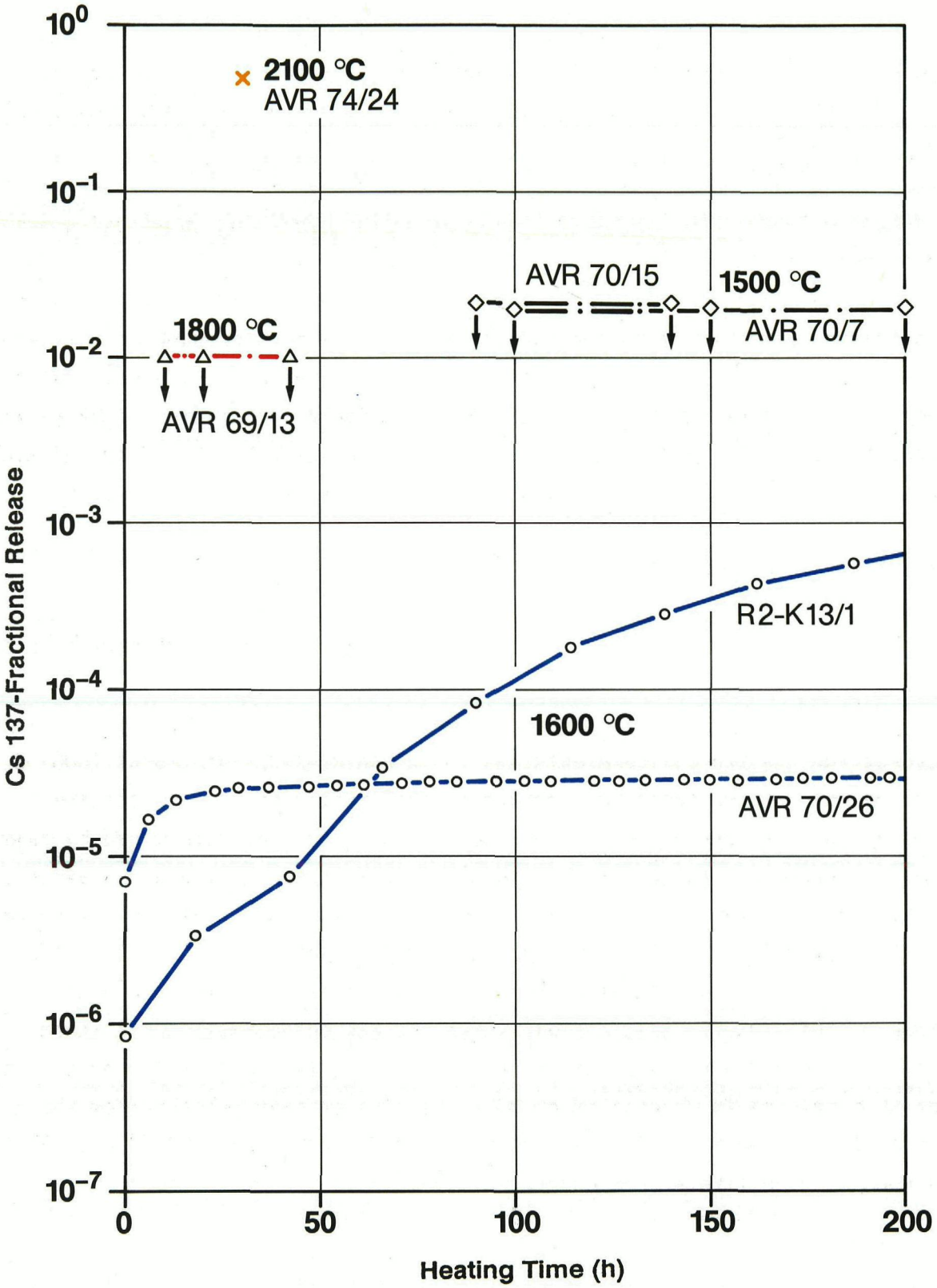

Fig. 18: Cs 137 release from fuel elements with TRISO mixed oxide particles

3.1.4 Release of krypton

The Kr 85 release from fuel elements with TRISO mixed oxide particles with isothermal heat treatment at temperatures between 1500 and 2100 °C is shown in Fig. 19.

The low krypton release at 1500 °C and 1600 °C was partly below the limit of detection (this limit was reduced by improvement of the equipment for the experiment with the R2-K13/1 fuel element and later tests).

Only in fuel element AVR 70/15 one or two particles failed after 48 and after 65 hours respectively, where 49 and 38 % respectively of the particle fission gas inventory were spontaneously released. This means that for three particles with low strength due to manufacture, pressure vessel failure occurred, i.e. a simultaneous defect in the SiC layer and the two surrounding pyrocarbon layers, or there was existing damage on one or two layers and a defect occurred to the remaining coating.

At 1800 °C and in much shorter time at 2100 °C, corrosion in the SiC led to permeability of this layer. Fission gases therefore diffused to a greater extent through the largely intact pyrocarbon layers.

The Kr 85 release during heating up from 1250 °C to a maximum of 2500 °C at about 50 °C per hour is shown plotted against the temperature in Fig. 20. As the mechanisms destroying the SiC are time-dependent, the release at 2100 °C, i.e. at a higher temperature than the isothermal loading, is very small. The release of fission gas rises with the SiC becoming defective, from 2150 °C for the fuel element with 10.3 % burnup (AVR 74/17), but only from higher than 2200 °C for the fuel element with 7.1 % burnup. In addition to fission product corrosion, the SiC is destroyed at these temperatures by decomposition. (See chapter 3.4.2)

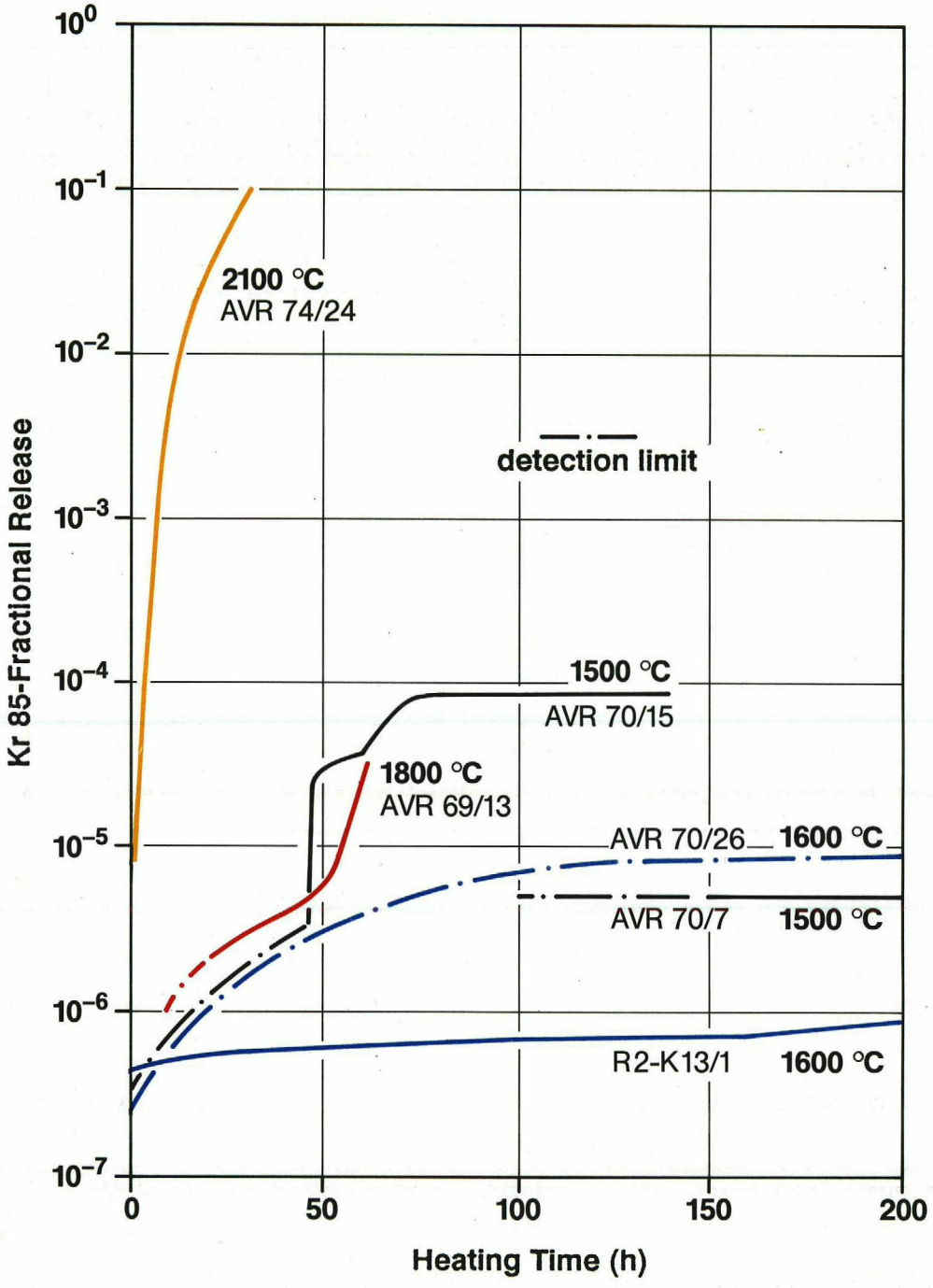

Fig. 19: Kr 85 release from fuel elements with TRISO mixed oxide particles with isothermal treatment

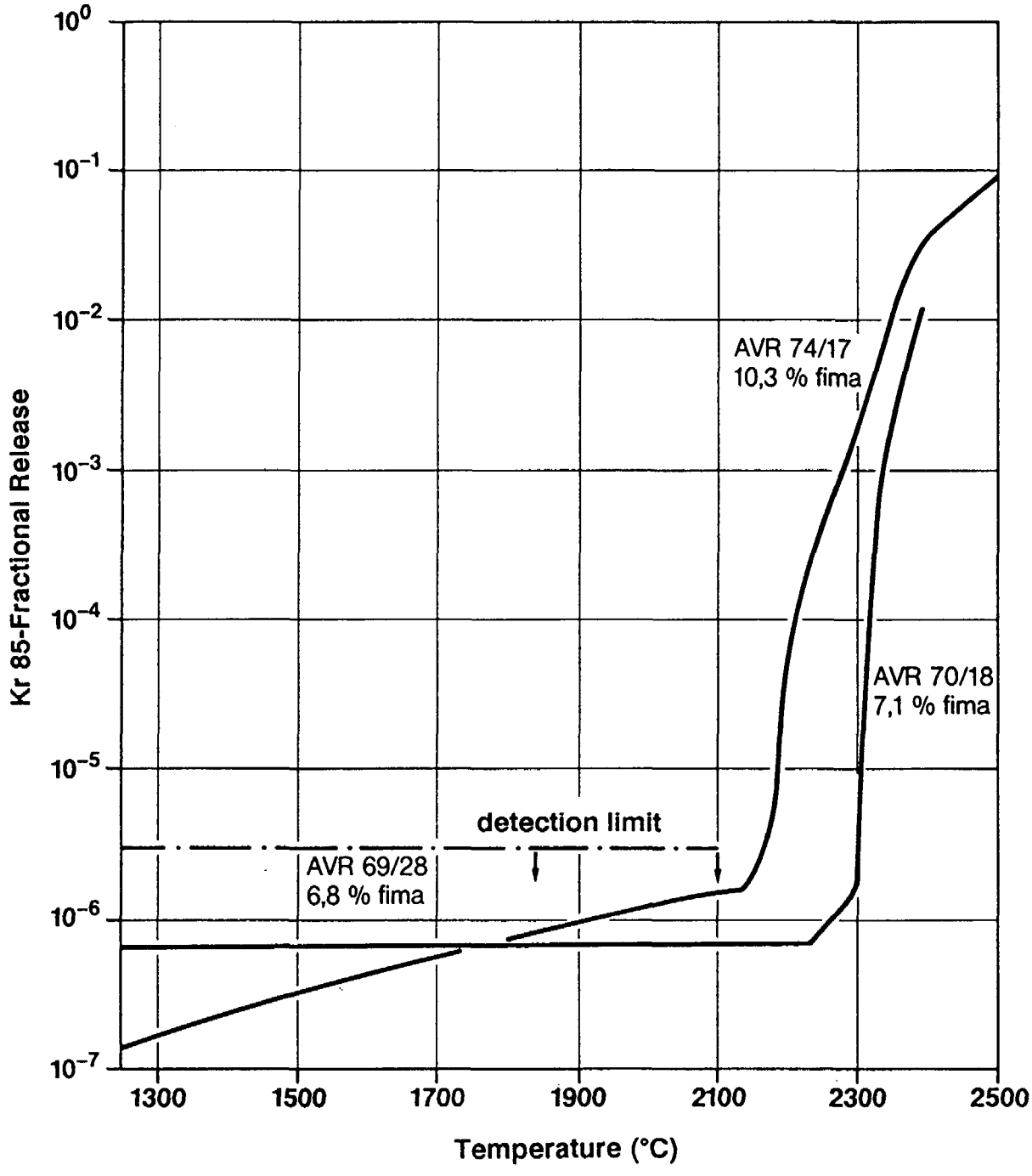

Fig. 20: Kr 85 release during heating up (at 50 °C/hour) from three fuel elements with TRISO mixed oxide particles

The Kr 85 equilibrium releases, determined from simulations of operational temperatures of 1050 and 1250 °C, are shown in Table 7. All equilibrium release rates were less than 2×10^{-11} per sec, related to the inventory.

The limit of detection was considerably lowered by improvement of the equipment, so that relatively accurate measurements were possible for three fuel elements (R2-K13/1, AVR 74/17 and 74/24).

FE	Burnup % FIMA	Heating Time (h) 1050 °C	1250 °C	* R/N-Kr 85 (s^{-1}) 1050 °C	1250 °C	* R/NXe 133 (s^{-1}) at end of irradiation
R2-K13/1	10,3	6	16	<2 E-13	2 E-13	6,1 E-13
69/28	6,8	5	7,5	<2 E-11	<2 E-11	
70/15	7,1	16	8	<2 E-11	<2 E-11	
70/18	7,1	9	8	<2 E-11	<2 E-11	
70/7	7,3	5	9	<2 E-11	<2 E-11	
70/26	8,2	5	17	<2 E-11	<2 E-11	
69/13	8,6	5	8	<2 E-11	<2 E-11	
74/17	10,3	10	18	<3,2 E-12	3,2 E-12	
74/24	11,2	5	7	<2,8 E-12	2,8 E-12	

* relative equilibrium release rate calculated for end of irradiation

Table 7: Results of operating conditions test phase of accident simulation tests on fuel elements with TRISO mixed oxide particles

3.1.5 Fission product distribution in fuel elements

a) Distribution in fuel free zone of two fuel elements containing TRISO mixed oxide particles heated to 1600 °C.

Rotating samples were taken from the fuel free shell of the sphere of fuel elements R2-K13/1 and AVR 69/13 before and after each heating test, these samples were measured by gamma spectrometry to determine the fission product profiles in the matrix graphite (see chapter 2.5.1 above).

The two profiles for Cs 134 and 137 before and after the 1600 °C test on sphere R2-K13/1 are shown in Fig. 21 and the four Cs 137 profiles before and after the three 1800 °C tests on sphere 70/26 are shown in Fig. 22.

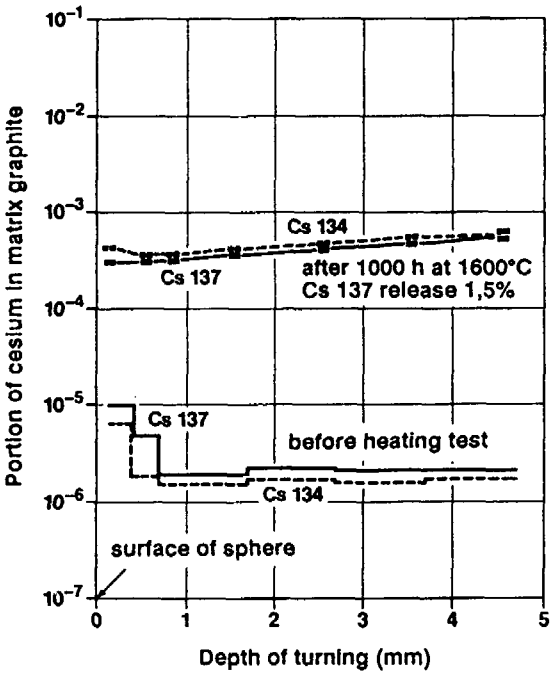

Fig. 21:
Cs 134 and Cs 137 profiles in fuel free zone of fuel element R2-K13/1 (TRISO mixed oxide particles) before and after heating test at 1600 °C

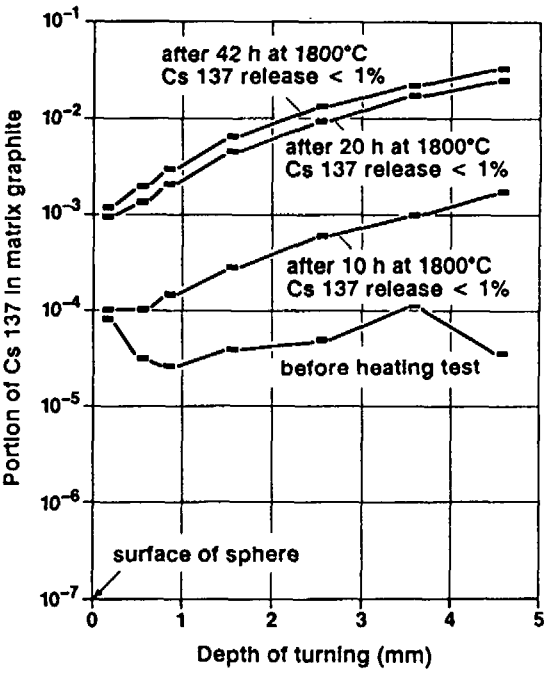

Fig. 22:
Cs 137 profiles in fuel free zone of fuel element AVR 69/13 with TRISO mixed oxide particles before and after 3 heating tests at 1800 °C

Common features of the two graphs are the flat initial profiles before heating and increased diffusion profiles rising towards the fuel zone after the accident simulation test. Comparing the profiles while including the measured caesium release rates, one can see that the level of caesium concentration in the fuel free zone depends not only on the released activity, as in that case the R2-K13/1 profile would be highest, but also on the level of initial concentration and the time behaviour of particle release.

b) Distribution in the fuel zone of a sphere heated to 2150 °C

The AVR 69/28 fuel element heated to 2150 °C was deconsolidated in profile (see chapter 2.5.1 above) and the caesium profiles in the fuel zone were obtained by gamma spectrometry measurements on the graphite samples (see Fig. 23). The flat profiles dropping off slightly towards the outside at a high level of activity are produced by great caesium release from the fuel particles.

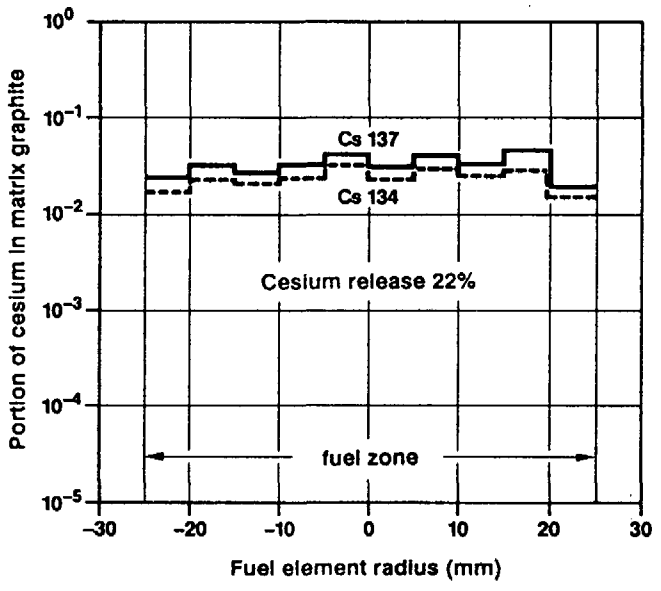

Fig. 23:
Caesium profiles in matrix graphite of the fuel zone of AVR 69/28 fuel element (TRISO mixed oxide particles) after heating test to 2150 °C

To determine the fission product distribution in the kernel and coating, 10 particles were taken from three particle fractions obtained from deconsolidation of sphere 69/28, i.e. an outer fraction, a central fraction and a fraction between these two. The particles were crushed and kernels and pieces of coatings were measured separately by gamma spectrometry. The caesium distribution in the particles and the release from the particles in the matrix graphite and from the fuel element are shown in Table 8.

	Cs 137-distribution %			
	Edge zone	Intermediate zone	Centre	Total
Kernel (K)	11	21	36	24
Coating (C)	60	50	41	51
Particle (K+C)	71	71	77	75
Matrix				3
Release from FE				22

Table 8: Cs 137 distribution of a fuel element with TRISO mixed oxide particles (AVR 69/28) after slow heating to 2150 °C

The ceramographic examination (see next chapter, Fig. 24 middle) of particles from sphere 69/28, and the caesium releases in the matrix graphite and from the fuel element show the start of failure of the SiC. The proportion of caesium varying by a factor of seven, which was found in the 30 particle examinations of the coatings, show that the degree of damage to the particles was very different. For this reason, and because of the small number of particles examined, it is not absolutely clear whether release of caesium from kernels and particles in the edge zone is really higher than from the centre, as the figures in Table 8 appear to indicate.

3.1.6 Ceramography

TRISO mixed oxide particles of three heated fuel elements were examined ceramographically /28/. Polished sections of a particle from every sphere and magnified sections of the SiC layer are shown in Fig. 24.

The effects of the 140 hours of treatment at 1500 °C are clear in the particle (top picture) in formation of coarse grains and gas inclusions in the centre of the $(Th,U)O_2$ kernel and the cracks in the buffer layer. The white SiC layer, which is the main barrier against fission product release, appears to be intact and unchanged.

For particles heated to 2150 °C (centre of picture), the fission gas pores in the kernels increased in size and so did the gap between buffer and pyrocarbon layer. It is, however, of greater importance that in this case the SiC layer also changed. The dark points inside the SiC layer are due to damage. The corrosive attack of fission products on the inner surface of the SiC layer can be seen particularly clearly on the section with the greatest magnification. For the particle heated to 2400 °C (lower picture) the SiC layer is greatly damaged by thermal decomposition (see chapter 3.4.12).
One can see that the SiC layer is getting thinner from the outside and is no longer in existence in places. The tangential section of a SiC layer (bottom right) shows that during the heating test, grains have formed in the SiC, where decomposition has started at the grain boundaries.

3.1.7 Summary of heating experiments

Table 9 shows the accident heating programme and fission product total releases of the fuel elements with TRISO mixed oxide particles examined, except for sphere FRJ2-K11/3 (see chapter 3.1.1 above).

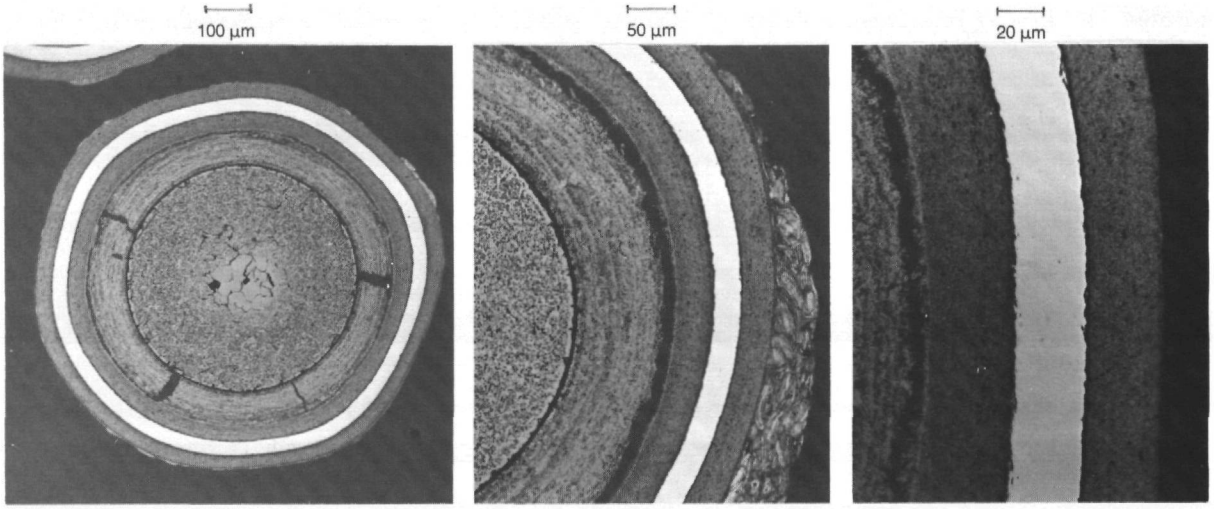

1500° C, 140 h $F_{Cs\ 137} < 2 \times 10^{-2}$ (AVR 70/15, 7,1 % fima)

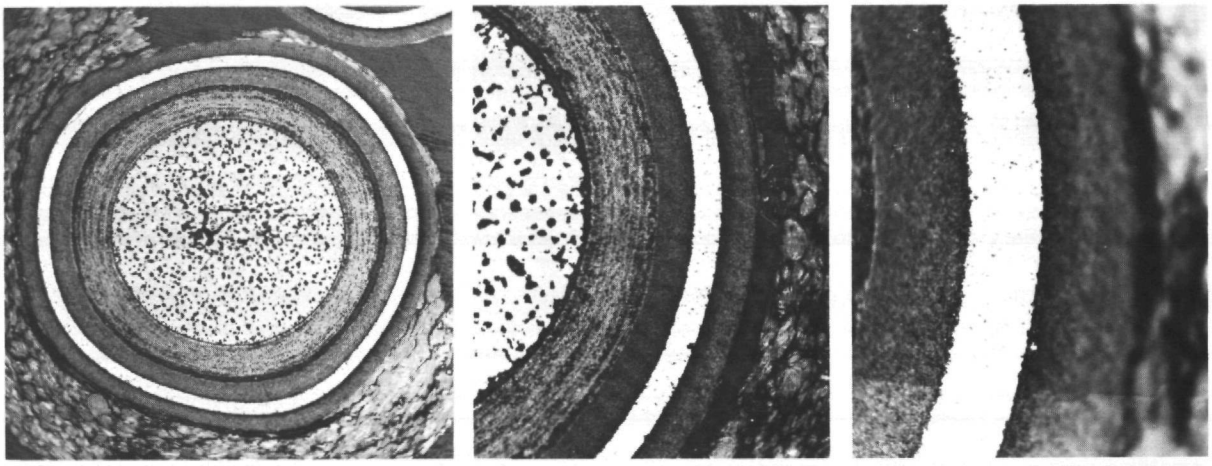

2150°C, 6 h slow heating up $F_{Cs\ 137}$ 2,2 x 10^{-1} (AVR 69/28, 6,8 % fima)

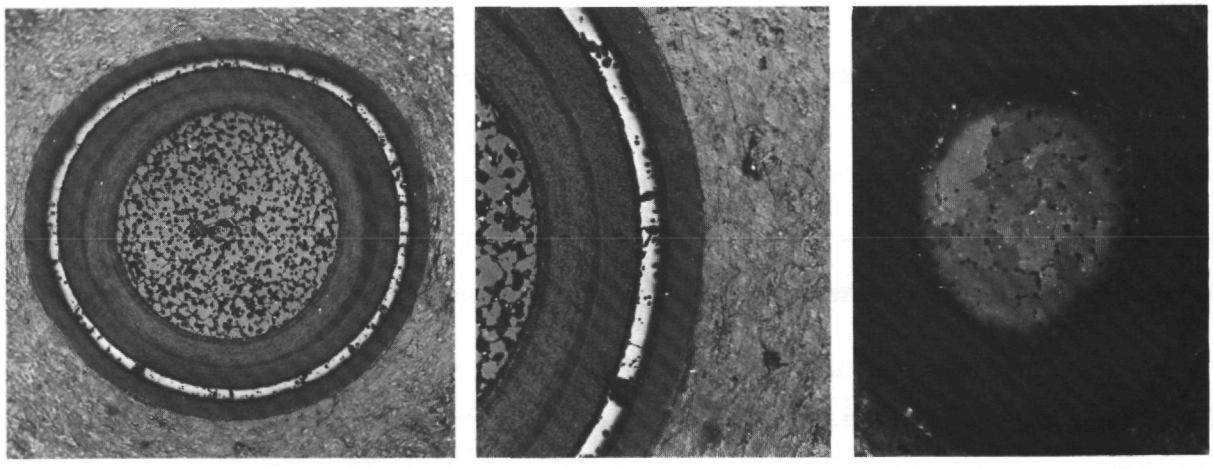

2400° C $F_{Cs\ 137}$ 8,2 x 10^{-1} (AVR 70/18, 7,1 % fima)

Fig. 24: TRISO mixed oxide particles from heated fuel elements

FE	Burnup (% FIMA)	Heating Programme			Release Fraction				
		max. Temp. (°C)	1250...T (hours)	Heating Time T (hours)	Kr 85	Cs 134	Cs 137	Sr 90*	Ag 110m*
70/7	7,3	1500	1,5	100	<7 E-6	<2 E-2	<2 E-2		
		1500	1,5	50	5 E-6	<2 E-2	<2 E-2		
		1500	1,5	50	<3 E-6	<2 E-2	<2 E-2		
				200	<2 E-5	<2 E-2	<2 E-2	-	-
70/15	7,1	1500	7	90	8 E-5	<2 E-2	<2 E-2		
		1500	1,5	50	<3 E-6	<2 E-2	<2 E-2		
				140	8 E-5	<2 E-2	<2 E-2	-	-
70/26	8,2	1600	1,5	312	<1 E-5	**	3 E-5	1,7 E-5	1,9 E-2
R2-K13/1	10,3	1600	7,5	1000	3,5 E-4	1,6 E-2	1,5 E-2	1,2 E-3	1
69/13	8,6	1800	14	10	<1 E-6	<1 E-2	<1 E-2		
			2,5	10	<1 E-6	<1 E-2	<1 E-2		
			3,5	22	3 E-5	<1 E-2	<1 E-2		
				42	3 E-5	<1 E-2	<1 E-2	-	-
74/24	11,2	2100	18	30	1 E-1	5,0 E-1	5,0 E-1	-	-
69/28	6,8	2150	58	6	4 E-5	2,2 E-1	2,2 E-1	-	-
70/18	7,1	2400	28	-	1,2 E-2	**	8,2 E-1	-	-
74/17	10,3	2500	27	-	1,2 E-1	8,3 E-1	8,3 E-1	-	-

* Only measured in 2 experiments with cold finger apparatus

** Not evaluated or inexact measurement

Table 9: Table of accident simulation test results of fuel elements with TRISO mixed oxide particles

3.2 Fuel elements with UO_2 TRISO particles

Fuel elements with UO_2 TRISO particles of low enrichment are intended for use in future HTR's such as the Module HTR or the HTR 500. The investigation of these fuel elements is therefore of great importance.

3.2.1 Fuel and irradiation data

The particle data are given in table 10 and the loading data of the fuel elements with UO_2 TRISO particles in table 11. The fuel elements used in the AVR and in the irradiation experiments HFR-K3 and FRJ2-K13 are nearly the same. Kernel diameter and particle coating are similar to those of TRISO mixed oxide particles. The heavy metal contamination in the fuel elements (Table 11) is again very small.

Experiment Particle batch	AVR 19 HT 232-245	HFR-K3/FRJ2-K13 EUO 2308
Kernel composition	UO_2	UO_2
Kernel diameter (µm)	500 ± 2 %	497 ± 3 %
Kernel density (g/cm^3)	10,80	10,81
Thickness of coating (µm)		
Buffer layer	93 ± 14 %	94 ± 11 %
Inner PyC layer	38 ± 10 %	41 ± 10 %
SiC layer	35 ± 6 %	36 ± 5 %
Outer PyC layer	40 ± 9 %	40 ± 6 %
Density of coating (g/cm^3)		
Buffer layer	1,01	1,00
Inner PyC layer	1,86	no value
SiC layer	3,19	3,20
Outer PyC layer	1,89	1,88

Table 10: Data of UO_2 TRISO particles

Experiment	AVR 19	HFR-K3/FRJ2-K13
Type of sphere	AVR-GLE 3	HFR-K3/FRJ2-K13
Type of graphite	N U K E M A3-27	
Loading		
U 235 (g/FE)	1	1
Heavy metal (g/FE)	10	10
U 235- enrichment (%)	9,82	9,82
Particles in FE	16400	16400
Proportion of heavy metal (Burn-Leach results)		
Particles	no value	$<5 \times 10^{-8}$
Fuel element	5×10^{-5}	$3,5 \times 10^{-5}$
Year of manufacture	1981	1981

Table 11: Data of fuel elements with low enriched UO_2 TRISO particles

Table 12 shows the irradiation data of the fuel elements examined and compares the planned mean final irradiation data for module HTR and HTR 500. The AVR fuel elements available so far only have small or medium values for burnup and remain well below the target values for the module HTR and HTR 500.

Of the four fuel elements used in the irradiation experiments, three with about 8 % reached the final burnup intended for the module HTR and sphere 1 from experiment HFR-K3 nearly reached the HTR 500 final burnup. While the fluence of fast neutrons for the fuel elements placed in research reactor FRJ2 (DIDO) at Jülich is very small, the target values for the module HTR and HTR 500 were exceeded in the material test reactor HFR at Petten (Netherlands). The fuel element temperatures reached in the irradiation experiments are also comparatively very high.

Fuel element	Burnup (% FIMA)	Fluence [a] x 10^{25} m^{-2} E > 0,1 MeV	Full [a] power days	Mean [b] irradiation temperature (°C)
FRJ2-K13/2	8,0	0,1	396	1000 - 1200
FRJ2-K13/4	7,6	0,1	396	1000 - 1200
HFR-K3/1	7,7	3,9	359	1000 - 1200
HFR-K3/3	10,2	6	359	800 - 1000
AVR 70/33	1,6	0,2	210	~700
AVR 71/7	1,8	0,2	240	~700
AVR 70/19	2,2	0,3	290	~700
AVR 74/8	2,9	0,4	390	~700
AVR 73/12	3,1	0,4	410	~700
AVR 71/22	3,5	0,5	470	~700
AVR 74/10	5,5	0,8	740	~700
AVR 74/6	5,6	0,8	750	~700
AVR 74/11	6,2	0,9	830	~700
Modul	9	2,1	1000 [c]	max. 800
HTR 500	10,8	3,3	700 [d]	max. 880

a) AVR values from interpolation of calculated data

b) AVR temperatures of 700 °C are a rough estimate, max. surface temperatures of 1000 to 1300 °C were measured

c) After fuel elements passing through several times

d) Single passage through

Table 12: Irradiation data of examined fuel elements with UO_2 TRISO particles

3.2.2 Fission product release profiles from HFR-K3 fuel elements at 1600 and 1800 °C

The two fuel elements irradiated in experiment HFR-K3 are close to the values aimed at for future HTR's as regards burnup, fast neutron fluence and irradiation temperature. The two heating tests at 1600 and 1800 °C clearly show the excellent retention capacity of the SiC coating for fission products, but also the limitations of this material.

The fission product releases measured on fuel element HFR-K3/1 in the 500 hour 1600 °C experiment are plotted in Fig. 25. The releases, except for Ag 110m, are very low and are due to heavy metal contamination in the fuel element in the first 200 hours. The Cs 137 release increases greatly after more than 200 hours, which is explained by the start of SiC corrosion. The Kr 85 and Sr 90 release rates also increase with time delay and to a lesser extent than for Cs 137. Strontium diffuses more slowly through the kernel material and matrix graphite, while noble gases are retained better by the pyrocarbon than caesium.

When 1600 °C is reached, the Ag 110m release is already more than 1 %, which is traced back to the high irradiation temperature. Ag 110m is the only fission product which can diffuse from intact TRISO particles after a prolonged period at 1200 °C. Ag 110m decays considerably more quickly than Cs 137 and the Ag 110m activity in the fuel element is about two orders of magnitude lower than that of Cs 137. In Fig. 26 the fission product release curves for the first 100 hours of sphere HFR K3/1 are compared with the release profiles for fuel element HFR-K3/3 heated for 25 hours at 1800 °C.

The standardised rise of all the release curves in the 1800 °C test shows that in the initial phase of the 1800 °C treatment, SiC damage has already occurred due to fission product corrosion, which leads to noticeable release of caesium and a great deal of silver after only 25 hours.

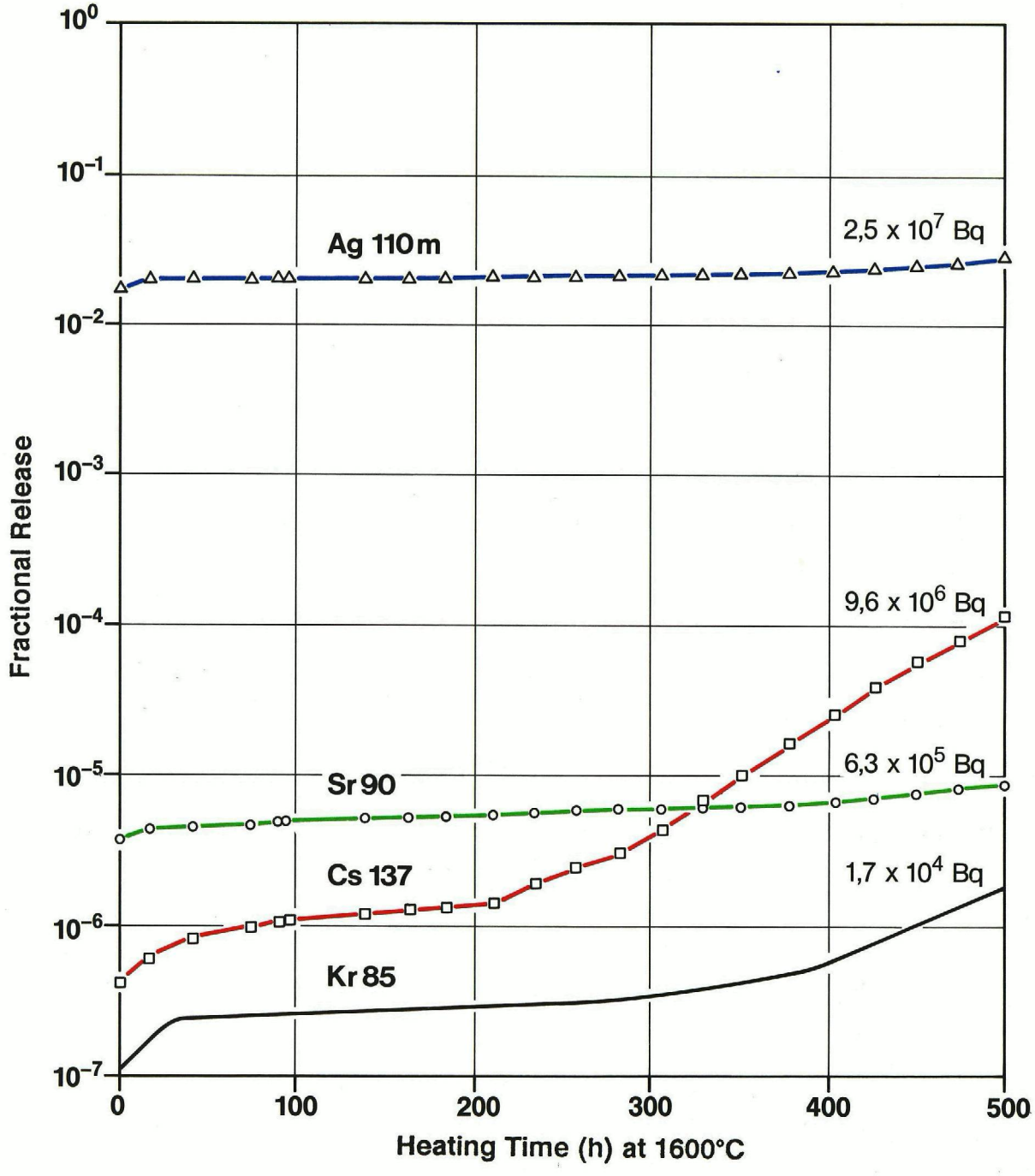

Fig. 25: Fission product release from a fuel element with UO_2 TRISO particles (HFR-K3/1) at 1600 °C

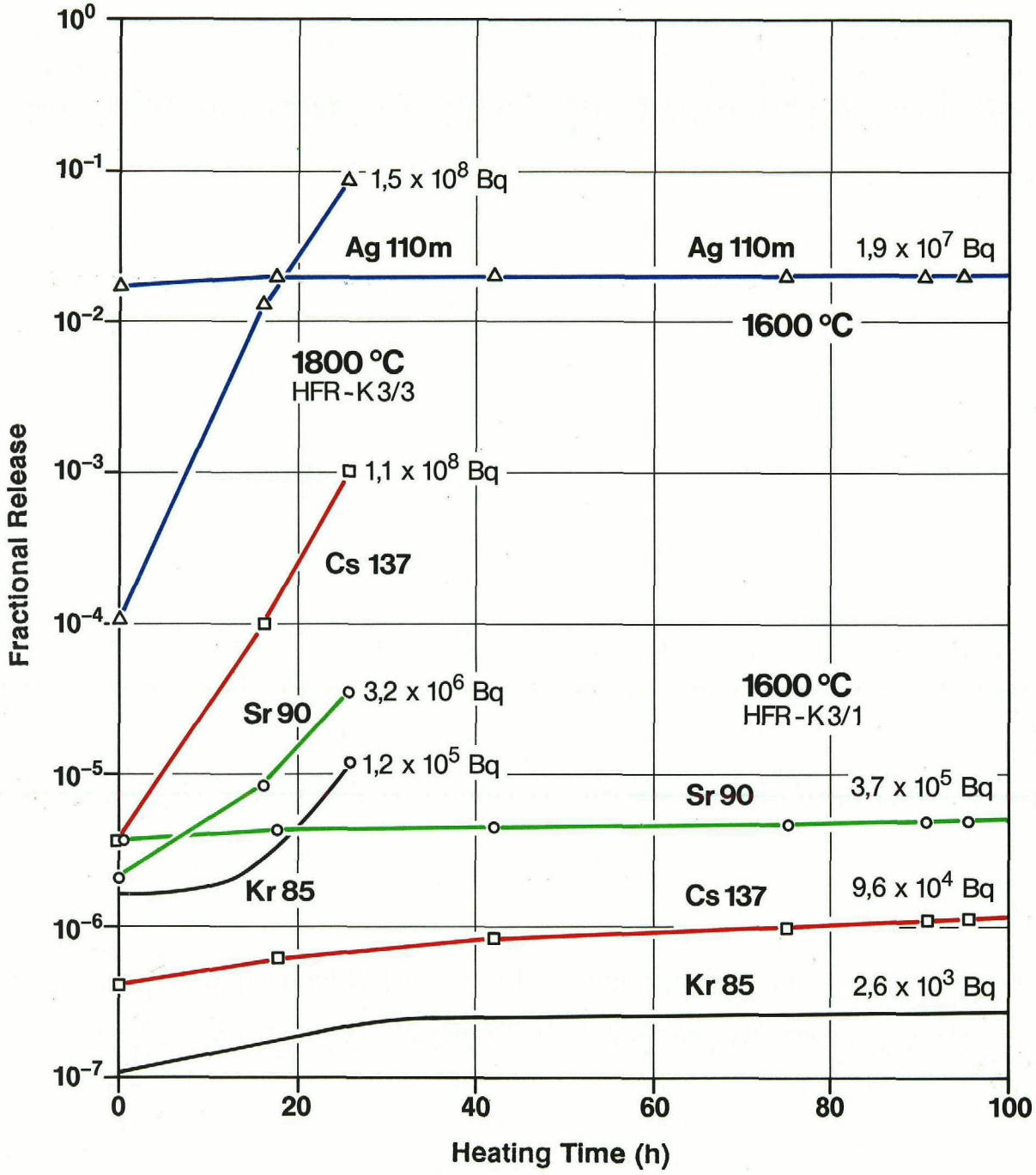

Fig. 26: Fission product release from fuel elements with UO_2 TRISO particles at 1600 °C (HFR-K3/1) and 1800 °C (HFR-K3/3)

When 1800 °C is reached, the release of silver from this fuel element, which was about 200 °C colder during irradiation, is lower by two orders of magnitude than that from sphere 1 when it reaches 1600 °C.
Fig. 27 again shows the results of the two experiments compared. The proportion of release due to contamination was deducted from the total release, so that only the part stemming from the particles is plotted here. The temperature-time dependence of fission product release becomes particularly clear in this graph.

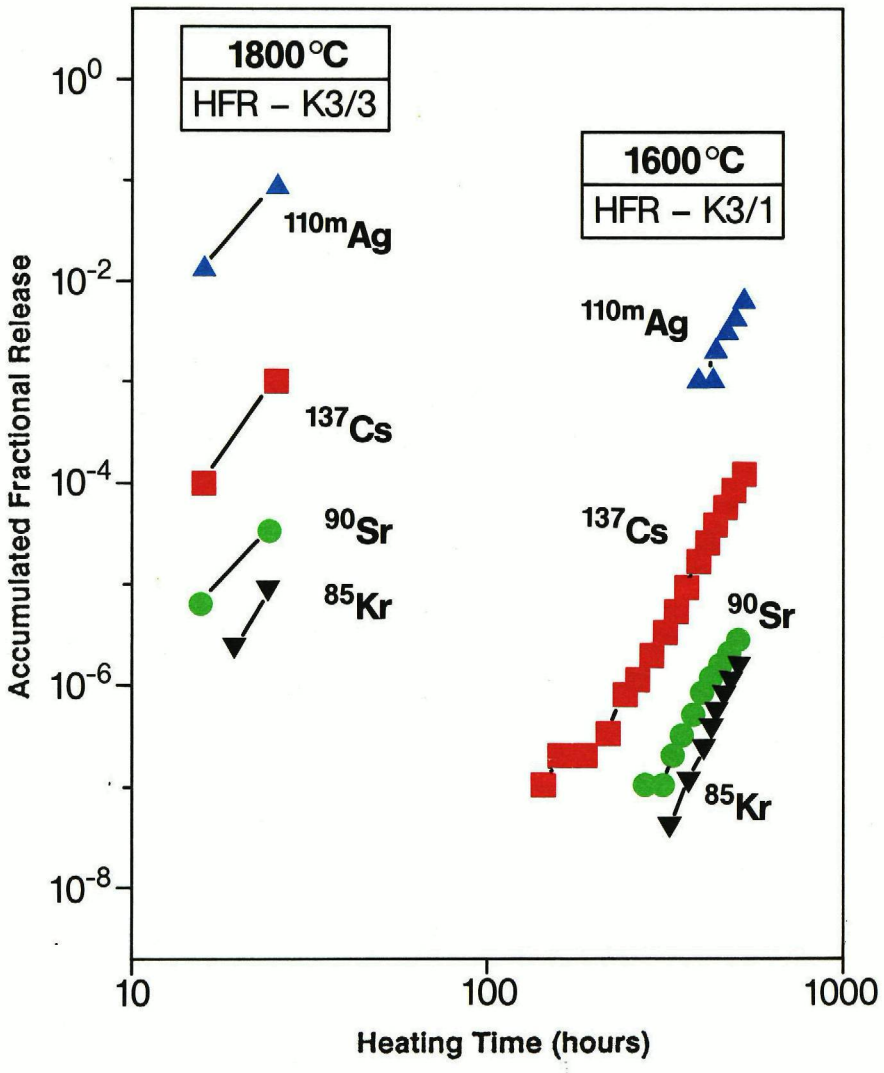

Fig. 27: Fission product release from two fuel elements with UO_2 TRISO particles without the part due to contamination /31/

3.2.3 Release of caesium

The Cs 137 releases from UO_2 TRISO fuel elements measured at constant temperature are plotted in Fig. 28.

In the two 500 hour experiments at 1600 °C, only the release curve of the HFR-K3/1 fuel element with much higher exposure during irradiation shows an increased upward tendency after 200 hours. This shows, as in the two 1600 °C experiments on the fuel elements with TRISO mixed oxide particles (see chapter 3.1.2) that with increased irradiation exposure, SiC defects due to corrosion will occur sooner at 1600 °C. The Cs 137 releases at 1600 °C from fuel elements FRJ2-K13/4 and HFR-K3/1 correspond to those from fuel elements with intact UO_2 TRISO particles. The higher levels of spheres FRJ2-K13/2 and AVR 71/22 are attributed to one defective particle or contamination from the AVR (see chapter 3.1.2 above).

A similar caesium release behaviour depending on irradiation can also be seen at 1800 °C. The releases from the fuel elements occur in the sequence of irradiation exposure, slowest from fuel element AVR 70/33 (1.6 %), very quickly from FRJ2-K13/4 (7.6 %) and fastest of all from sphere HFR-K3/3 (10.3 %).

For two AVR fuel elements with low burnup (AVR 70/19, 2.2 %, AVR 74/8, 2.9 %) which were heated at about 50 °C per hour from 1250 °C to 2400 and 2500 °C, the Cs 137 release was 3 and 25 % respectively.

3.2.4 Release of strontium

In Fig. 29 the measured Sr 90 releases are plotted. The Sr 90 releases remain very low after 500 hours at 1600 °C. At 1700 °C the Sr 90 release rises with the duration of the test.

At 1800 °C, if extensive SiC defects occur due to corrosion, the strontium release increases. The retention in the kernel and matrix graphite prevents fast strontium release from fuel elements with high burnup at 1800 °C.

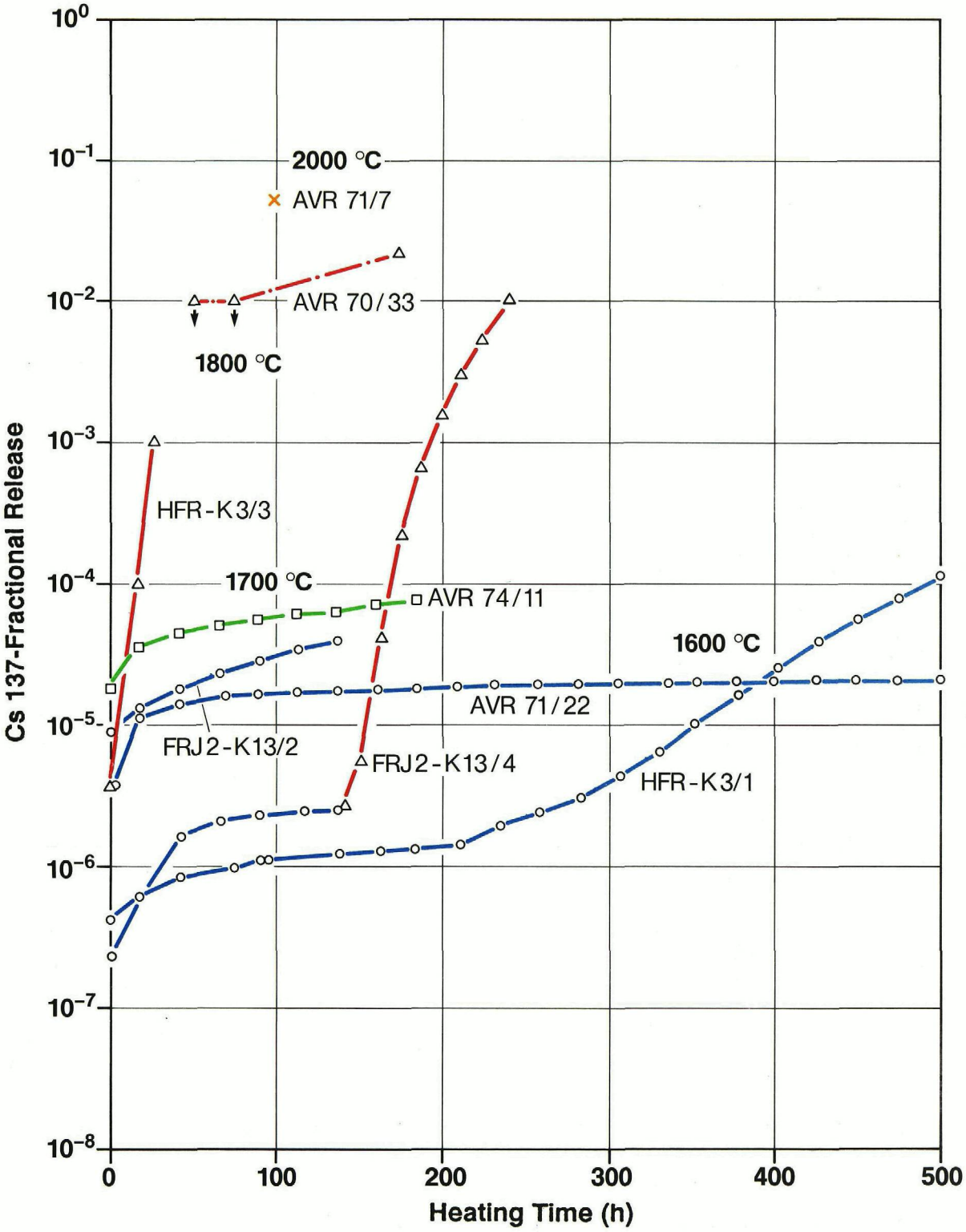

Fig. 28: Cs 137 release from fuel elements with UO_2 TRISO particles

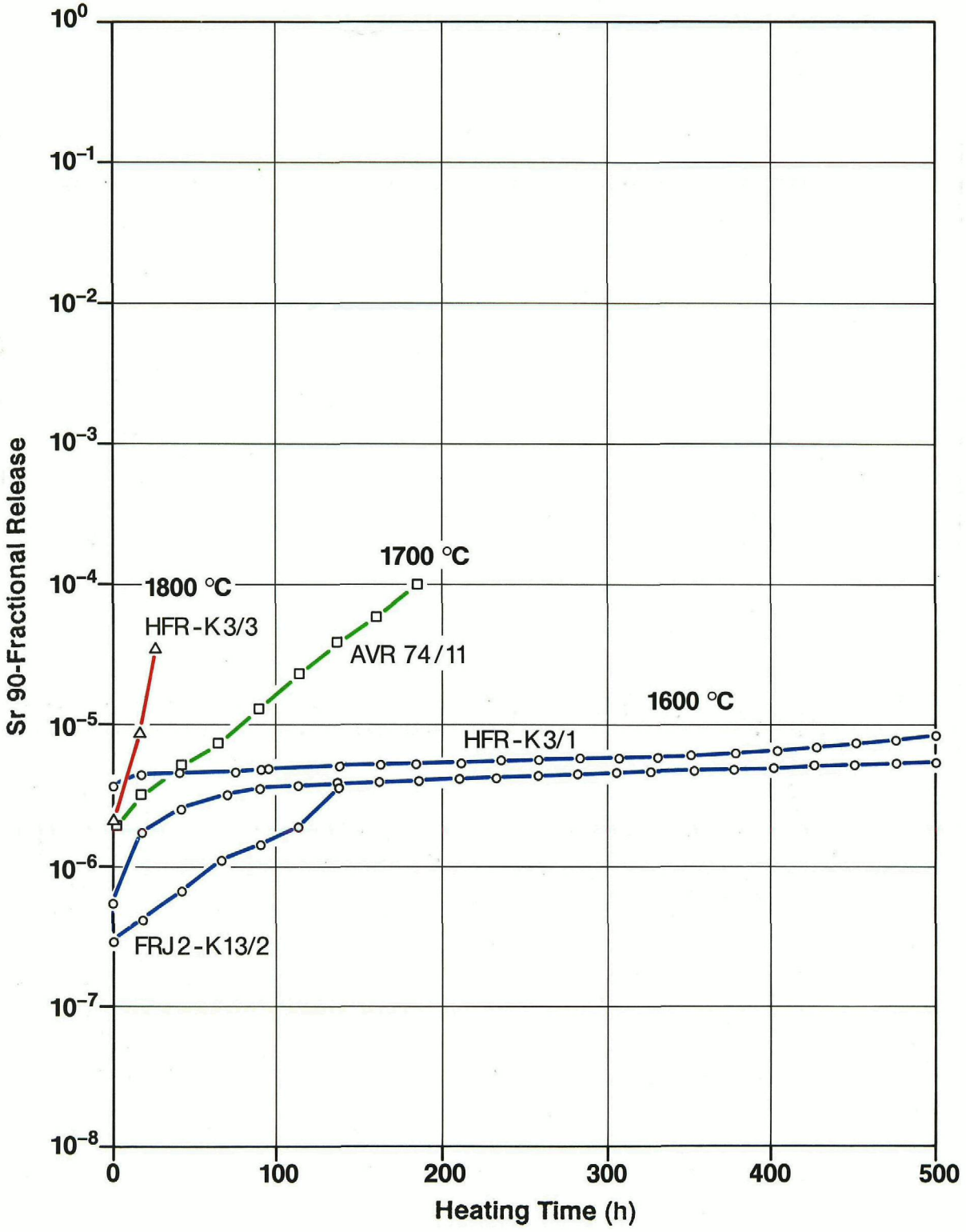

Fig. 29: Sr 90 release from fuel elements with UO_2 TRISO particles

3.2.5 Release of Krypton

The Kr 85 release curves at constant accident temperatures for fuel elements with UO_2 TRISO particles are shown in Fig. 30. The release in 1600 °C tests remains very small.

During the 1700 °C test on AVR fuel element 74/11, one particle failed and during the 1800 °C test on FRJ2-K13 sphere 4, two particles were damaged, where 30 to 46 % of the Kr 85 inventory of the particles was spontaneously released (see Table 13). The rise in Kr 85 release at 32 hours at 1800 °C and on reaching 1800 °C during the second heating test for fuel element AVR 70/33 leads one to conclude that there were total failures on several particle coatings. At these and particularly at higher temperatures, it is difficult, however, to distinguish between increased Kr 85 diffusion through pyrocarbon layers after SiC corrosion and release from particles with failed coatings.

FE	Temp. (°C)	Duration hours	Particle defects		Kr 85 release (%)
			Number	Proportion	
74/11	1700	84	1	6,1 E-5	32
70/33	1800	32...40	32	2,0 E-3	40
	1800	0*	8	4,9 E-4	40
			40	2,5 E-3	
FRJ2-K13/4	1800	8	1	6,1 E-5	46
		94,5	1	6,1 E-5	30
			2	1,2 E-4	

* 2nd heating test on reaching 1800 °C

Table 13: Particle defects with total coating failure in fuel elements with UO_2 TRISO particles at accident temperatures

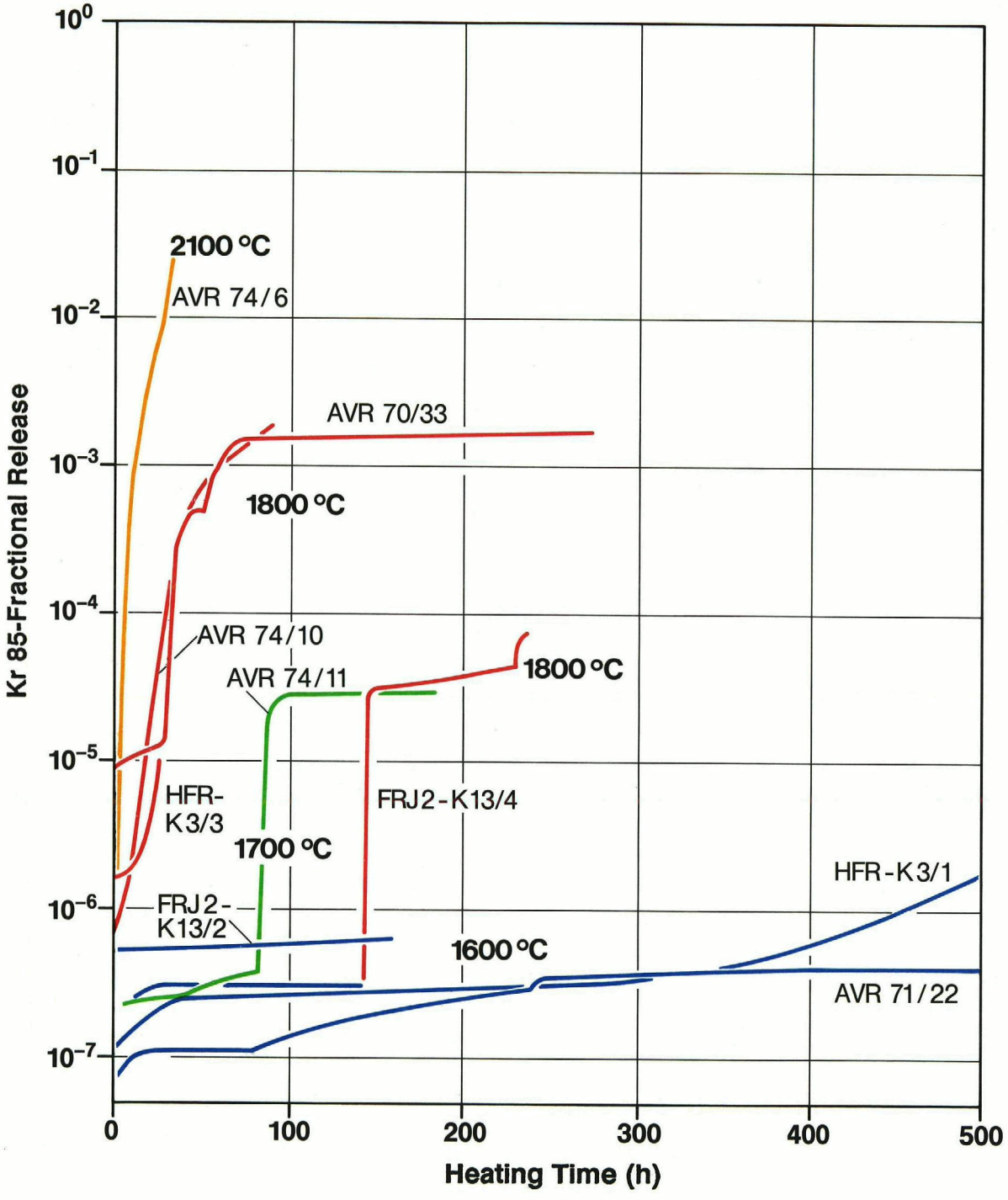

Fig. 30: Kr 85 release from fuel elements with UO_2 TRISO particles

In order not to make Fig. 30 too complicated, the Kr 85 releases from two fuel elements with low burnup and relatively low release are not included (AVR 73/12, 3.1 % and 71/7, 1.8 %, see Table 16, chapter 3.2.9).

Fig. 31 shows the Kr 85 mean values of release for a period relevant for an HTR accident for fuel elements heated at 1600 and 1800 °C. It is clear that, in spite of the particle defects which occurred at 1800 °C, the release is relatively low during this period. Because of the relatively high initial release from fuel elements AVR 70/33 and 74/10 at working temperatures, which may be due to contamination in the AVR core, the release curve for heating from 1250 to 1800 °C starts above that for heating from 1250 to 1600 °C.

The release of Kr 85 in ramp tests, where spherical fuel elements are heated at 50 °C per hour to a maximum of 2500 °C, is shown plotted against temperature in Fig. 32. The release of Kr 85 rises slightly due to SiC corrosion from 2100 °C and then increases from 2200 °C when SiC decomposition contributes to increasing the damage (see chapter 3.4.2 and 3.4.3). The pyrocarbon layers which remained largely intact prevent total release of the fission gas above 2200 °C.

The Kr 85 equilibrium release, which were determined from the operational simulation phase of the experiment at 1050 and 1250 °C are given in Table 14.

The very low release rates are frequently below the limit of detection of the equipment. The highest equilibrium release rates were measured on AVR sphere 70/33. It is possible that for the relatively short heating times of 5 and 8 hours at 1050 and 1250 °C on this fuel element, no equilibrium release was reached and that the release was therefore overestimated (with Kr 85 release superimposed with the burst due to heating up). Superimposition by bursts was measured on fuel elements FRJ2-K13/4 and AVR 74/11. If Kr 85 release due to bursts occur during heating, then durations of heating up to 10 hours are too short to determine equilibrium releases. Dwell times at one temperature of 20 hours or more are sensible.

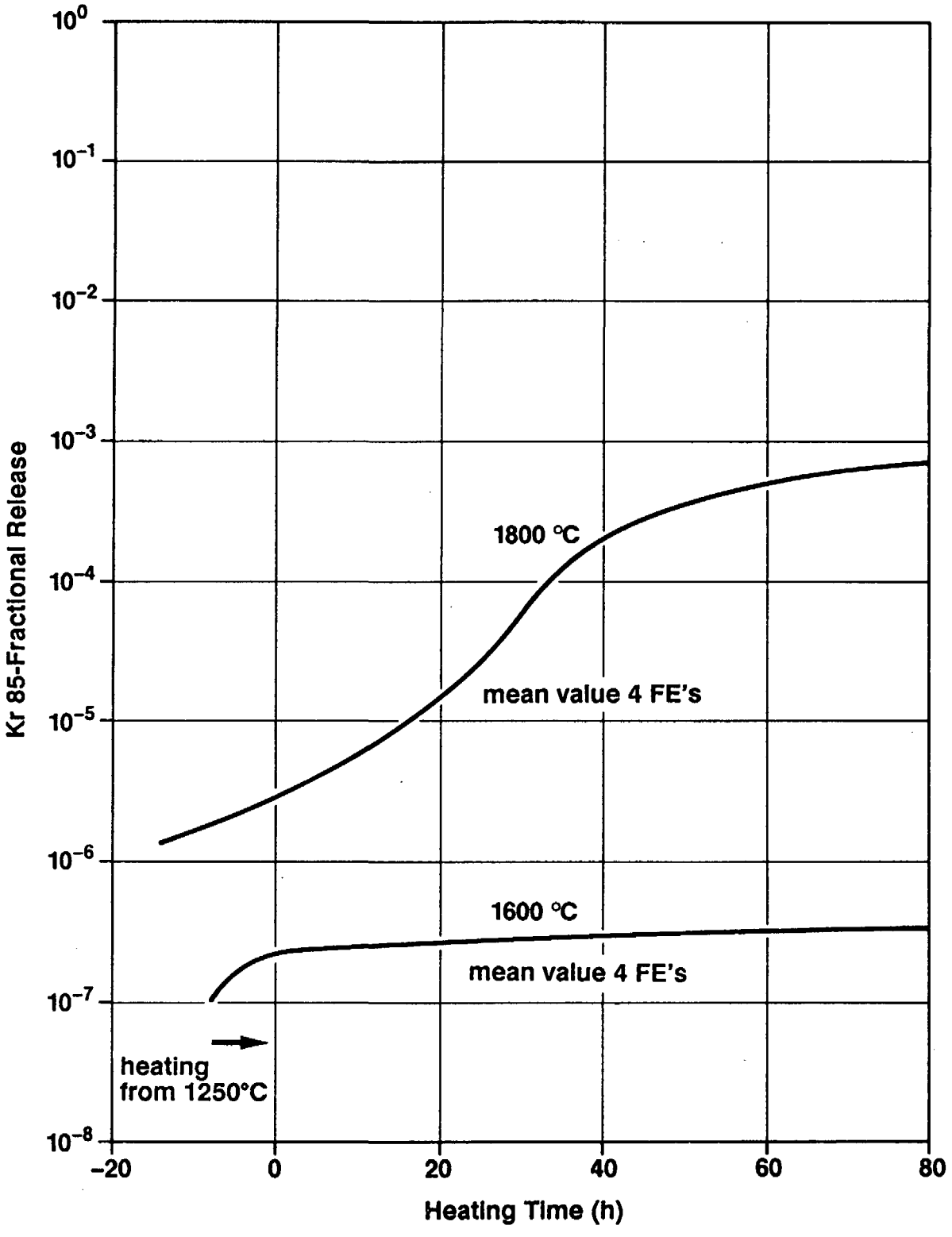

Fig. 31: Mean Kr 85 release during heating and during 80 hours at 1600 and 1800 °C from fuel elements with UO_2 TRISO particles

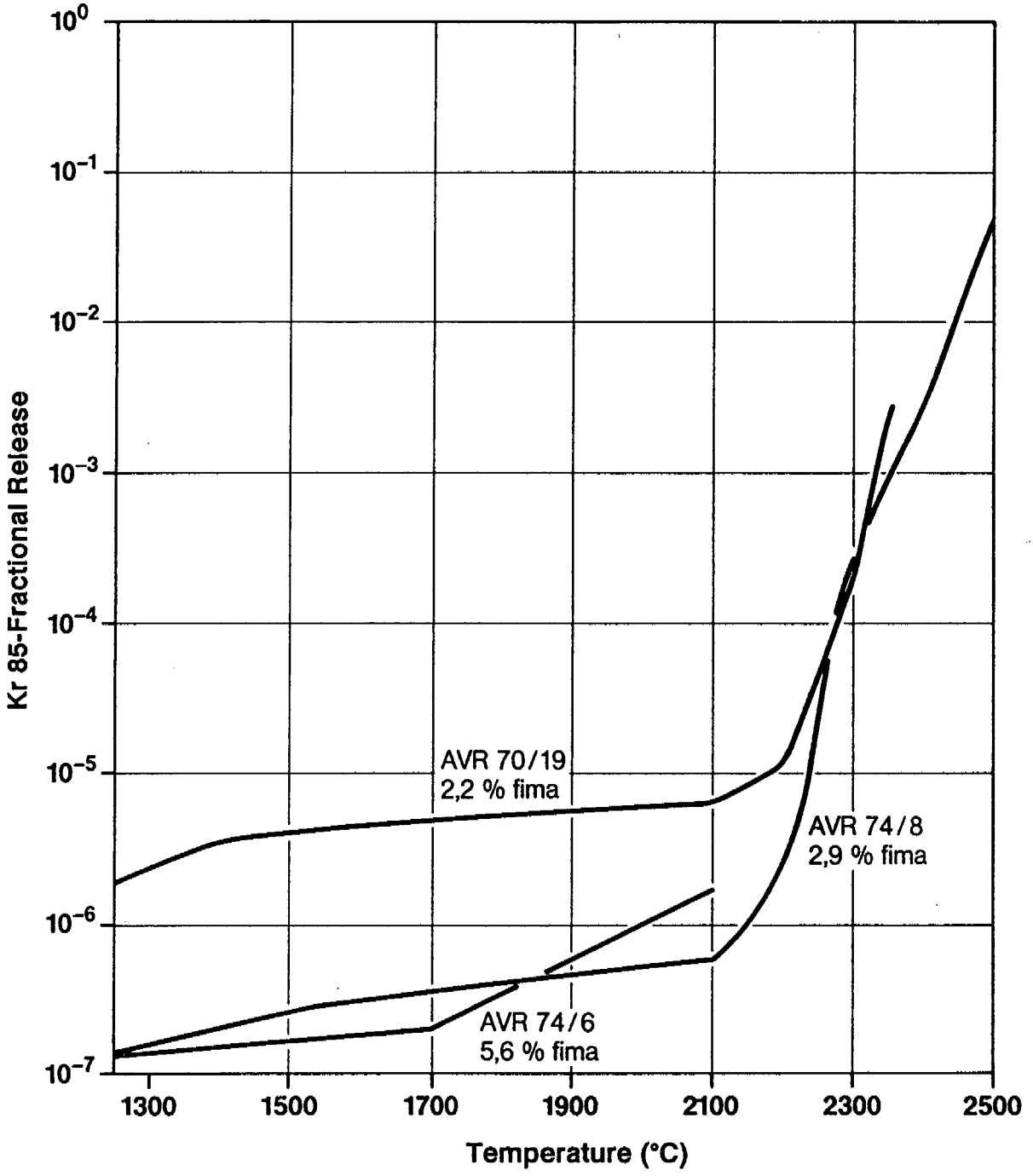

Fig. 32: Kr 85 release during heating (50 °C/hour) from fuel elements with UO_2 TRISO particles

FE	Burnup (% FIMA)	Heating Time (h) 1050 °C	1250 °C	* R/N-Kr 85 (s^{-1}) 1050 °C	1250 °C	* R/N-Xe 133 (s^{-1}) at end of irradiation
FRJ2-K13/2	8,0	23	21	<1,2 E-12	<1,2 E-12	2,8 E-14
FRJ2-K13/4	7,6	7	9	no equilibrium release		
HFR-K3/1	7,7	5	16,5	<6,8 E-13	6,8 E-13	6,1 E-13
HFR-K3/3	10,2	5	13,5	3,5 E-12	8,8 E-12	3,0 E-13
AVR 70/33	1,6	5	8	4,2 E-11	7,0 E-11	
AVR 71/7	1,8	10	7	<2,2 E-11	<2,2 E-12	
AVR 70/19	2,2	8	10	<5,2 E-11	<5,2 E-11	
AVR 74/8	2,9	7	17	<4,0 E-12	<4,0 E-12	
AVR 73/12	3,1	10	8	<4,5 E-12	<4,5 E-12	
AVR 71/22	3,5	15	23	<1,2 E-12	1,2 E-12	
AVR 74/10	5,5	7	9	<2 E-11	<2 E-11	
AVR 74/6	5,6	10	6	<2,4 E-12	<2,4 E-12	
AVR 74/11	6,2	7	8	no equilibrium release		

* relative equilibrium release rate calculated for end of irradiation

Table 14: Results of operational simulation phase of accident simulation tests on fuel elements with UO_2 TRISO particles

Long heating phases mean a greater accuracy of measurement, as the very small rise in the curve has to be evaluated (Fig. 13). Table 14 also gives the R/N values for the irradiation experiments FRJ2-K13 and HFR-K3 to the end of irradiation for comparison.

3.2.6 Release of silver

Silver 110m is the only fission product which diffuses at high irradiation temperatures (1000 to 1200 °C) through intact SiC coatings and from fuel elements. Table 15 compares the fractions released during irradiation with those in an accident simulation test. It is shown that after long irradiation at 1000 to 1200 °C, Ag 110m is released in similar quantities as after a few hundred hours at 1600 °C.

Fuel element	Irradiation			Heating Test		
	Duration (hours)	Temp. (°C)	Ag 110m release	Duration (hours)	Temp. (°C)	Ag 110m release
FRJ2-K13/2	9504	1000...1200	8,7 E-3	138	1600	2,8 E-3
FRJ2-K13/4	9504	1000...1200	1,2 E-2	138	1600	1,0 E-3
				100	1800	1,0
HFR-K3/1	8616	1000...1200	2,2 E-3	500	1600	2,7 E-2
HFR-K3/3	8616	1000	1,6 E-4	25	1800	8,8 E-2

Table 15: Release of Ag 110m from fuel elements with UO_2 TRISO particles during irradiation and in accident simulation test

The Ag 110m releases measured in heating tests are plotted in Fig. 33.

The high release level of sphere HFR-K3/1 is traced back to high irradiation temperatures. The irradiation temperature of the fuel element FRJ2-K13/2 also heated to 1600 °C was also relatively high, while the release of Ag 110m was initially low. After 50 hours at 1600 °C, the release of silver from fuel element FRJ2-K13/2 starts to rise more steeply than that of the AVR fuel element heated to the same temperature. In release of silver, a comparatively great increase in release is found for the AVR 74/11 fuel element heated at 1700 °C compared with 71/22. At 1800 °C, when failures occur in the SiC layers due to corrosion, the silver is released relatively quickly. The Ag 110m release is complete after 70 hours at 1800 °C for sphere FRJ2-K13/4 which was first heated for 138 hours at 1600 °C and then at 1800 °C.

3.2.7 Fission product distribution in fuel-free zone

For the fuel element AVR 70/33 heated three times at 1800 °C, a total of four rotating samples were taken from the fuel-free zones before and after the tests (see chapter 2.5.1). The Cs 137 profiles determined from the gamma spectrometry measurements on the graphite samples are shown in Fig. 34.

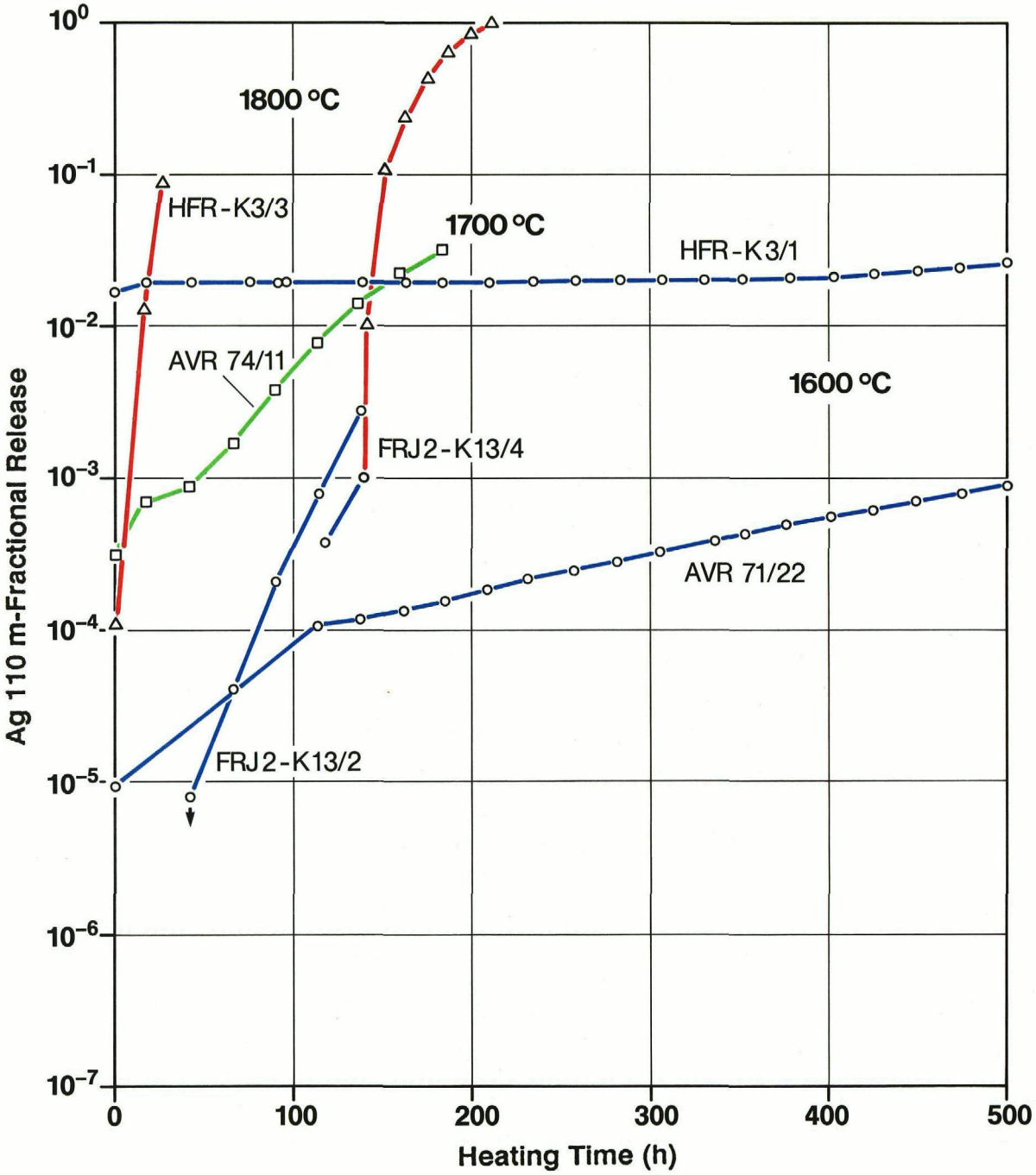

Fig. 33: Ag 110m release from fuel elements with UO_2 TRISO particles

Fuel element	Irradiation			Heating Test		
	Duration (hours)	Temp. (°C)	Ag 110m release	Duration (hours)	Temp. (°C)	Ag 110m release
FRJ2-K13/2	9504	1000...1200	8,7 E-3	138	1600	2,8 E-3
FRJ2-K13/4	9504	1000...1200	1,2 E-2	138	1600	1,0 E-3
				100	1800	1,0
HFR-K3/1	8616	1000...1200	2,2 E-3	500	1600	2,7 E-2
HFR-K3/3	8616	1000	1,6 E-4	25	1800	8,8 E-2

Table 15: Release of Ag 110m from fuel elements with UO_2 TRISO particles during irradiation and in accident simulation test

The Ag 110m releases measured in heating tests are plotted in Fig. 33.

The high release level of sphere HFR-K3/1 is traced back to high irradiation temperatures. The irradiation temperature of the fuel element FRJ2-K13/2 also heated to 1600 °C was also relatively high, while the release of Ag 110m was initially low. After 50 hours at 1600 °C, the release of silver from fuel element FRJ2-K13/2 starts to rise more steeply than that of the AVR fuel element heated to the same temperature. In release of silver, a comparatively great increase in release is found for the AVR 74/11 fuel element heated at 1700 °C compared with 71/22. At 1800 °C, when failures occur in the SiC layers due to corrosion, the silver is released relatively quickly. The Ag 110m release is complete after 70 hours at 1800 °C for sphere FRJ2-K13/4 which was first heated for 138 hours at 1600 °C and then at 1800 °C.

3.2.7 Fission product distribution in fuel-free zone

For the fuel element AVR 70/33 heated three times at 1800 °C, a total of four rotating samples were taken from the fuel-free zones before and after the tests (see chapter 2.5.1). The Cs 137 profiles determined from the gamma spectrometry measurements on the graphite samples are shown in Fig. 34.

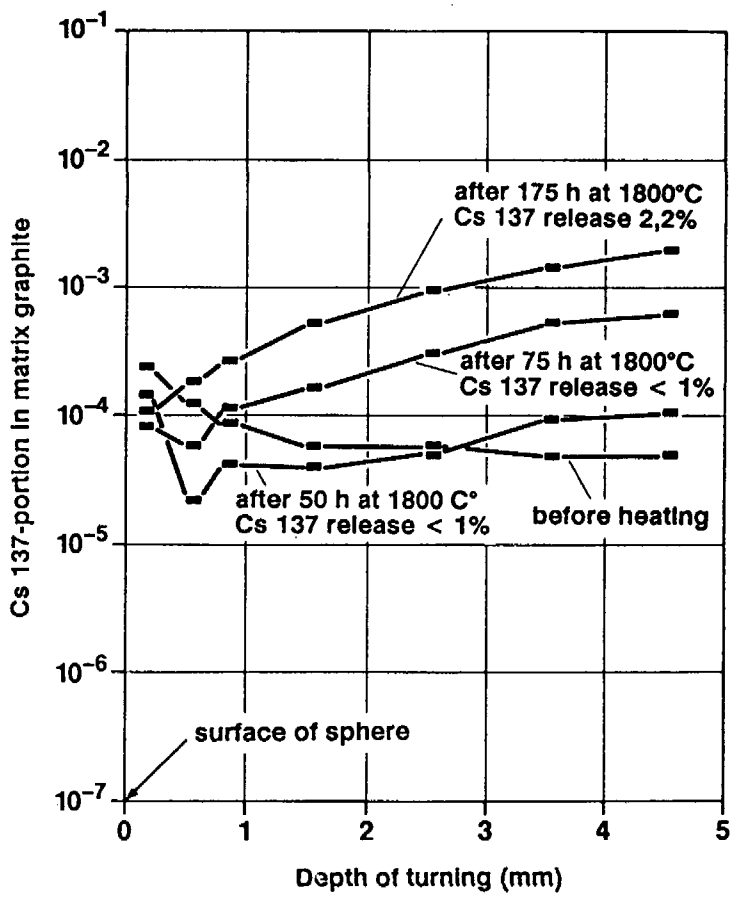

Fig. 34: Cs 137 profiles in fuel-free zone of fuel element AVR 70/33 with UO_2 TRISO particles before and after three heating tests at 1800 °C

Typically for AVR fuel elements with low heavy metal contamination, the Cs 137 concentration in the fuel-free zone increases towards the fuel surface, because caesium diffuses from outside into the sphere, due to cooling gas contamination. Slightly raised and increasing profiles towards the inside after the first heating test for 50 hours at 1800 °C show caesium diffusion from the fuel zone. This trend increased after the next two experiments, with increasing caesium release from the fuel element.

3.2.8 Ceramography

Figs. 35 and 36 show sections of UO_2 TRISO particles from five of the fuel elements examined by ceramography so far.

The investigations on particles from three of the fuel elements heated to 1600 °C (Fig. 35) show:

- the degree of damage to SiC depends on the duration of heating at 1600 °C. After 160 hours, no damage can yet be seen (top picture)
- the degree of damage at 1600 °C depends on the irradiation exposure. For the low exposure fuel element AVR 71/22 (centre picture), the SiC corrosion by fission products starting from the inside is relatively slight. However, the corrosion on fuel element HFR-K3/1 also heated for 500 hours at 1600 °C, which had much higher irradiation exposure, is considerably greater (Table 12). This is also shown in the Cs 137 release profile of both spheres (Fig. 28).
- the degree of damage to SiC in the particles of a fuel element differs. This becomes clear from the SiC sections of three different particles from both the fuel elements heated for 500 hours at 1600 °C (centre and bottom of picture).

For these two fuel elements heated at 1600 °C, the five to ten particles examined coming from the edge area and centre did not have different degrees of damage. However, the SiC corrosion on particles from the centre of sphere 74/11, which were heated at 1700 °C for 185 hours, was greater than for particles from the edge of the fuel zone (Fig. 35 top and centre). The number of particles is, however, too small and the SiC damage in the samples examined is too different to be able to interpret different damage behaviour in these fuel elements.
In one particles from the fuel element heated for 27 hours from 1250 to 2400 °C (Fig. 36, bottom), thermal decomposition, the dominant SiC failure mechanism above 2200 °C, is noticeable at the edge of the SiC layer. The SiC tangential section (bottom right) shows grain formation caused by temperature. The SiC decomposition starts at the grain boundaries, as can be seen on the TRISO mixed oxide particles also heated to 2400 °C (Fig. 24, bottom right).

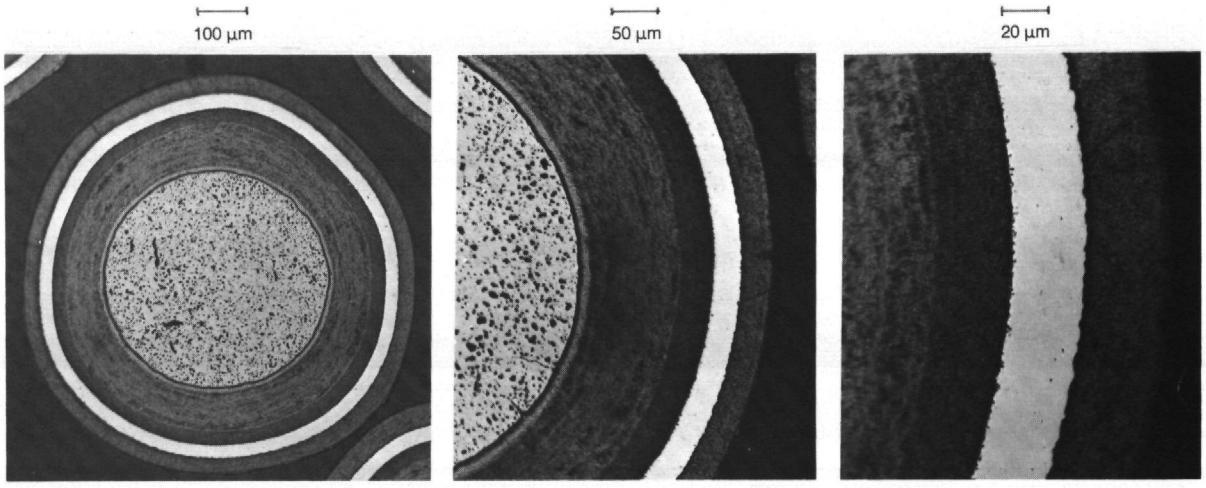

1600° C, 160 h $F_{Cs\ 137}$ 4 x 10^{-5} (FRJ2-K13/2, 8 % fima)

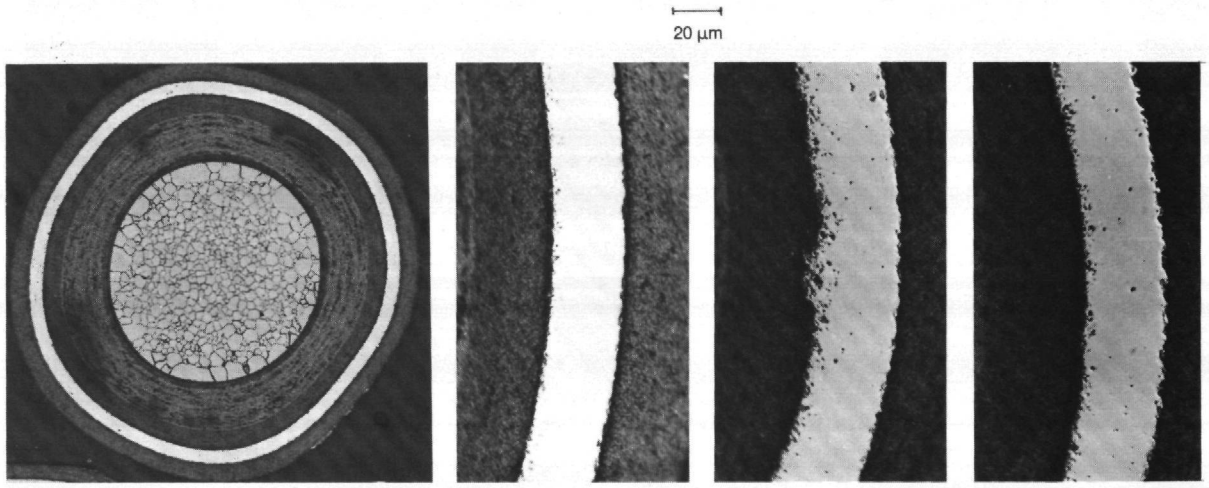

1600° C, 500 h $F_{Cs\ 137}$ 2 x 10^{-5} (AVR 71/22, 3,5 % fima)

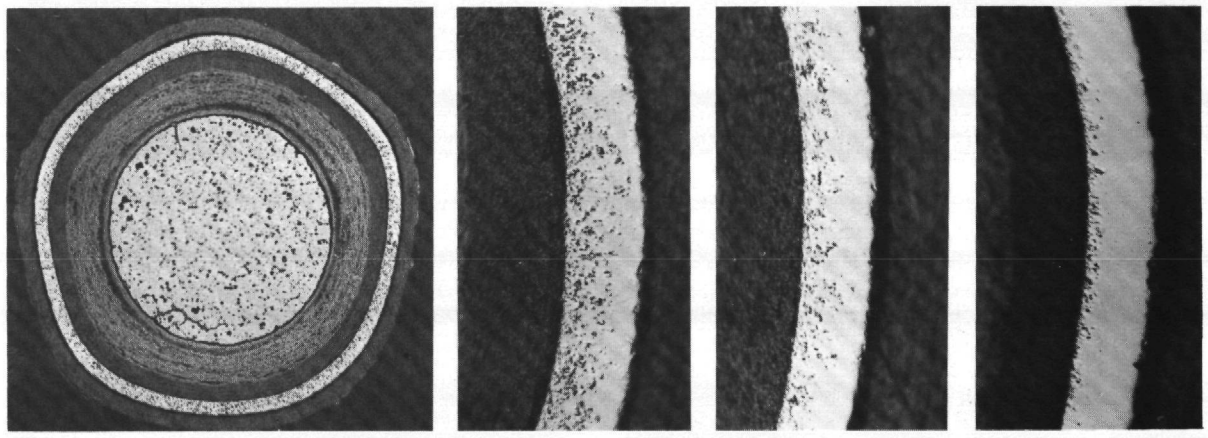

1600° C, 500 h $F_{Cs\ 137}$ 1 x 10^{-4} (HFR-K3/1, 7,7 % fima)

Fig. 35: UO_2 TRISO particles from fuel elements heated at 1600 °C

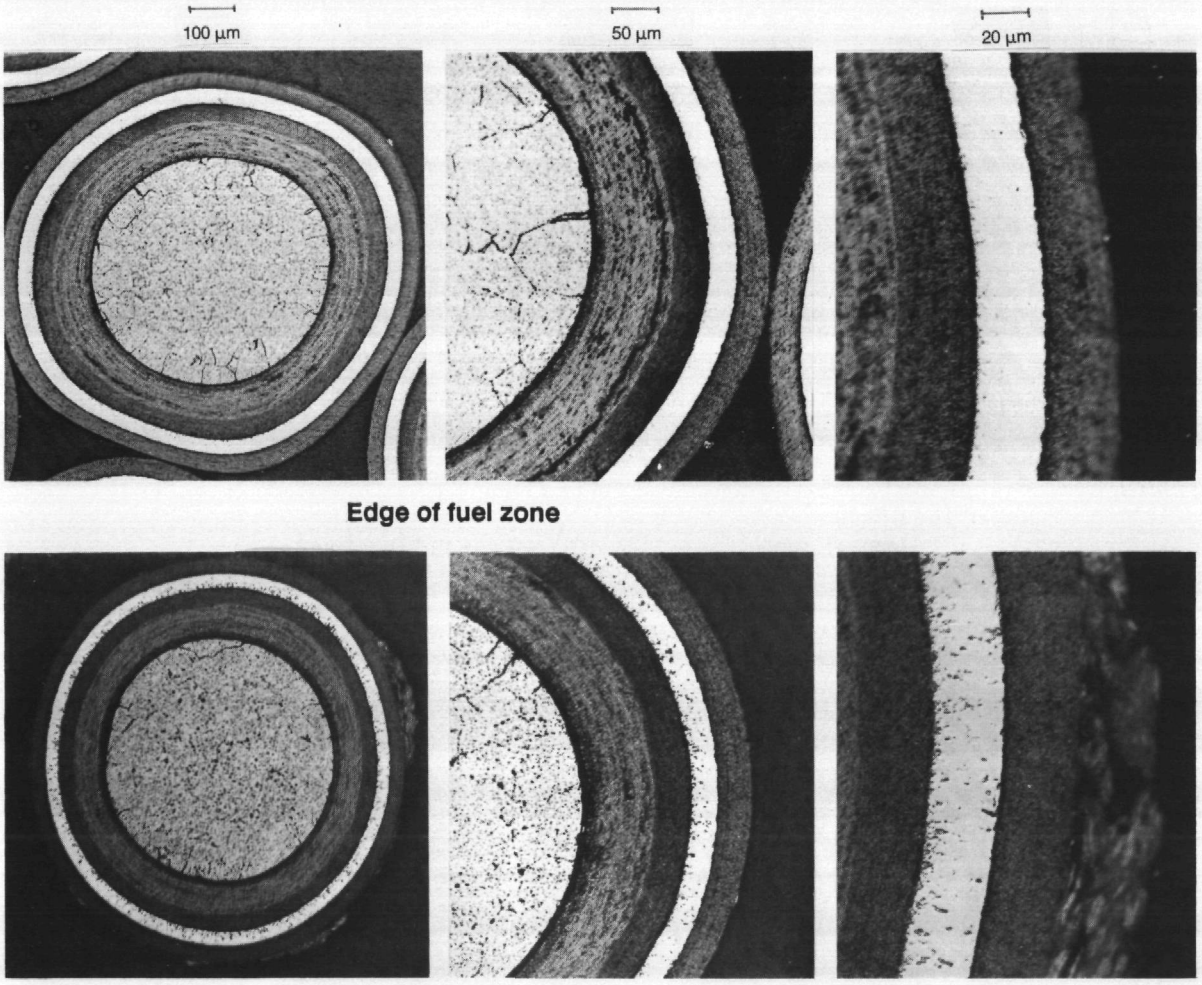

Fig. 36: UO_2 TRISO particles from fuel elements heated at 1700 and 2400 °C

3.2.9 Summary of heating experiments

Table 16 shows the accident heating programme and total fission product release for the fuel elements with UO_2 TRISO particles examined so far.

Fuel element	Burnup (% FIMA)	Heating programme			Fraction released				
		Temp. (°C)	1250...T (h)	Duration at T (h)	Kr 85	Cs 134	Cs 137	Sr 90*	Ag 110m*
FRJ2-K13/2	8,0	1600	7,5	138 (160)	6,4 E-7	1,0 E-4	3,9 E-5	3,8 E-6	2,8 E-3
HFR-K3/1	7,7	1600	9	500	1,8 E-6	1,3 E-4	1,1 E-4	8,3 E-6	2,7 E-2
71/22	3,5	1600	7,5	500	4,0 E-7	6,9 E-5	2,0 E-5	5,3 E-6	9,0 E-4
74/11	6,2	1700	9	184,5	3,0 E-5	8,4 E-5	7,6 E-5	8,3 E-5	3,2 E-2
FRJ2-K13/4	7,6	1600	7,5	138	3,0 E-7	5,7 E-6	2,5 E-6		1,0 E-3
		1800	2	100	7,2 E-5	9,7 E-3	9.9 E-3		1,0
HFR-K3/3	10,2	1800	12	25	1,1 E-5	1,2 E-3	1,0 E-3	3,6 E-5	8,8 E-2
74/10	5,5	1800	14	30	1,3 E-4	<1,0 E-2	<1,0 E-2		
		1800	12	30	8,3 E-4	5,0 E-2	3,7 E-2		
		1800	12	30	8,3 E-4	3,5 E-2	4,2 E-2		
		1800		90	1,8 E-3	8,5 E-2	7,9 E-2		
70/33	1,6	1800	14	50	5,1 E-4	<1,0 E-2	<1,0 E-2		
		1800	3,5	24,5	9,9 E-4	<1,0 E-2	<1,0 E-2		
		1800	3,5	100	2,2 E-4	*	2,2 E-2		
		1800		174,5	1,7 E-3		2,2 E-2		
73/12	3,1	1900	15	50	1,6 E-5	<1,0 E-2	<1,0 E-2		
		1900	15	50	1,2 E-4				
		1900		100	1,4 E-4				
71/7	1,8	2000	18	50	2,5 E-6	*	5,0 E-2		
		2000	18	50	8,3 E-5	*	4,2 E-2		
				100	8,6 E-5		9,2 E-2		
74/6	5,6	2100	18	30	2,4 E-2	5,0 E-1	4,7 E-1		
70/19	2,2	2400	27	-	1,0 E-2	3,1 E-2	3,0 E-2		
74/8	2,9	2500	27	-	4,6 E-2	2,5 E-1	2,5 E-1		

* inaccurate measurement

Table 16: Table of accident simulation test results for fuel elements with UO_2 TRISO particles

3.3 Fuel samples with UO_2 kernels and UO_2 TRISO particles

Samples with UO_2 kernels and UO_2 TRISO particles were heated in order to measure the release profile of I 131 from HTR fuel. These experiments led to important results on the release behaviour of caesium, strontium and silver from defective or failed particles, which improved the methods of interpreting accident simulation tests on spherical fuel elements.

3.3.1 Fuel and irradiation data

In irradiation experiment FRJ2-P28, fission product release from artificially defective UO_2 fuel particles of low enrichment were to be determined at irradiation temperatures of 800 to 1200 °C. In experiment FRJ2-P27, by contrast, information was to be obtained on the fission product retention, above all of Sr 90, Ag 110m, I 131 and Cs 137 in TRISO coated UO_2 particles at irradiation temperatures of 900 to 1300 °C.
The particle data are given in Table 17 and the data on the samples examined in Table 18.

Experiment Type of particle	FRJ2-P28 UOS 331 with buffer layer	FRJ2-P27 EUO 2308
Kernel composition	UO_2	UO_2
Kernel diameter (µm)	497 ± 3 %	497 ± 3 %
Kernel density (g/cm^3)	10,81	10,81
Thickness of coating (µm)		
Buffer layer	94	94 ± 11 %
Inner PyC layer	-	41 ± 10 %
SiC layer	-	36 ± 5 %
Outer PyC layer	-	40 ± 6 %
Density of coating (g/cm^3)		
Buffer layer	1,00	1,00
Inner PyC layer	-	No Value
SiC layer	-	3,20
Outer PyC layer	-	1,88

Table 17: Data of UO_2 fuel kernels and UO_2 TRISO particles examined

Experiment	FRJ2-P28	FRJ2-P27	
Sample	Coupon	Coupon	Compact
Matrix graphite	N U K E M	A3 (compressed hot)	
Loading per sample			
U 235 (mg)	0,30	2,09	148,78
U 238 (mg)	2,76	19,17	1366,29
U 235 enrichment (%)	9,82	9,82	9,82
Particles	5	34	2424

Table 18: Loading data of fuel samples examined

The FRJ2-P28 "defective particles" are fuel kernels which are surrounded only by porous buffer layer. The particles in the two FRJ2-P27 samples are of the same type as those used in irradiation experiments FRJ2-K13 and HFR-K3.
The irradiation data of the fuel samples examined are given in Table 19.

Description of sample	Irradiation experiment			Activation in FRJ1	
	Burnup (% FIMA)	Full power Days	Mean Irr. Temp. °C	Burnup (% FIMA)	Full power Days
FRJ2-P28					
Coupon C1	8,1	251	940	0,6	25
Coupon C6	8,1	251	1020	0,6	25
Coupon C2	8,2	251	940	0,4	25
Coupon C7	-	-	-	0,4	23
Coupon C8	-	-	-	0,4	23
FRJ2-P27					
Coupon 8/2	9,0	232	1220...1320	-	-
Compact 15	7,6	232	1080...1130	-	-

Table 19: Irradiation of fuel samples examinedd

In order to measure the I 131 release on the FRJ2-P28 coupons containing five UO_2 fuel kernels each, the samples irradiated in FRJ2 had to be activated again in the KFA research reactor FRJ1. Two similar unirraddiated coupons were also activated.

As the two FRJ2-P27 samples were heated shortly after the end of irradiation, the relatively short-lived I 131 (half life of 8 days) was still present in sufficient quantities.

3.3.2 Fission product release profile up to 1400 °C

The two coupons with 5 UO_2 kernels each and the two samples with UO_2 TRISO particles were examined up to a maximum of 1400 °C. After a heating phase at the irradiation temperature, the temperature was raised to 1400 °C in 30 hours, and after 10 hours at 1400 °C, it was lowered in another 30 hours to the irradiation temperature. Only the compact 15 sample was kept at 1400 °C for 24 hours, and cooled in one hour.

The heating programme and release results of coupon C1 are shown in Fig. 37. While the I 131 and Xe 133 activities are similarly high and several percent are released at the end of the test, the release of Ag 110m is clearly higher and that of Cs 137 is lower.

In the heating test on the FRJ2-P27 coupon 8/2 with 34 UO_2 TRISO particles, one of which was defective, the release behaviour from this defective particle is similar to that of the coupons with UO_2 kernels (Fig. 38).

Only Ag 110m is released to a significant extent from Compact 15 with intact UO_2 TRISO particles irradiated at relatively high temperatures, while the amounts of Cs 137, I 131 and Xe 133 released from contamination are very low.

One of the aims of these experiments was to clear up the question whether iodine and noble gas releases from HTR fuel samples are similar, as generally assumed. The I 131 and Xe 133 releases from UO_2 kernels and from intact UO_2 TRISO particles plotted in Fig. 39 show that in the temperature range examined, there was agreement between the measured release profiles. This makes it clear that the release during heating does not rise at the same rate as the temperature, but has a delayed relatively steep rise (burst), which changes to a much lower release.

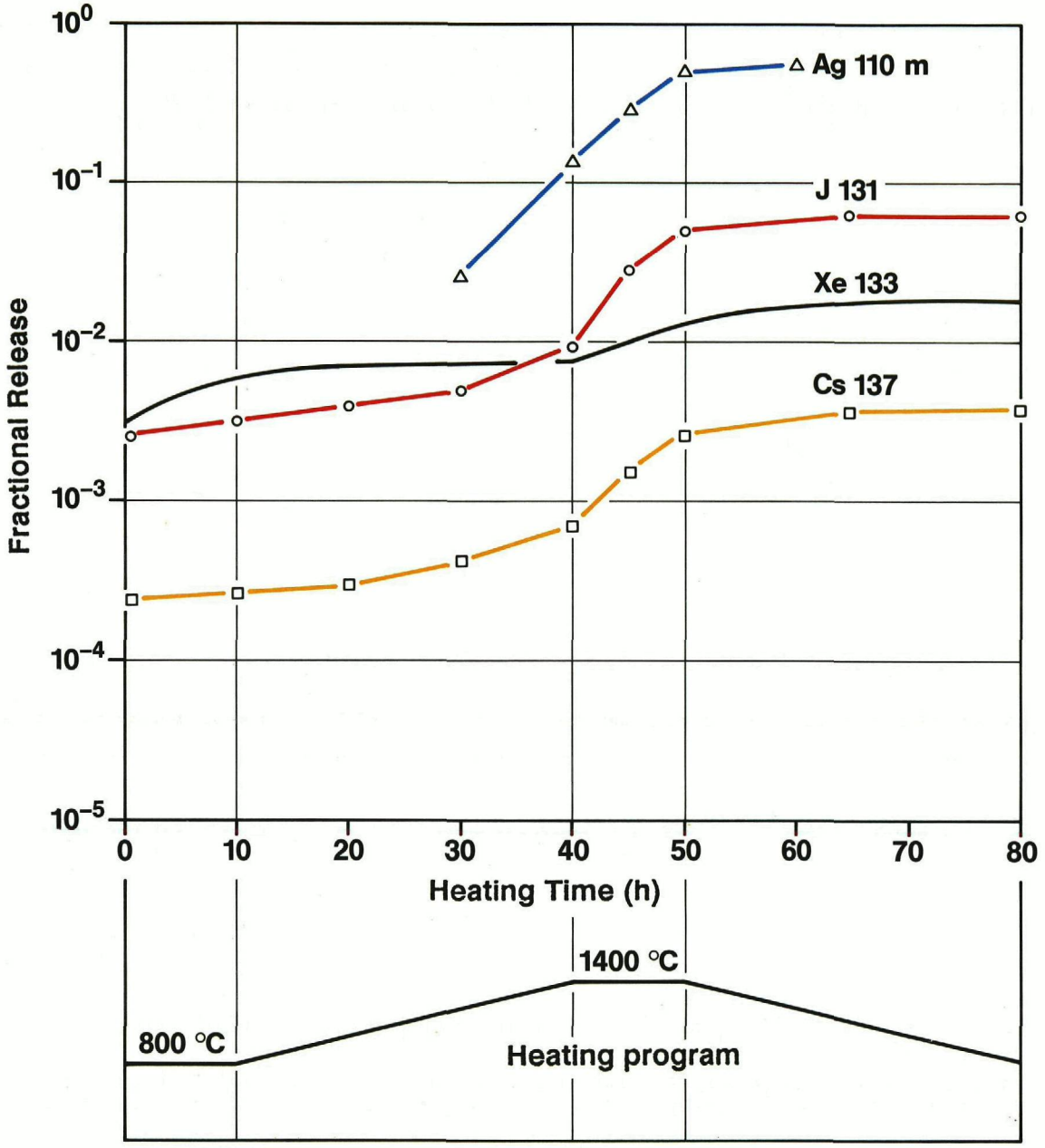

Fig. 37: Fission product release from UO_2 kernels (FRJ2-P28/C1) during heating test up to 1400 °C

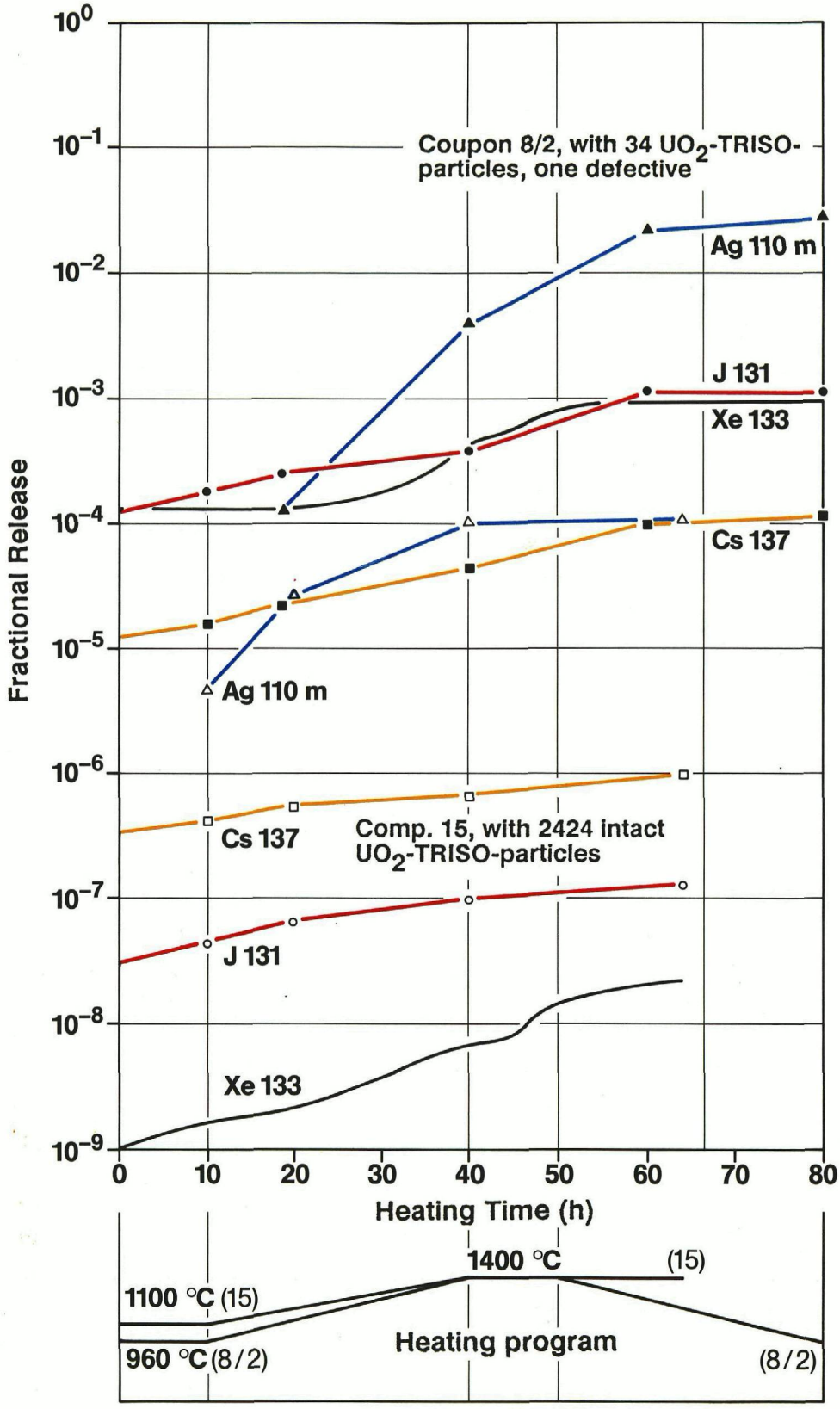

Fig. 38: Fission product release in heating test up to 1400 °C on the samples with UO_2 TRISO particles (FRJ2-P27)

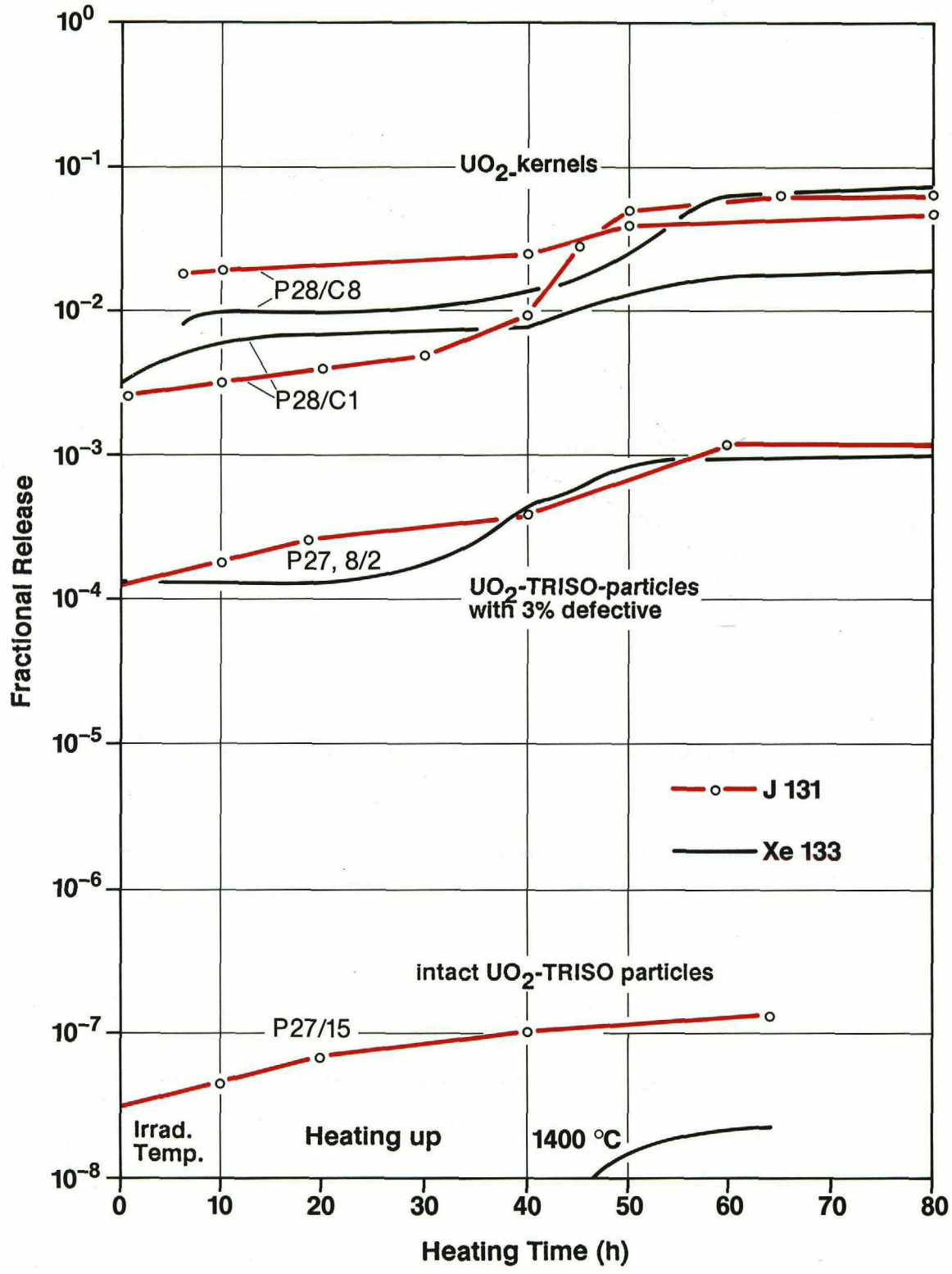

Fig. 39: I 131 and Xe 133 release during heating tests up to 1400 °C from UO_2 kernels and UO_2 TRISO particles

3.3.3 Fission product release profile up to 1800 °C

Fig. 40 shows the fission product release from a coupon with 5 UO_2 fuel kernels during a heating test up to 1600 °C. During heating up, release of I 131 and Xe 133 is already very high, and after 20 hours at 1600 °C more than half the Cs 137 has been released. The Sr 90 release remains comparatively very low during the whole 192 hours at 1600 °C.

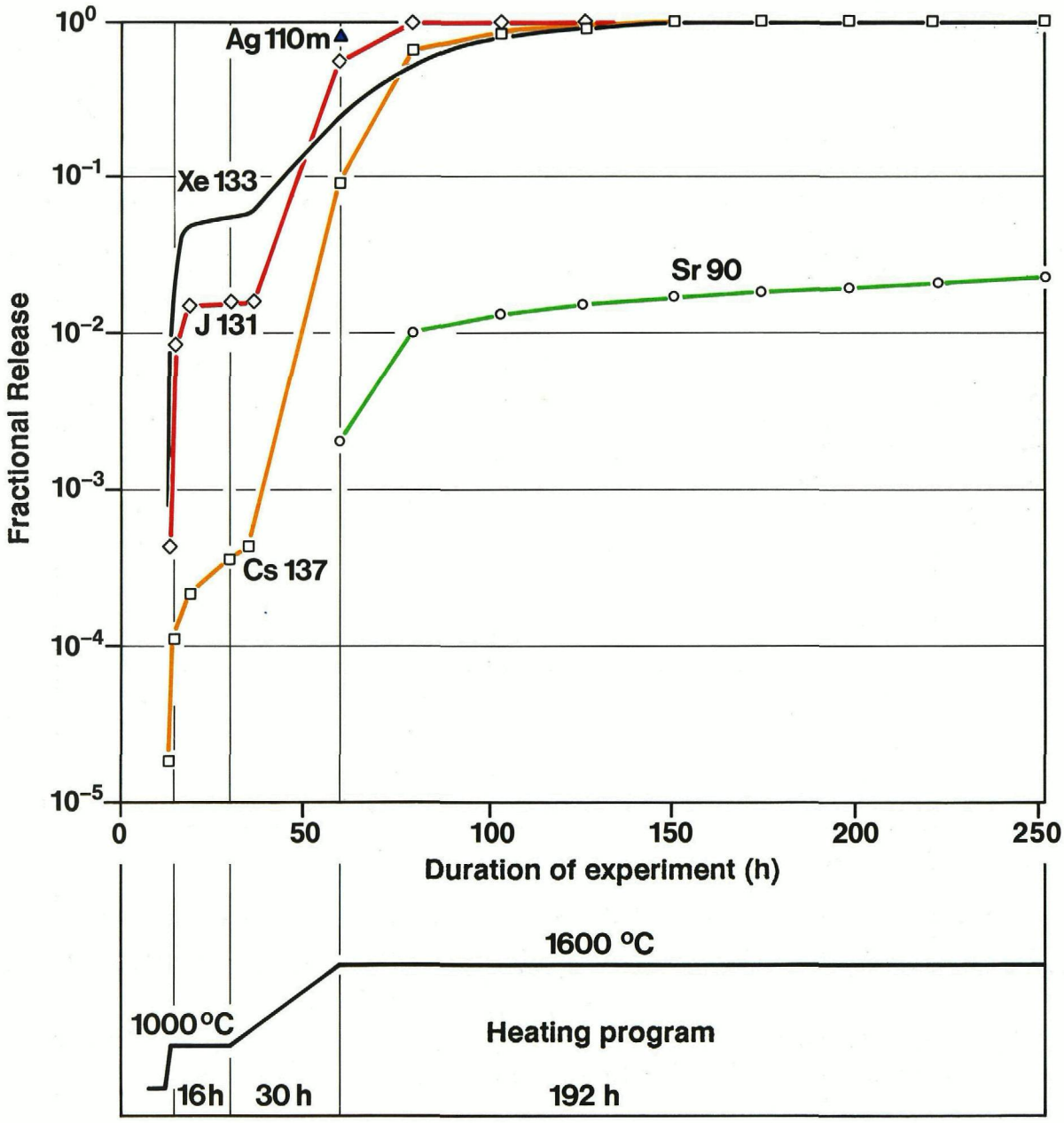

Fig. 40: Fission product release from UO_2 kernels (FRJ2-P28/C6) during heating test at 1600 °C

When comparing the Cs 137 and I 131 release curves at 1400 and 1600 °C (Fig. 41) it is found that the I 131 and Cs 137 release at 1600 °C is nearly two orders of magnitude higher than that at 1400 °C at the end of the heating up period.

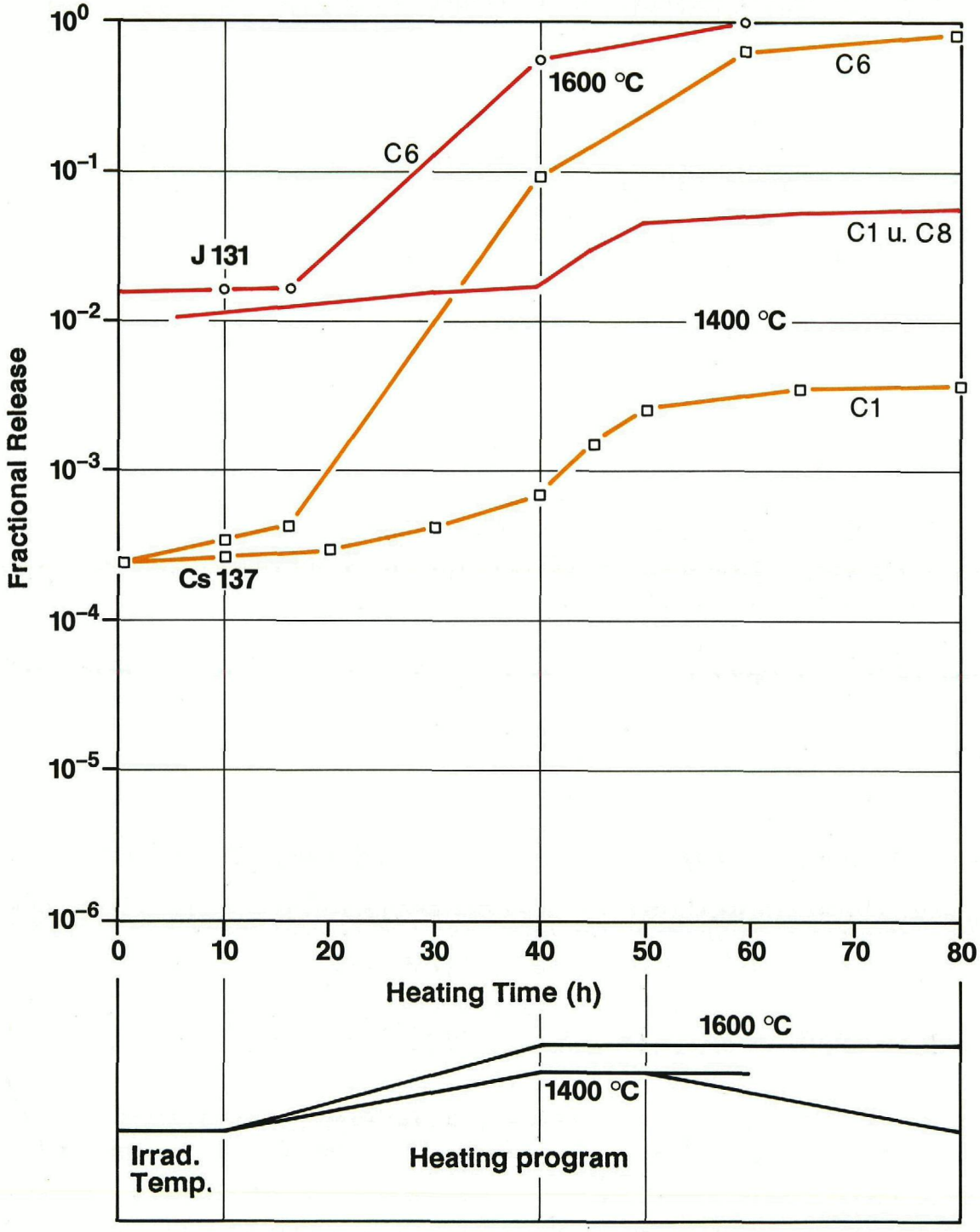

Fig. 41: Fission product release from UO_2 kernels (FRJ2-P28 coupons) at 1400 and 1600 °C

The graph of all the measured iodine release profiles from UO_2 kernels to a maximum of 1800 °C (Fig. 42) again shows the rise in releases at high temperature. However, it is clear that the release at accident temperatures from UO_2 kernels with low burnup occurs more slowly. The effect of burnup at the relatively low release at 1400 °C from coupon C8 seems to be less than the release from coupon C7 at 1700 °C which is higher by an order of magnitude. Clearly the release from the fuel kernels with low burnup occurs in the initial phase, when fission products are released from the edge zones, at the same speed as from particles with high burnup. Inside the fuel kernels with low burnup, the fission product release is greatly hindered by the denser material, compared with kernels with high burnup (see Fig. 43).

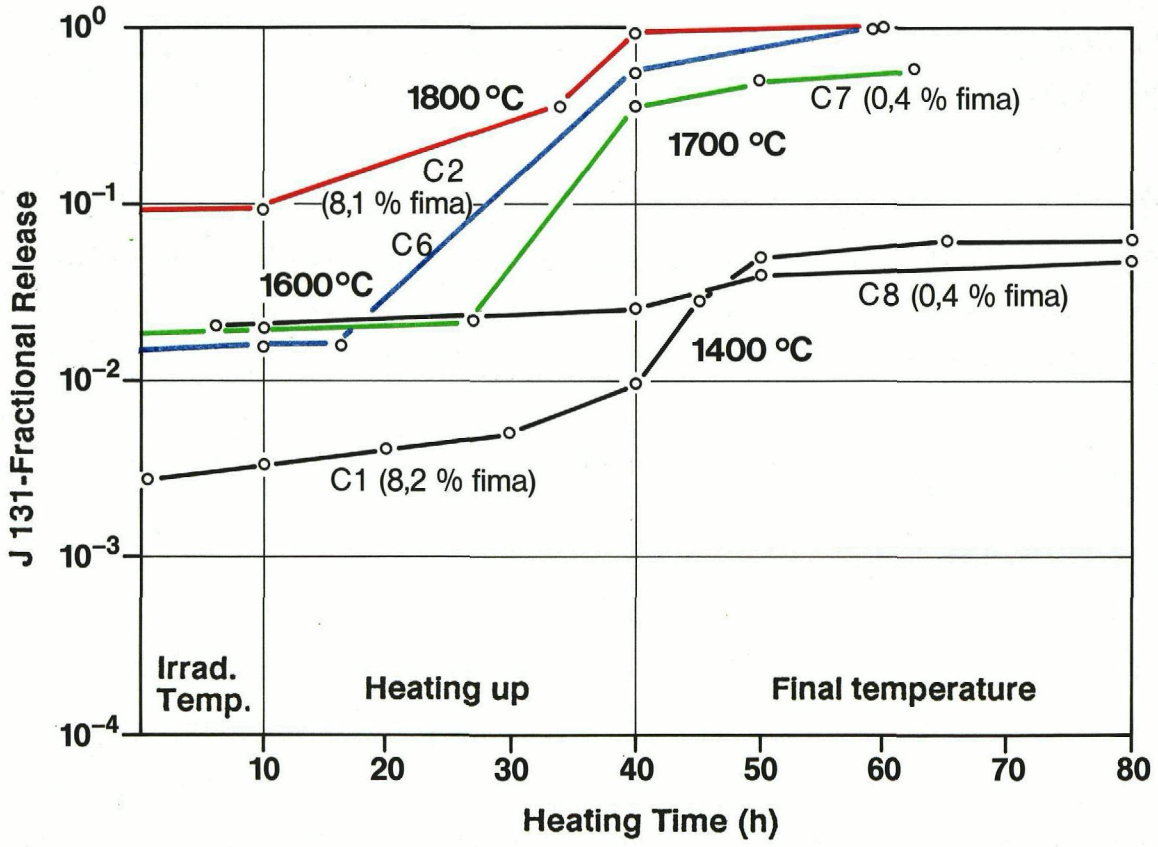

Fig. 42: Iodine release from fuel kernels with different burnup (FRJ2-P28 coupons) at temperatures from 1400 to 1800 °C

3.3.4 Ceramography

Fig. 43 shows the ceramographic section of an intact UO_2 TRISO particle from coupon 8/2 heated to 1400 °C. On the microradiography photograph next to it, one can clearly see the defective particle from the same coupon, where the defect is clearly due to manufacture.

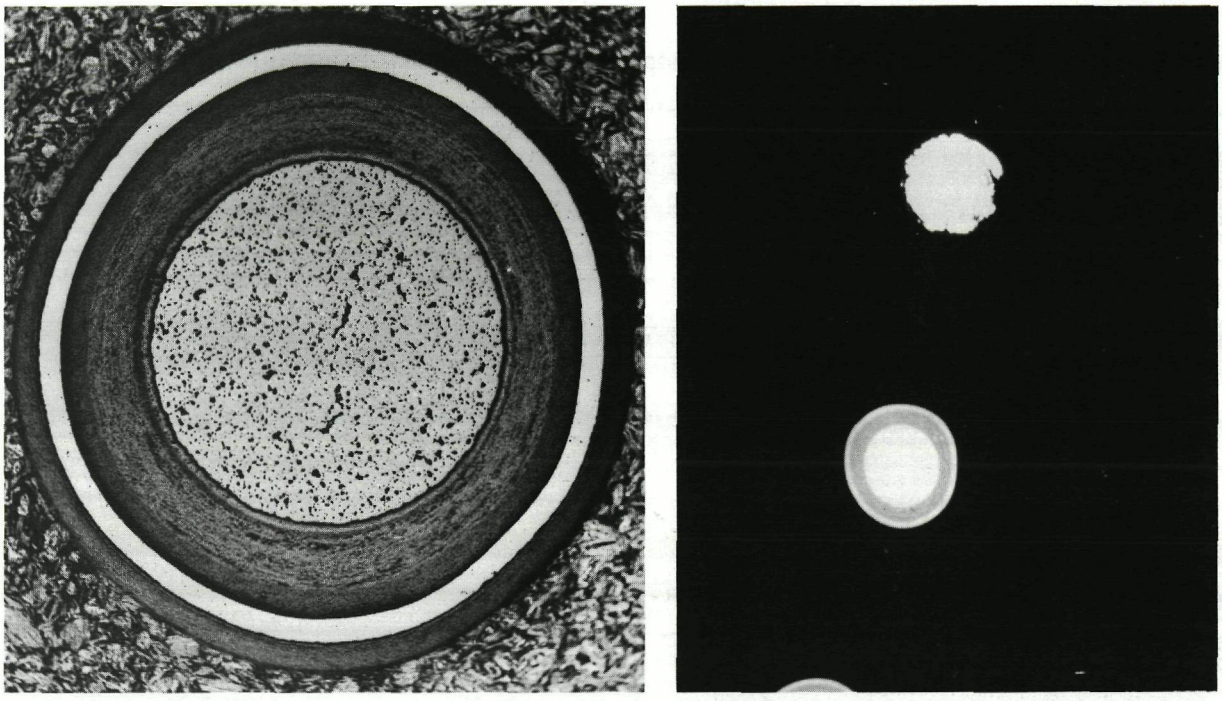

Fig. 43: Particles from FRJ2-P27 coupon 8/2 after heating test up to 1400 °C
Left: ceramography of an intact particle
Right: microradiography of a defective particle next to an intact one

UO_2 kernels from coupons heated from 1400 to 1800 °C, which are only surrounded by a porous buffer layer, are shown in Fig. 44. The two kernels with low burnup (on left hand side of picture) look similar and appear to be intact, in spite of very different temperature treatment.

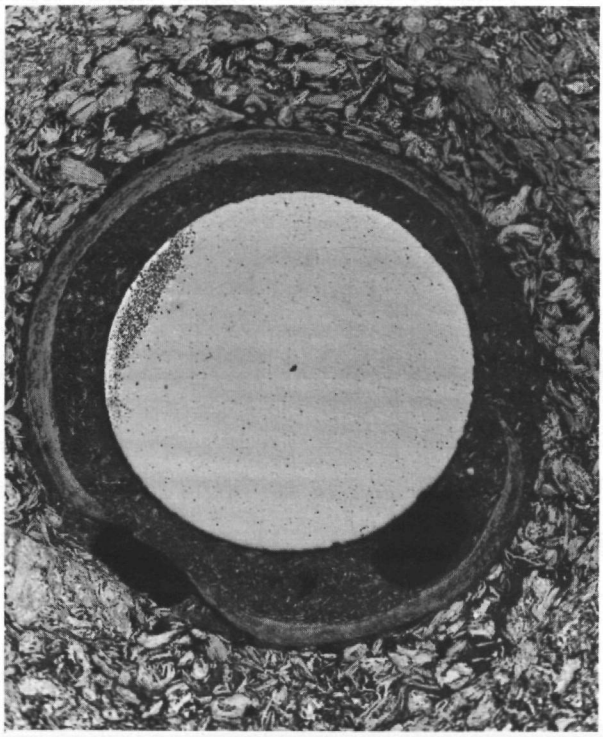

0,4 % fima (C8)

1400° C, 10 h

100 µm

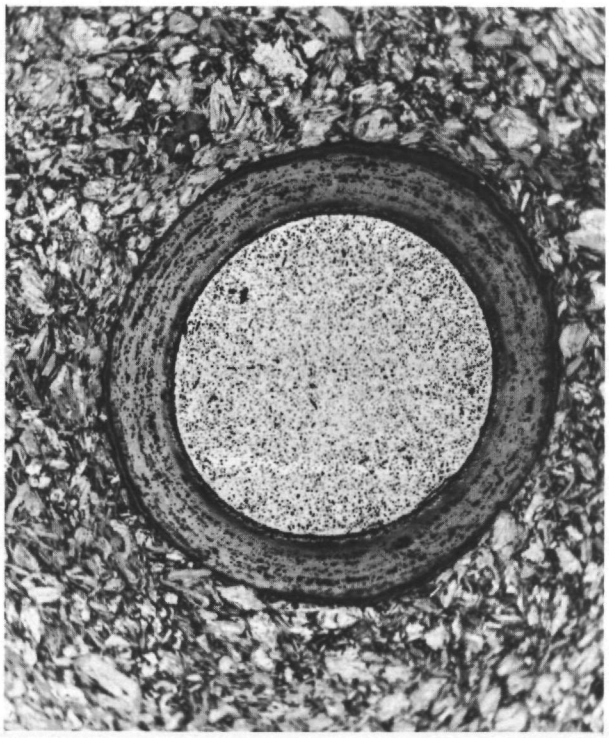

8,7 % fima (C1)

1400° C, 10 h

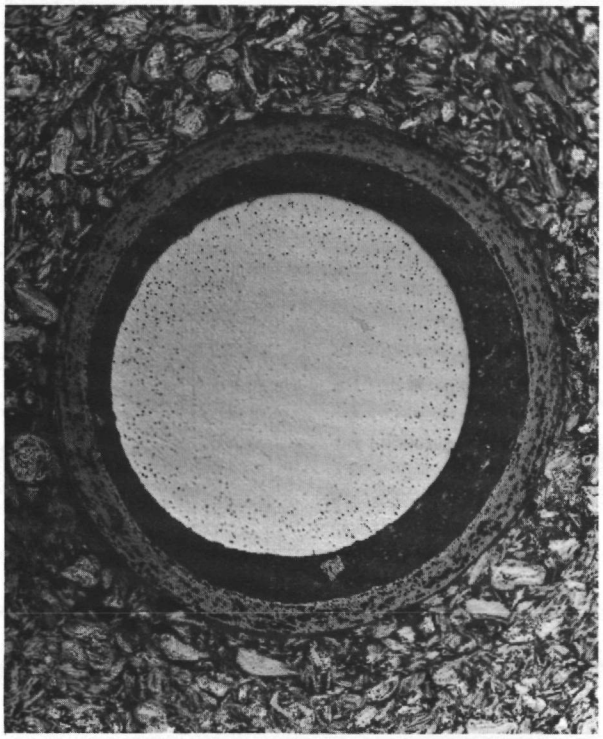

0,4 % fima (C7)

1700° C, 22,5 h

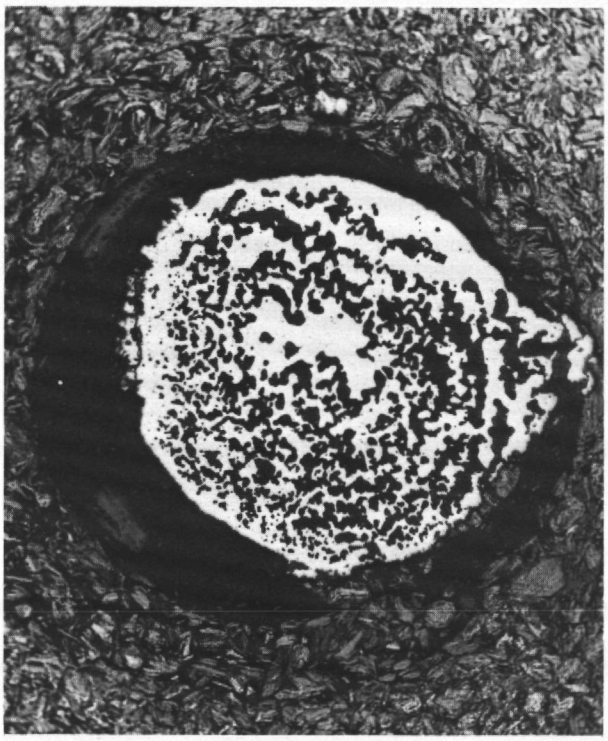

8,6 % fima (C2)

1800° C, 70 h

Fig. 44: UO_2 kernels with buffer layer (FRJ2-P28) after accident simulation tests at 1400 to 1800 °C

By contrast, the particles with high burnup heated to 1800 °C (bottom right) changed greatly compared with those treated at 1400 °C (top right). Large gas inclusions formed due to treatment at 1800 °C and the kernel material has partly split off in the edge zones.

The comparison of the two bottom sections of kernels heated to 1700° and 1800 °C respectively explains why the fission product release occurs more quickly from the greatly changed particles with high burnup than from the intact particles with low burnup.

3.3.5 Summary of heating experiments

Table 20 shows the total releases in heating tests on fuel particles with UO_2 kernels and UO_2 TRISO particles.

Description of sample	Particles	Burnup (% FIMA)	Heating test ** max. T (°C)	Duration (h)	Release Fraction J 131	Xe 133	Cs 137	Sr 90	Ag 110m
FRJ2-P27									
Compact 15	2424 UO_2-TRISO	7,6	1400	24	1,3 E-7	2,3 E-8	1,0 E-6	*	1,1 E-4
Coupon 8/2	34 UO_2-TRISO, one of them defective	9,0	1400	10	1,2 E-3	1,0 E-3	1,2 E-4	1,4 E-4	2,9 E-2
FRJ2-P28									
Coupon C1		8,7	1400	10	1,8 E-2	6,4 E-2	3,6 E-3	*	5,4 E-1
Coupon C8		0,4	1400	10	7,1 E-2	4,4 E-2	*	*	*
Coupon C6	5 UO_2 kernels	8,7	1600	192	1,0	1,0	1,0	2,2 E-2	1,0
Coupon C7	each	0,4	1700	22,5	1,0	5,8 E-1	3,0 E-1	*	1,0
Coupon C2		8,6	1800	20	1,0	1,0	1,0	6,0 E-2	1,0
				50	-	-	-	1,9 E-1	-

* below limit of detection

** in 30 hours from irradiation temperature (800 to 1100 °C) to maximum temperature

Table 20: Results of heating of fuel samples with UO_2 kernels and UO_2 TRISO particles

During the experiment on coupon C2, the release of the measured fission products was complete after 20 hours at 1800 °C, with the exception of Sr 90 (only 6 %). As in the 1600 °C test on coupon C6, the comparatively good Sr 90 retention in the fuel kernel at these temperatures is clearly shown. All measured releases from the coupons with UO_2 kernels were related to the inventory after activation. During irradiation in experiment FRJ2-P28, considerable quantities of fission products were released from fuel kernels. Table 21 compares the releases during irradiation with similar releases in heating tests on two coupons from the same irradiation capsule. After 10 hours at 1400 °C (C1) and after heating to 1600 °C (C6) similar high fractions of Ag 110m and Cs 137 released from UO_2 kernels are reached as after 261 days at about 940 or 1020 °C during irradiation.

	Temp. (°C)	Duration (h)	Fraction Released From UO_2 Kernels Ag 110m	Cs 137
Capsule 1 - Irradiation	940	6264	6,9 E-1	1,6 E-2
C1/K1 - Heating Test	1400	10	5,4 E-1	3,6 E-3
Capsule 3 - Irradiation	1020	6264	1	1,1 E-1
C6/K3 - Heating Test	1600	-	8,3 E-1	9,2 E-2

Table 21: Fission product release from UO_2 kernels during irradiation and heating tests

3.4 The SiC layer

For fuel elements which contain particles with a TRISO coating, the SiC intermediate layer is the main fission product barrier up to temperatures of about 1800 °C and at short times at temperature to above 2000 °C. During accident temperatures up to and including 1600 °C, fission products, with the exception of Ag 110m, are only released from particles with defective SiC layers, either due to manufacture or irradiation, and to a very small extent from heavy metal contamination due to manufacture.

3.4.1 Defects in SiC due to manufacture and irradiation /29/

SiC defects due to manufacture can be found in unirradiated spherical fuel elements by the manufacturer HOBEG at Hanau with the burn-leach test. The outer pyrocarbon is completely burnt off in the first stage. The heavy metal is then leached out of particles with defective SiC layers. The number of defective particles can be determined from the quantity of heavy metal obtained.

Fig. 45 (left) plots the frequency distribution of SiC defects per sphere of 5 fuel elements with mixed oxide TRISO particles examined from 4 manufacturing batches (i.e., a total of 20 fuel elements).

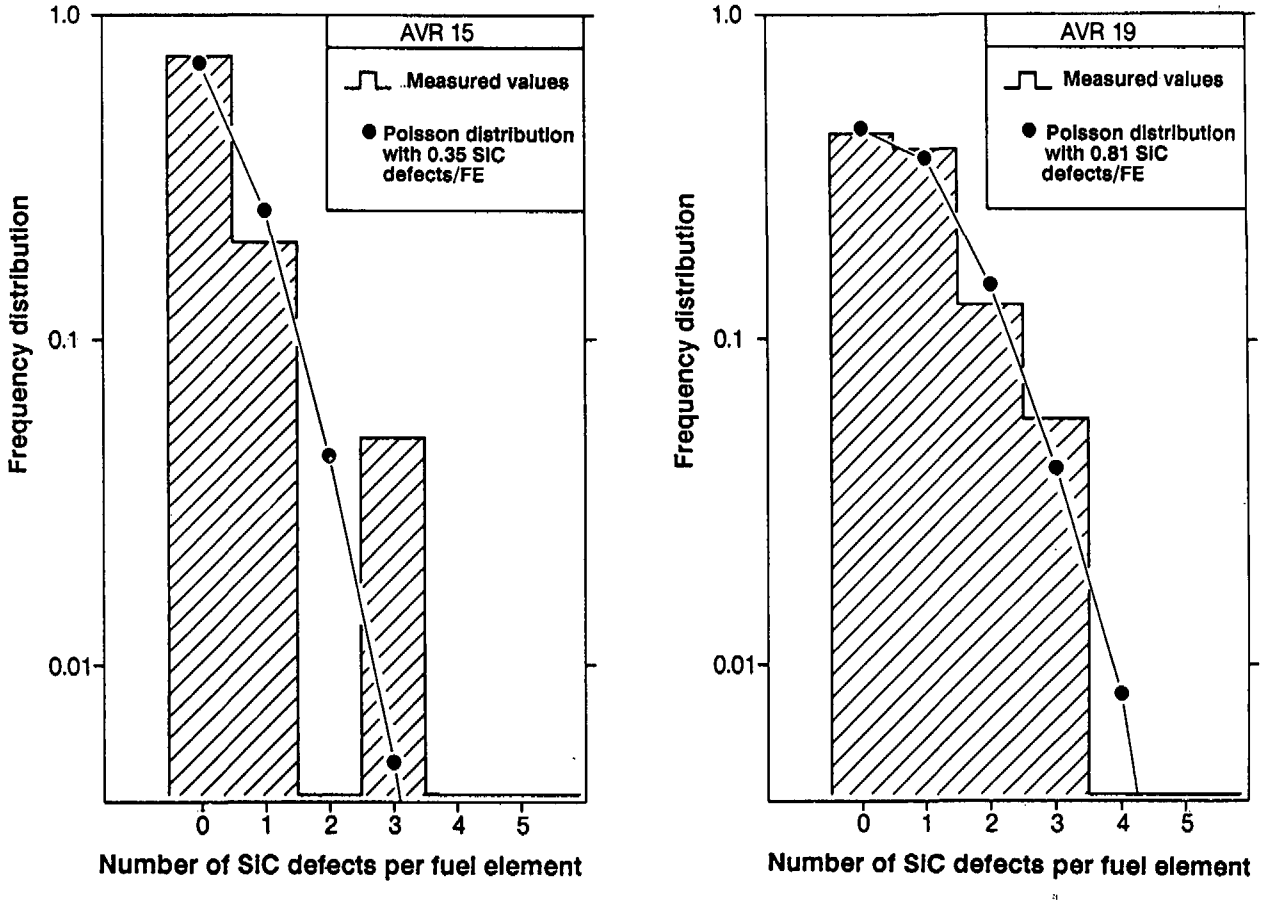

Fig. 45: SiC defects due to manufacture on 20 fuel elements with mixed oxide TRISO particles (left) and 70 fuel elements with UO_2 TRISO particles (right)

The coating of the particles for AVR 15 was done in 3 kg batches, and a total of 6000 fuel elements were manufactured for use in the AVR reactor.

The frequency distribution of SiC defects for 5 spheres from 14 batches, i.e. a total of 70 fuel elements with UO_2 TRISO particles from 5 kg coating batches, from which 24000 AVR fuel elements were manufactured, is plotted in Fig. 45 (right). The Poisson distribution contained in the two graphs shows that with the number of fuel elements examined, one can achieve satisfactory information on the statistical distribution of SiC defects due to manufacture in spherical fuel elements.

A proportion of SiC defects of 5×10^{-5} was determined for fuel elements with mixed oxide TRISO particles, (i.e. about two defective SiC layers per three spheres) and for fuel elements with UO_2 TRISO particles, the proportion of defects was 3.5×10^{-5} (i.e. about one SiC layer per three spheres). The fission product release from fuel samples with TRISO particles in 9 irradiation experiments with UO_2 TRISO and 6 irradiation experiments with mixed oxide TRISO fuel elements are plotted in Fig. 46 against the irradiation temperature.

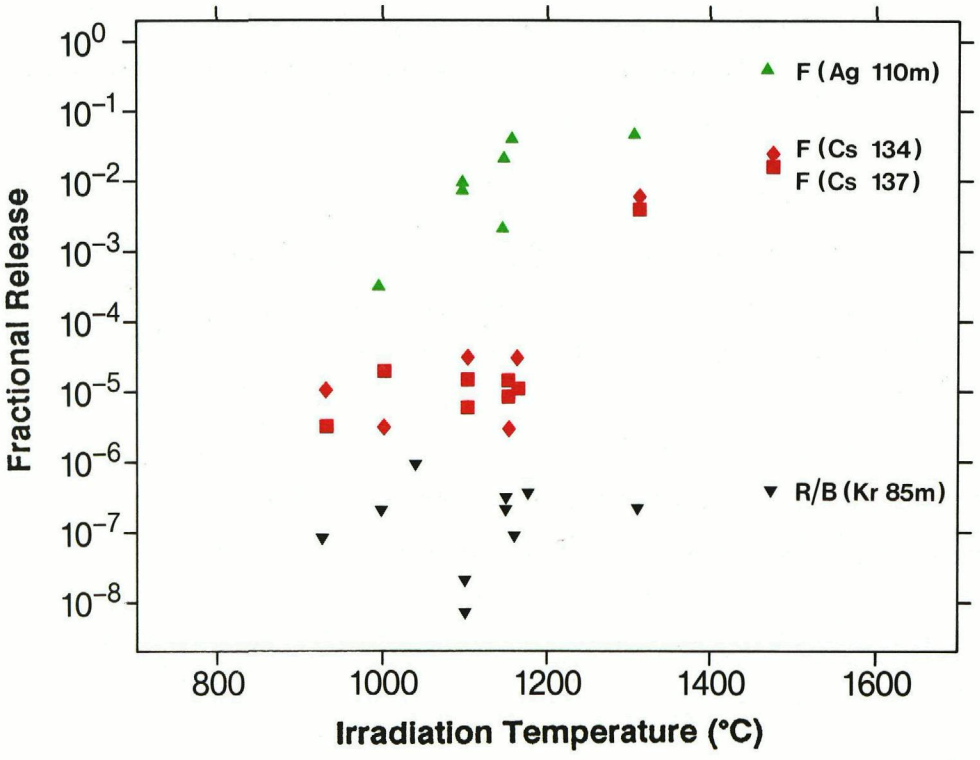

Fig. 46: Fission product release during irradiation from fuel samples with TRISO particles

The Kr 85 equilibrium releases at the end of irradiation and the proportions of caesium and silver measured later outside the fuel samples were used. It is found that silver is released at irradiation temperatures above 1000 °C and caesium above 1250 °C (the irradiation temperatures in the HTR 500 and HTR module are 800 to 900 °C). Below these high irradiation temperatures, the release remains in the region of the free heavy metal quantities due to manufacture. The fission gas equilibrium releases are very low at irradiation temperatures up to about 1500 °C. In maximum irradiation conditions in HTR's, no particle failure due to irradiation was found.

3.4.2 SiC failure mechanisms

Corrosion and decomposition lead to additional damage of SiC in accident simulation tests.

Two different laboratory tests were done on corrosion of SiC by fission products.

In order to be able to judge the corrosive effect of individual groups of fission products, unirradiated UO_2 TRISO particles were tested at 1600 to 2400 °C, to which various fission products were added during manufacture. It was found that rare metals, particularly caused the greatest damage to SiC /32/.

In heating tests between 1600 and 1900 °C on irradiated particles, which were exposed to a steep temperature gradient, the degradation rate of the SiC layer was determined (Fig. 47) /33/. These experiments give relatively unfavourable results, because high fission product concentrations occur on the hot particle side, which accelerate the SiC corrosion. The temperature gradient in a fuel particle is very small during an accident.

The decomposition of the SiC layer was only examined on unirradiated particles.

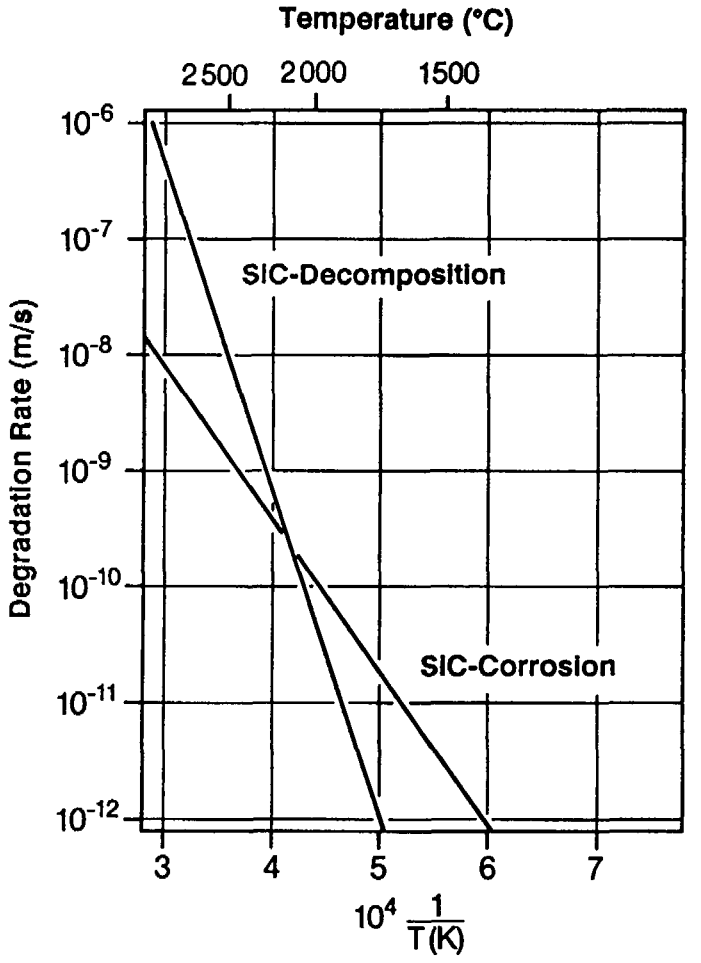

Fig. 47: Temperature dependence of SiC degradation rate due to corrosion and decomposition

After heating tests on UO_2 TRISO particles, the start of SiC decomposition became noticeable in the edge zones after one hour at 2300 °C /34,35/.

In another experiment, an effective degradation rate of the SiC layer was determined (Fig. 47) /36/.

The TRISO particles without an outer pyrocarbon layer were tested at 2000, 2100 and 2200 °C, which again created conservative conditions, because the protective effect of the outer pyrocarbon layer was missing.

The degradation rates in Fig. 47 intersect at 2100 °C. Below this temperature, corrosion dominates and above it decomposition of SiC dominates. The results show the effect of SiC defect mechanisms at high temperatures in fuel elements with TRISO particles very well.

3.4.3 SiC defects in accident simulation tests

The start of SiC damage is of the greatest importance for fission product release in accidents, because this means the start of release for fission products from fuel particles relevant for accidents.

The fission product releases in heating tests at 1600 °C on fuel elements with UO_2 and $(Th,U)O_2$ TRISO particles, which are attributed to SiC corrosion, clearly depend on the irradiation exposure (i.e., on the amount of burnup, the fast neutron fluence and the temperature). The existing results do not permit any conclusion about the individual importance of these three parameters.

Fig. 48 shows the Cs 137 releases after 500 hours at 1600 °C from three fuel elements with different irradiation exposures plotted against the fast neutron fluence.

The profile and level of release show that only caesium due to contamination was released from AVR sphere 71/22. However, in experiments on HFR-K3/1 fuel elements after 200 hours and after less than 50 hours on R2-K13/1 fuel elements, the release of Cs 137 from the fuel particles was measured (see also Figs. 25 and 18). Clearly, Cs 137 is completely retained by intact TRISO particles at 1600 °C.

The release from the fuel particles is presumably due to corrosion of SiC due to fission products starting at the grain boundaries. The corrosion could be accelerated at higher burnups due to higher fission product concentration, at higher irradiation temperatures due to greater diffusion of the fission products and at higher fast neutron fluences due to increased numbers of defects in the SiC structure.

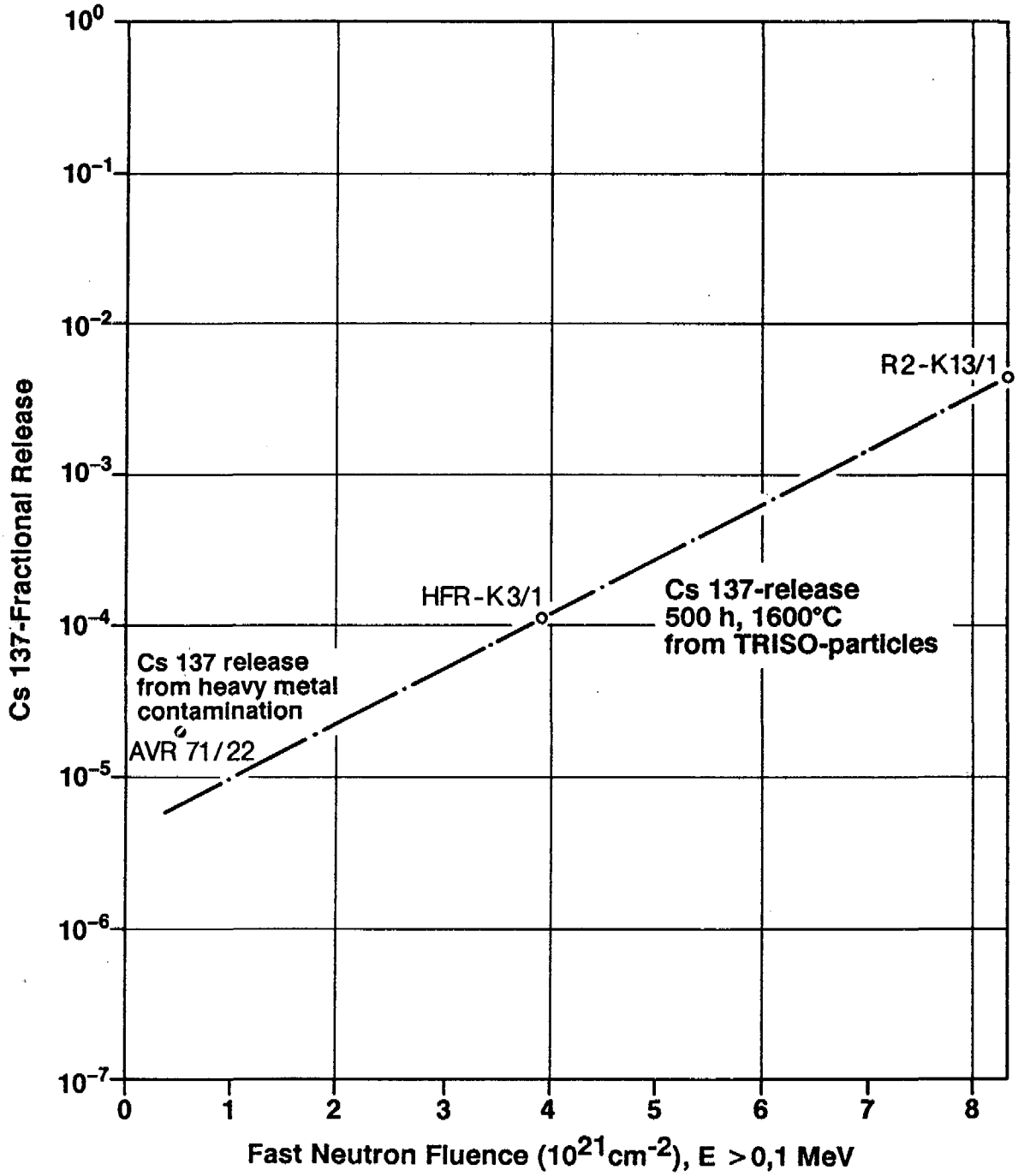

Fig. 48: Cs 137 release from fuel elements with TRISO particles after 500 hours at 1600 °C

At 1600 °C, SiC defects occurred within 100 hours only in fuel element R2-K13/1, which was irradiated above the target values for the HTR module and HTR 500 as regards temperature and fast neutron fluence.

The knowledge obtained from caesium release is confirmed and supplemented by ceramographic results. Fig. 49 at the top compares the coating sections from UO_2 TRISO particles from three fuel elements heated at 1600 °C with a particle from a fuel element which was not heated.

While the particle in fuel element FRJ2-K13/2 heated at 1600 °C for 160 hours does not show any SiC damage, one can see fission product corrosion starting after 500 hours at 1600 °C on the particle from sphere AVR 71/22 and advanced corrosion after the same heat treatment on the particle from fuel element HFR-K3/1 with higher irradiation. The degree of damage to the SiC layer inside a fuel element varies. In all cases no damage, or damage only just starting could be seen on particles from fuel element 71/22, while all the 10 particles examined from sphere HFR-K3/1 were damaged, some of them over the whole width of the layer (see Fig. 35). An example of different degrees of damage within a fuel element are the two particle sections from fuel element 70/11, which was heated at 1700 °C (Fig. 49, bottom).

In individual cases at 1500 and 1700 °C, and more often at 1800 °C (max. about 40 particles) pressure vessel failure occurred, i.e. particle coatings became defective right through, where 30 to 50 % of the fission gas inventory was released. The damage is less noticeable at 1800 °C, due to SiC defects, and relatively high release of caesium, than in release of fission gas and iodine.

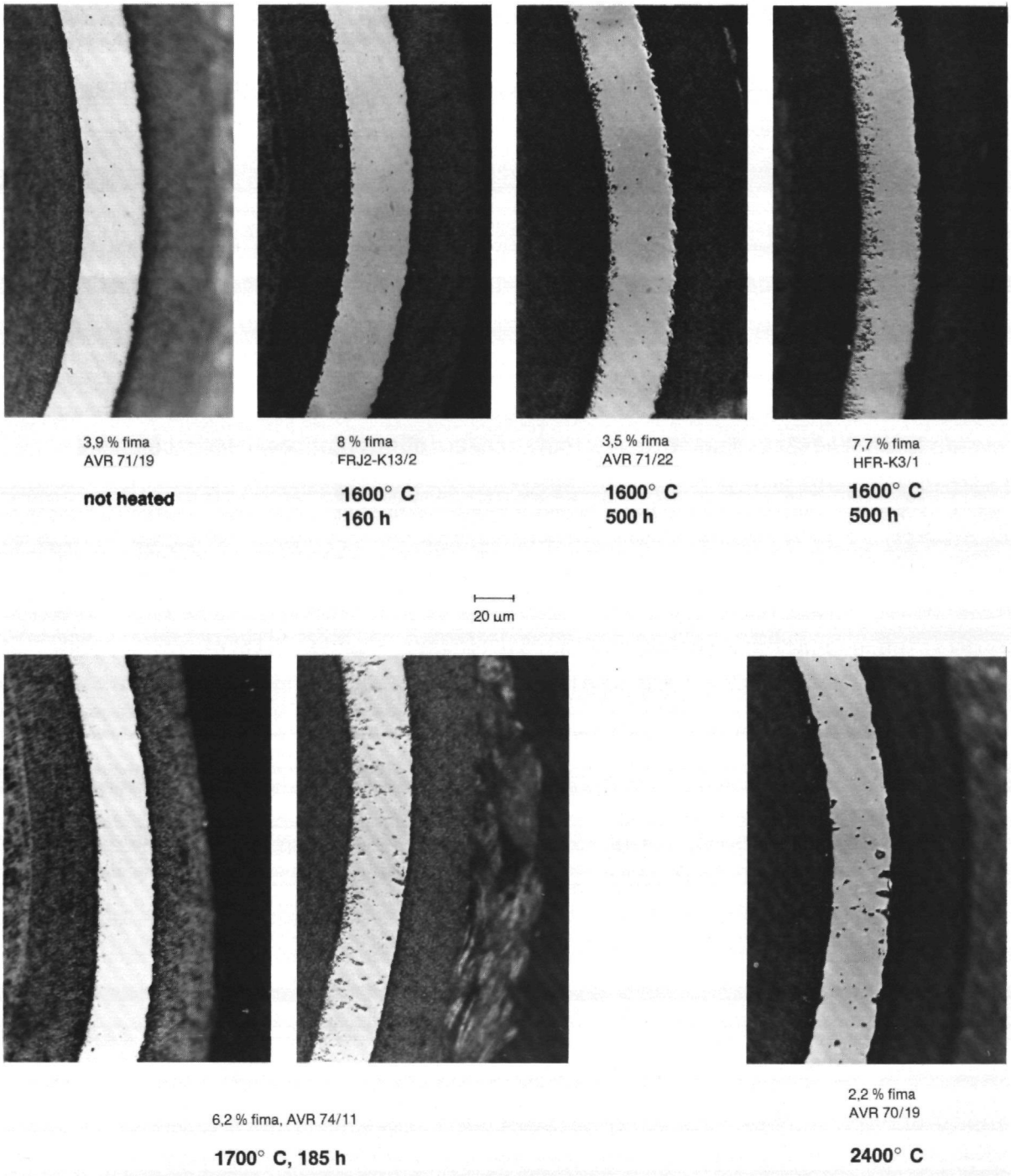

Fig. 49: Coating sections with SiC layers of UO_2 TRISO particles from heated fuel elements

SiC decomposition occurs relatively quickly above about 2200 °C.
In heating tests where spherical fuel elements with UO_2 and $(Th,U)O_2$ TRISO particles with different burnups were heated from 1250 to a maximum of 2500 °C at about 50 °C per hour, the rise in fission gas release due to SiC failure starts at 2200 to 2300 °C (Fig. 50). One cannot distinguish between increased fission gas diffusion through intact pyrocarbon layers and additional isolated cases of pressure vessel failure.

Start of SiC decomposition for a UO_2 TRISO particle from fuel element 70/19 heated to 2400 °C can be seen in Fig. 49, bottom. The tangential section of a TRISO mixed oxide particle, also from a sphere heated to 2400 °C (Fig. 24) shows that decomposition in the SiC layer starts from the grain boundaries.

Summarising the SiC damage behaviour in accidents can be described as follows (Fig. 51):

- No SiC failure were found up to 200 hours at 1600 °C

- Fission product corrosion in the SiC layers starts within 100 hours at 1700 to 1800 °C, and increases with higher temperatures and longer periods of heating

- Above 2000 °C, the SiC is also decomposed by heat.
  This damage mechanism leads to SiC damage above 2200 °C, during heating at 50 °C per hour.

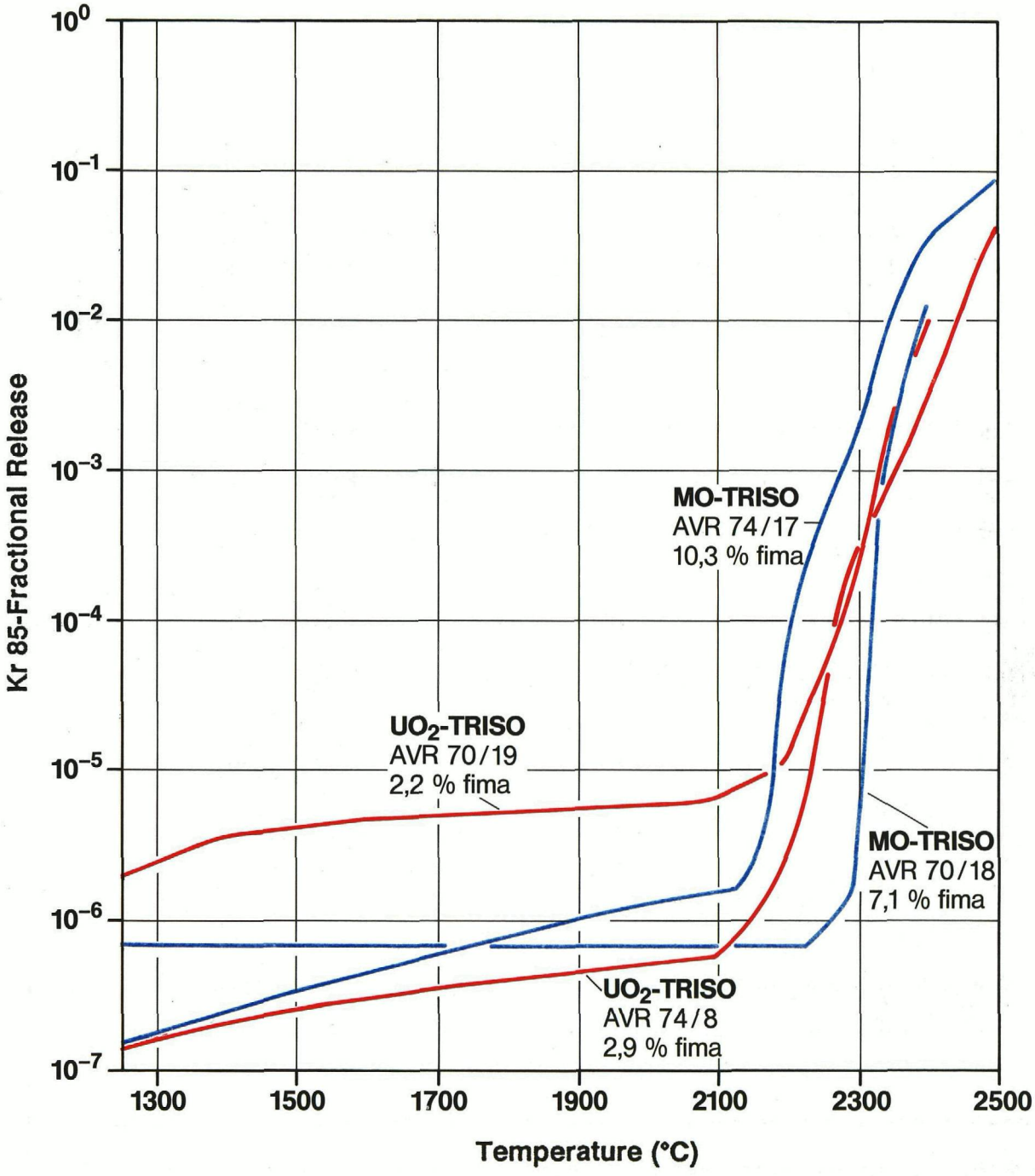

Fig. 50: Release of Kr 85 during heating (~50 °C/hour) from fuel elements with TRISO particles

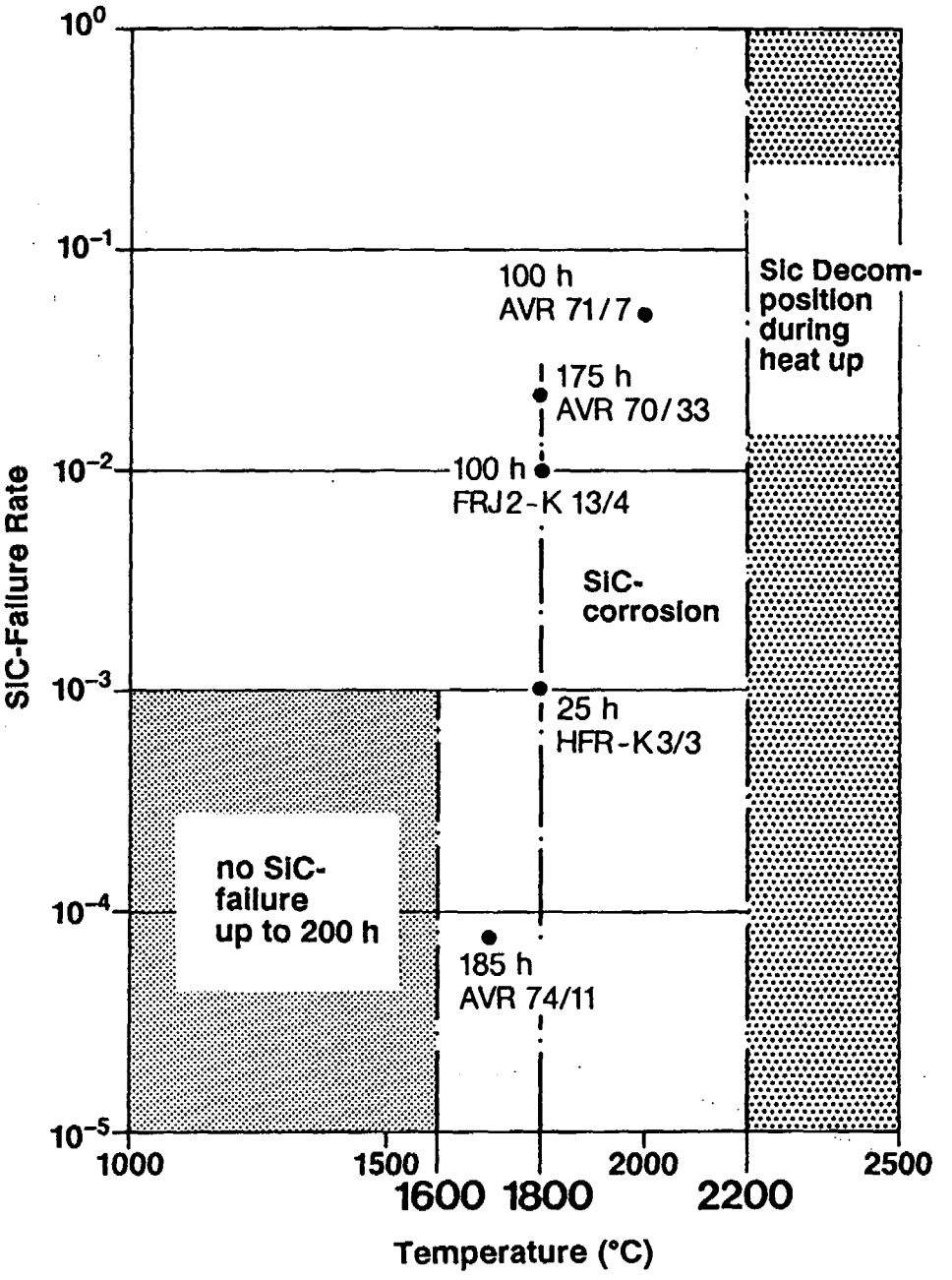

Fig. 51: SiC failure in fuel elements with UO_2 TRISO particles derived from release of caesium

3.5 Previous accident simulation programmes and results

Accident simulation tests have been done on spherical fuel elements since 1977. The quality of the experiments and the fission product retention with modern TRISO fuel elements have improved considerably in the period up to 1986 with the construction of the cold finger apparatus.

3.5.1 Accident simulation programmes

Table 22 gives a survey on the tests done so far for accident simulation in hot cells at KFA Jülich and the most important results obtained.

With the first generation of the two high temperature furnaces of the heating equipment (A test) from 1977 to 1981, hypothetical accidents up to 2500 °C were simulated. A large number of experiments were also done at 1400 to 1800 °C, at temperatures at which caesium release starts. The main point of the tests was use of fuel elements with HTI-BISO mixed oxide particles, such as were being used in the THTR 300 reactor. Other fuel elements of older types used in the AVR reactor were also heated. Of these types tested up to 1981, the fission product retention in fuel elements with BISO mixed oxide particles was best at accident temperatures.

After four years of operation (partly in extreme conditions), the first high temperature furnaces had to be shut down in 1981. Operation was restarted with new furnaces in 1983. In parallel with this, the cold finger apparatus was designed and constructed in just under 2 years and was comissioned at the beginning of 1984.

During collaboration (PWS-FD-11) parallel tests were done in 1983 at GA, San Diego and in the hot cells of KFA. Up to 100 particles of two American and two German types of fuel were heated to 2500 °C. The agreement in the results was satisfactory /19/. In ramp tests at 2500 °C with highly burnt-up American fuel samples, which were used in irradiation experiment R2-K13, an increasing number of particle failures were recorded from 1200 °C upwards /19/. The results of the accident simulation tests from the end of

Programme	FE or sample	Type of particle	Number of heated f.e./samples up to 1800 °C	up to 2500 °C	Result
1977 - 81	AVR-GO AVR-THTR DR-K4	$(Th,U)O_2$ BISO (HTI)	11	30	Cs 137 release above 1600 °C BISO coating intact up to 2500 °C, as long as good fission gas retention /3, 4, 14/
Simulation of hypothetical AVR-GK accidents (A Test)	AVR-GK	$(Th,U)C_2$ BISO (HTI)	5	4	Cs release above 1400 °C, above 2200 °C damage to coating and high Kr release /5/
	AVR-GLE 1 DR-K5	UO_2 BISO (LTI)	7	2	High Cs and Kr release above 1400 °C /5/
	AVR-GFB 2	UO_2 TRISO ThO_2 BISO (LTI)	3	6	High Cs and Kr release above 1400 °C /5/
	FRJ2-K11	$(Th,U)O_2$ TRISO	1		Results could not be used (see chapter 3.1.1)
1983 Simulation of hypothetical accidents collaboration with GA (A Test)	Loose particles	4 types		(4)	Comparison with GA-KFA satisfactory agreement /19/
	Block-Segm. Particles	UCO TRISO ThO_2 TRISO		(7)	High Kr release above irradiation temperature (16 % FIMA) /19/
1983 - 86 Simulation of design accidents (Küfa, A Test)	R2-K13/1	$(Th,U)O_2$ TRISO	1		Very little release up to 1600 °C, exception Ag 110m
	AVR-GO 2		4		
	FRJ2-K13	UO_2 TRISO	2		
	HFR-K3		2		
	AVR-GLE 3		4		
	FRJ2-P27		(2)		
	FRJ2-P28	UO_2 kernels	(5)		Iodine and inert gas release similar above 1600 °C, quick release of Cs
Simulation of hypothetical accidents	AVR-GO 2	$(Th,U)O_2$ TRISO		4	above 1800 °C high Cs release
	AVR-GLE 3	UO_2 TRISO		5	above 2200 °C high Cr release

Table 22: Accident simulation tests in hot cells of Institute for Reactor Materials at KFA Jülich

1983 to the beginning of 1986 with cold finger and heating apparatus are compiled in this report.

3.5.2 Release of fission products from different types of fuel elements

When comparing previously tested fuel elements, the excellent accident characteristics of fuel elements with modern TRISO particles became clear. Fig. 52 shows the Cs 137 release at 1600 °C from fuel elements with UO_2 TRISO particles, as designed for future HTR's, compared with that of fuel elements with mixed oxide and mixed carbide BISO particles. While caesium is retained completely at 1600 °C in TRISO particles, the BISO coating is no longer a sufficient barrier at this temperature.

The retention of fission gas in BISO particles is better. The fact that the Kr 85 release from fuel elements with BISO particles is higher than from spheres with UO_2 TRISO particles (Fig. 53) is attributed first of all to the higher heavy metal contamination due to manufacture of fuel elements with BISO particles. The mixed carbide BISO fuel element tested had a very high burnup, and in one of the four heated mixed oxide BISO spheres, several particles were damaged after about 50 hours by pressure vessel failure.

During the accident simulation tests under hypothetical accident conditions up to 2500 °C (Fig. 54), the release of fission gas from fuel elements with UO_2 TRISO particles again remains comparatively low, although these fuel elements were heated more slowly than other types, which favours damage to SiC. While spheres with medium burnup mixed oxide BISO particles and high burnup mixed carbide BISO particles showed good fission gas retention up to 2200 °C, failures at about 1600 °C in fuel elements with very high burnup mixed oxide BISO particles and burnt-up UO_2 TRISO and breeder ThO_2 BISO particles led to increased release. Tests showed that chlorine impurities in the SiC layer of the burnt-up UO_2 TRISO particles could lead to SiC corrosion during irradiation /37/. During accident simulation tests, the TRISO particles manufactured in 1973 started to be permeable to caesium at 1400 °C.

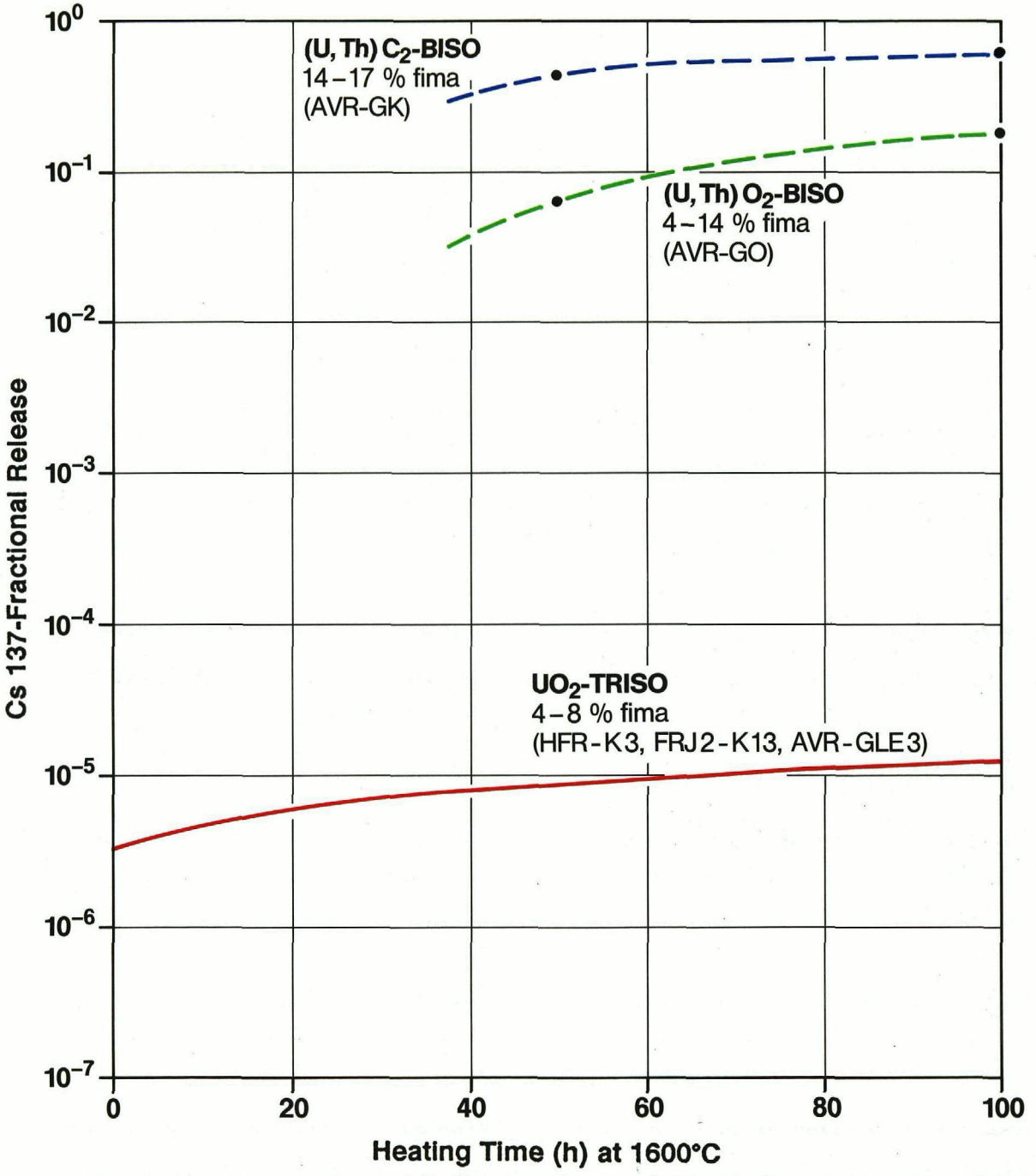

Fig. 52: Mean Cs 137 release at 1600 °C from different types of fuel

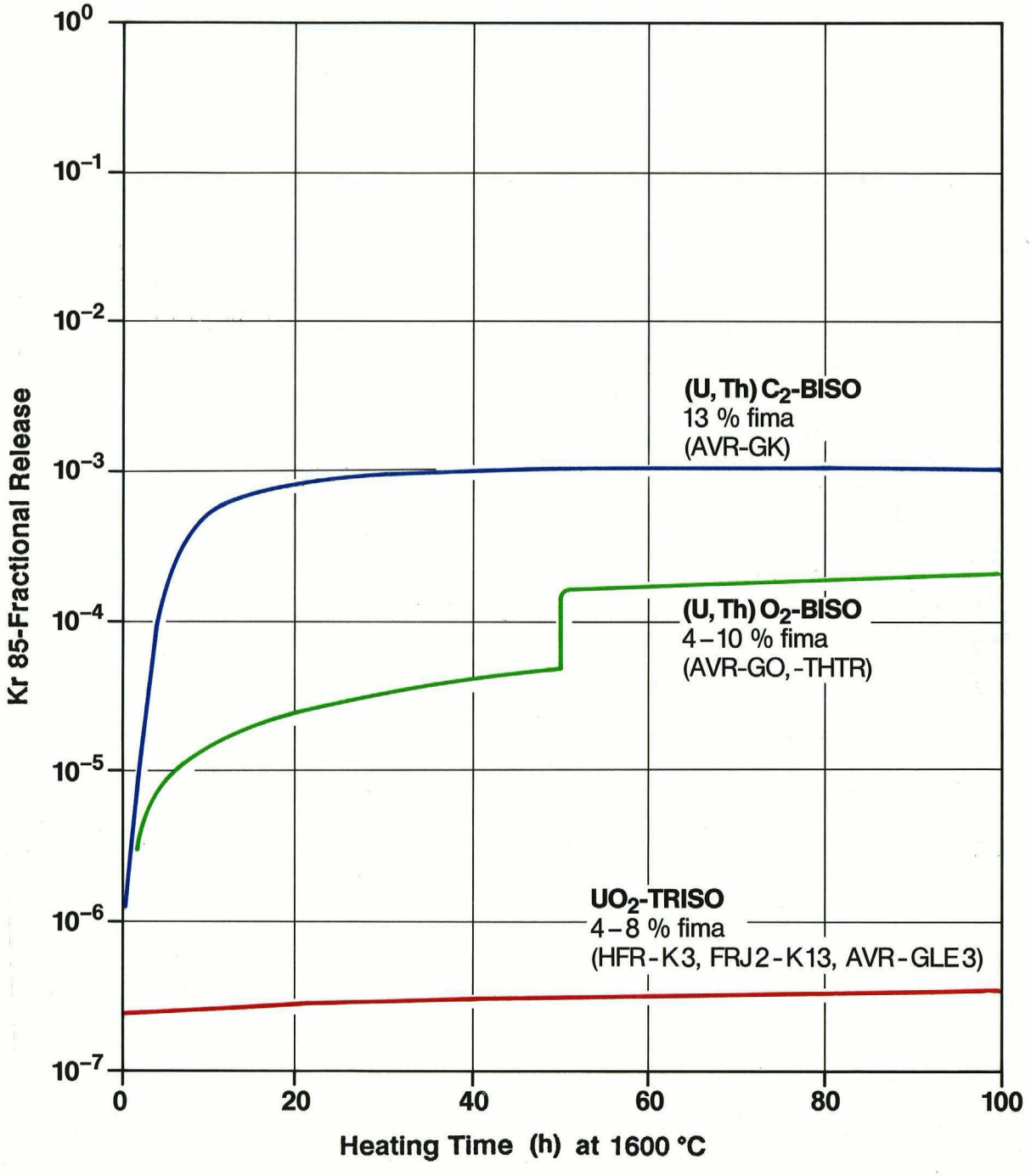

Fig. 53: Mean Kr 85 release at 1600 °C from different types of fuel

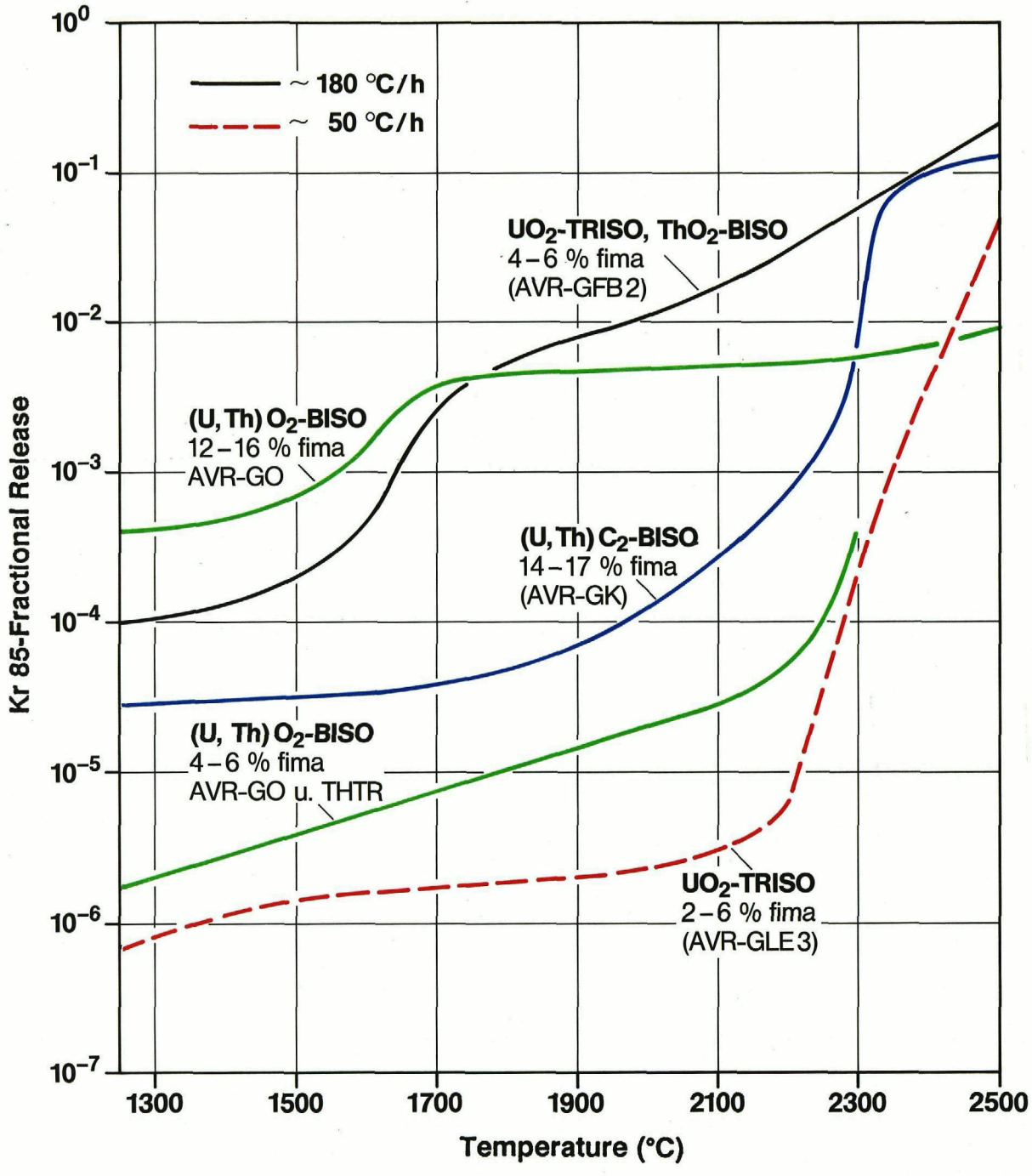

Fig. 54: Mean Kr 85 release during heating up to 2500 °C for different types of fuel elements

3.5.3 Changes in particles of different types

The sections of particles from heated fuel elements of different types shown in Fig. 55 have suffered changes due to temperature treatment. Mixed oxide BISO particles remain intact up to 2500 °C, with a few exceptions, where the CO partial pressure in particles with high burnup leads to ballooning of the HTI layer.

The importance of CO partial pressure in oxide particles is made clear in the comparison with the very highly burnt-up carbide particles similar to BISO mixed oxide particles as regards coating and dimensions, because of the missing oxygen, there was not nearly such a high internal pressure as in the mixed oxide particles. The heavy metal carbide which moves easily above 2000 °C penetrates into the coating and destroys the structure of the pyrolytic carbon.

The sections of TRISO particles in the lower half of Fig. 55 show the difference in quality of two kinds of SiC. The SiC layer of the modern UO_2 TRISO particle (FRJ2-K13/2) shows no damage after 160 hours at 1600 °C and so caesium is still completely retained in the particles. By contrast, the burnt-up UO_2 TRISO particle from old AVR-GFB2 fuel elements is already damaged after 60 hours at 1400 °C, due to the chlorine impurities in the SiC due to manufacture, so that 37 % of the Cs 137 is released from the sphere. The particles from the AVR-GFB2 fuel elements heated to higher temperatures also show greater damage than comparably irradiated particles from modern TRISO fuel elements.

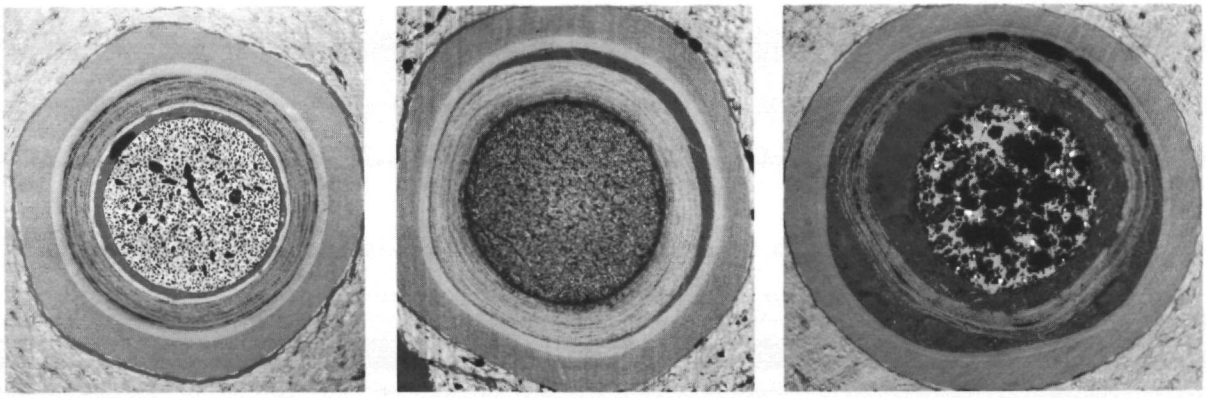

61/23-12,5 % fima
1600° C, 100 h

48/8-4,7 % fima
bis 2500° C

49/23-14,2 % fima
bis 2450° C

(Th, U) O_2-BISO-particles from AVR-GO-resp. THTR fuel elements

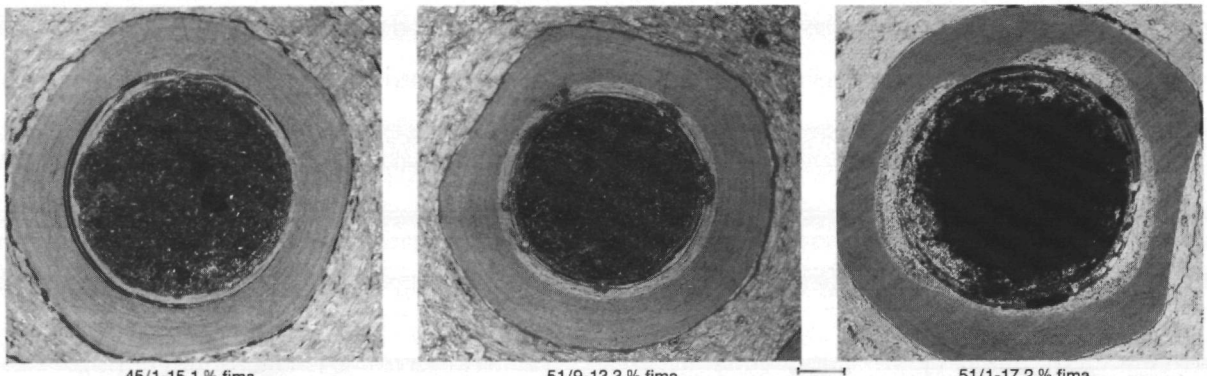

45/1-15,1 % fima
1400° C, 50 h

51/9-13,3 % fima
1600° C. 97 h

51/1-17,2 % fima
bis 2300° C

(Th, U) O_2-BISO-particles from AVR-GK-fuel elements

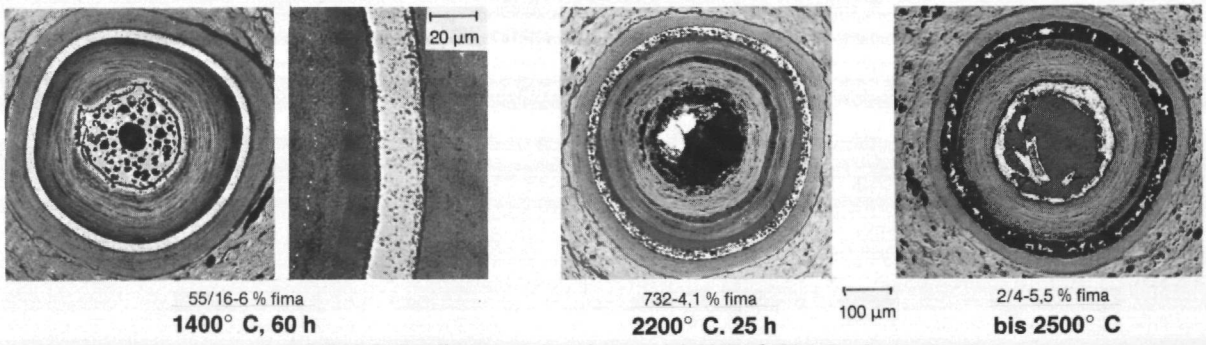

55/16-6 % fima
1400° C, 60 h

732-4,1 % fima
2200° C. 25 h

2/4-5,5 % fima
bis 2500° C

UO_2-TRISO-fissile particles from old AVR-GFB2-fuel elements

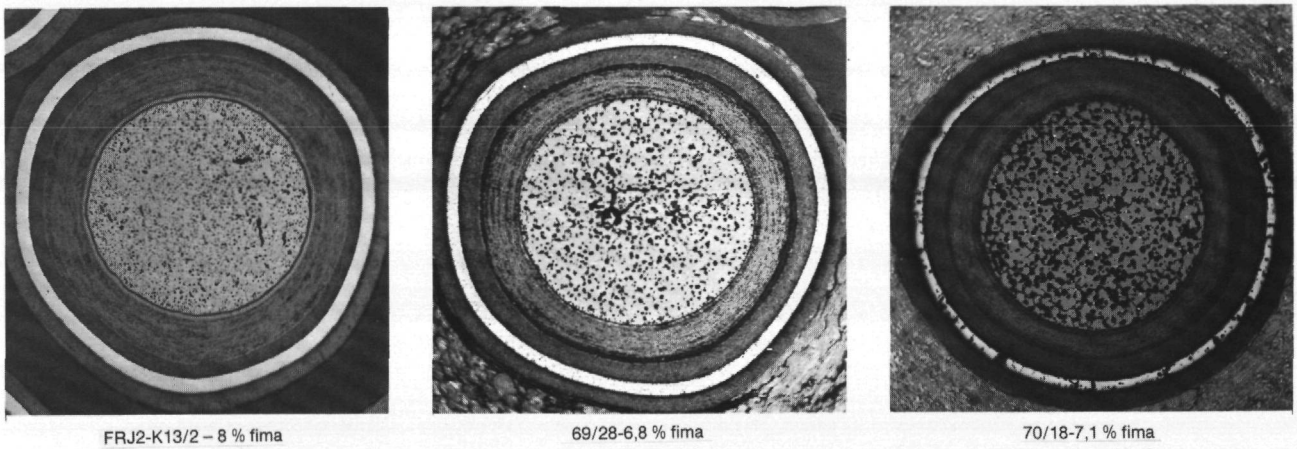

FRJ2-K13/2 – 8 % fima
1600° C, 160 h

69/28-6,8 % fima
2150° C, 6 h

70/18-7,1 % fima
bis 2400° C

TRISO particles from modern fuel elements

Fig. 55: Particles from differently heated spherical fuel elements compared

4. Model Calculations

For reactor design and the safety analyses of the firms HRB, Interatom and the risk analyses done at KFA the fission product release from fuel elements must be related mathematically to the description of the fuel elements, the results of manufacturing quality control and the fuel element exposure in normal operation and during accidents. It is also recommended for an extensive experimental programme, such as the heating programme for irradiated fuel elements here, that models should be used for reducing the data and for long term planning of experiments.

The models dealt with below refer largely to particle behaviour, as the retention of the fission products caesium, strontium, silver and iodine in the fuel element matrix above 1500 °C is small and that for the gases xenon and krypton is completely negligible. In this context, the term "particle damage" refers to damage or changes in the coating, where one must distinguish between fracture of particles (pressure vessel failure) and failures or defects in the intermediate SiC layer. In particle fracture, all the layers have failed. Defects can be determined in quality control using leaching of the fuel elements (see chapter 3.4.1), and failures can be determined during irradiation and heating tests by immediate release of gaseous fission products from failed particles and by later examination via chlorination of fuel elements with subsequent determination of the uranium released. Failed or defective SiC layers are more difficult to detect. The burn-leach process is used in quality control to determine manufacturing defects. The total of SiC defects in irradiation experiments due to manufacture and, if it occurs, due to irradiation, can only be determined semi-quantitatively by expensive techniques (electrolytic profile disintegration). SiC failures or defects result in increased release of caesium in heating tests. Using the profile disintegration of heated fuel elements and other methods (see chapter 2.5.1), additional information on the degree and extent of SiC damage can be obtained from the caesium distribution. Important information on damage mechanisms is obtained from ceramographic work.

The most extensive new data for developing models have come from heating tests with intact and defective UO_2 TRISO particles. The traditional models consist of the following components:

- The kernel release is calculated using a diffusion coefficient in the kernel

- Particle fracture is calculated from a pressure vessel model (codes CONVOL, PANAMA I)

- Fission product release from contamination, from defective particles and from particles with intact coatings has been treated with diffusion models previously (Codes SLIPPER, FRESCO, GETTER)

Heating tests with defective particles can be used for checking diffusion coefficients in UO_2.

The modelling of particle fracture and particle release due to diffusion was developed from the experimental data available in 1977-81. These results in the 1500-1800 °C range are no longer regarded as relevant, compared with the new measurements, in which caesium release after 100 hours at 1600 °C is smaller by a factor of 5×10^5. Therefore, predictions with these models and data are too high by several orders of magnitude. New formulae for predicting the release of metal and gaseous fission products are reported below, but there is no final assessment of all the accident experiments available yet.

4.1 Release of caesium from UO_2 fuel kernels

A simple diffusion model is normally used for the release of fission products with long half life from the particle kernel. The release during irradiation is given by

$$F_i = 1 - \frac{6}{\tau_i} \sum_{n=1}^{\infty} \frac{1 - e^{-n^2\pi^2\tau_i}}{n^4\pi^4} = 1 - \frac{1}{15\tau_i} + \frac{6}{\tau_i} \sum_{n=1}^{\infty} \frac{e^{-n^2\pi^2\tau_i}}{n^4\pi^4} \quad ,$$

where τ_i is the product of the reduced diffusion coefficient D' and the irradiation time t. The release in heating tests after irradiation is given by the Booth model

$$F_{i+a} = 1 - \sum_{n=1}^{\infty} \frac{1 - e^{-n^2\pi^2\tau_i}}{n^4\pi^4} e^{-n^2\pi^2\tau_a} = \frac{\tau F_i(\tau) - \tau_a F_i(\tau_a)}{\tau - \tau_a} \quad ,$$

where $\tau = \tau_i + \tau_a$ is the diffusion coefficient integrated over both irradiation time and heating time, and τ_a is the ddiffusion coefficient integrated just over the heating period.

A complete evaluation of the release measurements for UO_2, irradiated in experiments FRJ2-P27 and FRJ2-P28, is not yet available. Early attempts in modelling caesium and iodine release from simulated defective particles are shown below.

The recommended diffusion coefficient for predicting the release of Cs 137 from UO_2 kernels is given by /38/

$$\log_{10} D'(s^{-1}) = 3.92 - \frac{1.89 \times 10^4}{T(K)} \quad .$$

The value of this diffusion coefficient is too small by 2 orders of magnitude to reproduce the caesium release measured in experiment FRJ2-P28. Calculations from the irradiation experiment and heating test up to 1800 °C of coupon C2 from capsule 1 suggest the use of the diffusion coefficient

$$\log_{10} D'(s^{-1}) = 0.273 - \frac{1.13 \times 10^4}{T(K)}$$

(see Fig. 56). Measured and predicted caesium releases in irradiation and heating are shown in Fig. 57. The validity of this correlation has still to be confirmed by systematic evaluation of all available experimental data on caesium kernel release.

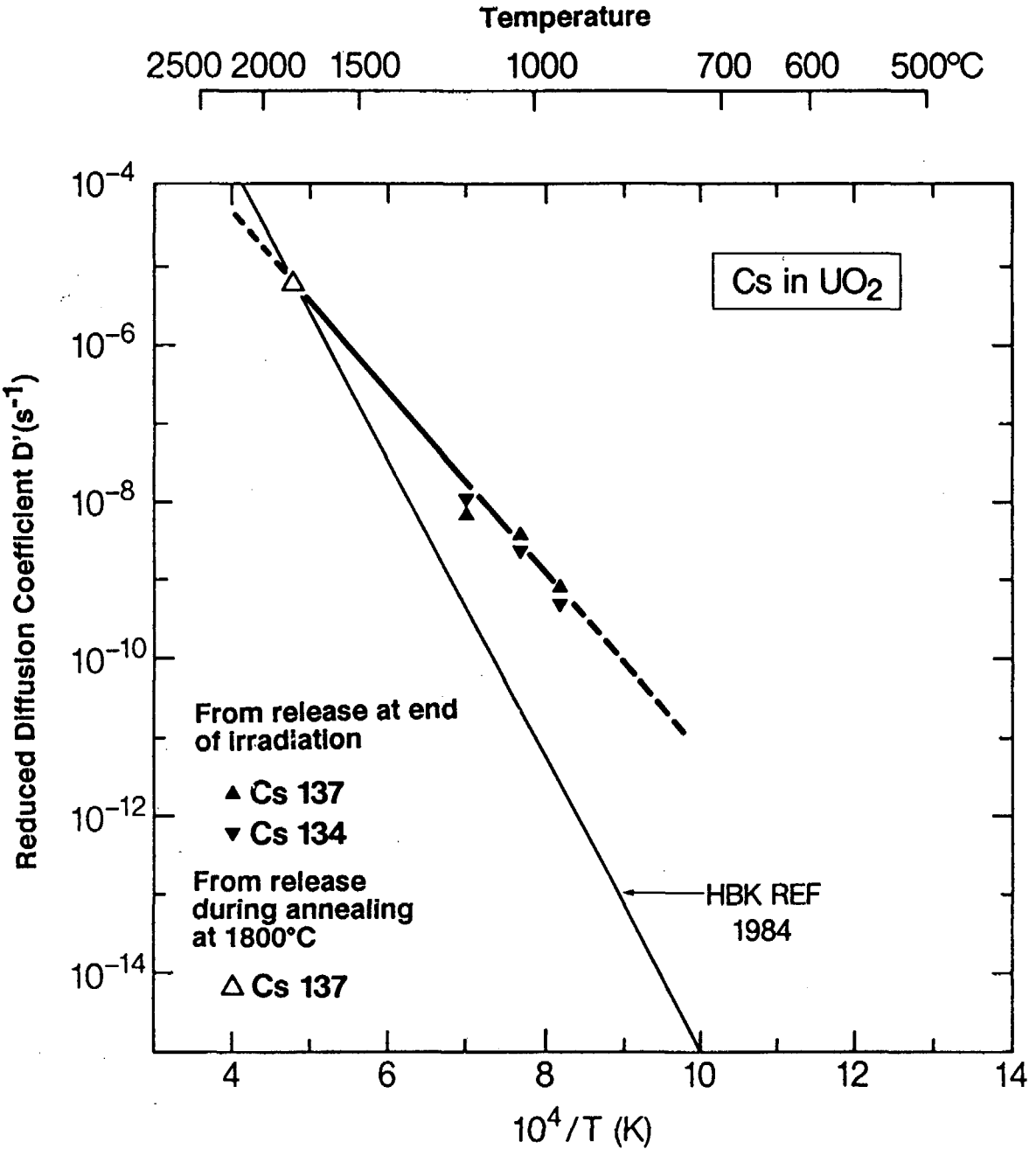

Fig. 56: Diffusion coefficient of caesium in UO_2 as a function of temperature. The diffusion coefficient required for calculation of inpile and out of pile releases is shown compared with the HBK reference value of 1984.

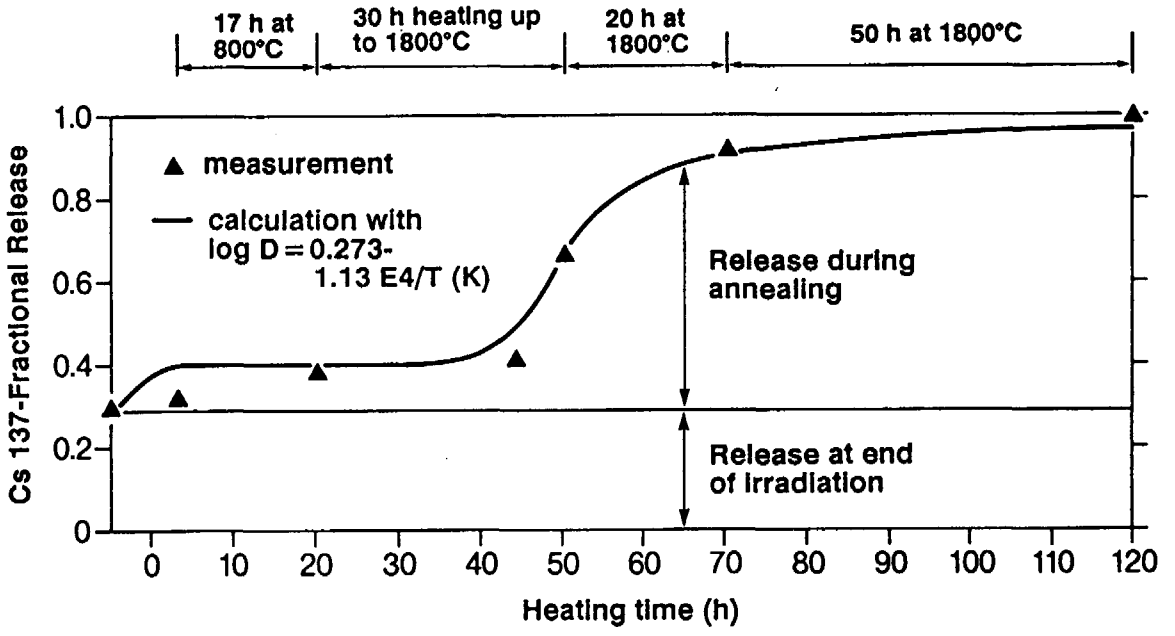

Fig. 57: Cumulative caesium release during irradiation and in heating tests on defective particles from FRJ2-P28/1 (coupon 2)

4.2 Release of iodine from UO_2 fuel kernels

Sample and irradiation data and heating results from experiments on FRJ2-P28 coupons with UO_2 kernels are given in section 3.3 above.

In order to be able to measure the iodine release from defective particles at accident temperatures one year after the end of irradiation, the coupons were re-activated in the Merlin reactor and annealed in the KÜFA shortly after being taken out of the reactor. Table 23 shows the temperatures during irradiation and annealing.

Experiment	Coupon	Mean irradiation temperature °C	Maximum annealing temperature °C
FRJ2-P28/1	C1	940	1400
	C2	940	1800
FRJ2-P28/2	C3	1160	-
	C4	1160	-
FRJ2-P28/3	C5	1020	-
	C6	1020	1600
MERLIN	C7	<200	1700
MERLIN	C8	<200	1800

Table 23: Coupons with defective particles were irradiated in the Dido reactor, cold activated in Merlin and annealed in the hot cells

The diffusion constant derived for krypton in $(Th,U)O_2$ was used experimentally as the diffusion coefficient of iodine in the UO_2 kernel with Q = 314 kJ/Mol activation energy /39/.

$$\log_{10} D'_{I_{in}\ UO_2}(s^{-1}) = 1.80 - \frac{1.649 \times 10^4}{T(K)}$$

The iodine releases calculated with the SLIPPER code /40/ are compared with measured results in Fig. 58.

The calculations lead to over-estimating the measured release at temperatures below 1600 °C. One exception to this is the measured release from coupon C2, which is above the calculated value by a factor of 3.5, with 9 % release after 17 hours at 800 °C. Above 1600 °C, the calculated values underestimate the measured release. The fact that the measured release from coupon C6 after 20 hours at 1600 °C is greater than that from coupon C7

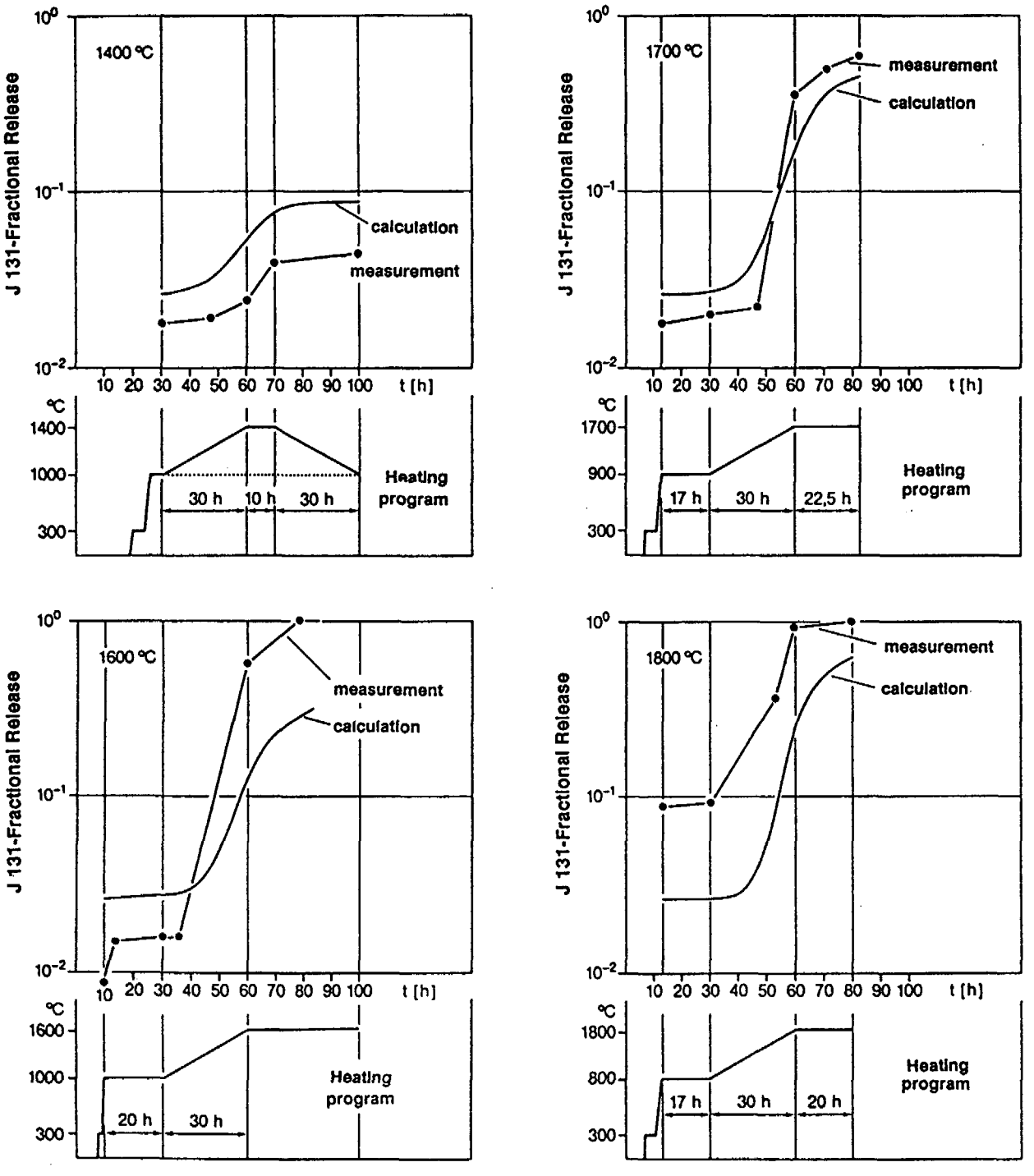

Fig. 58: Iodine release from UO_2 for transient at 1400, 1600, 1700 and 1800 °C. Comparison of SLIPPER calculations with results from this work

after 20 hours at 1700 °C is presumably due to different amounts of burnup. In order to reproduce the release at the end of irradiation (with the assumption I = Xe relese) and during annealing, one must assume two diffusion processes /41/:

$$Q_1 = 480\ kJ/Mol: \quad \log_{10} D_1'(s^{-1}) = 6.98 - \frac{2.51 \times 10^4}{T(K)} \quad ,$$

$$Q_2 = 54.4\ kJ/Mol: \quad \log_{10} D_2'(s^{-1}) = -6.85 - \frac{0.284 \times 10^4}{T(K)} \quad .$$

The combined diffusion coefficient is shown in Fig. 59.

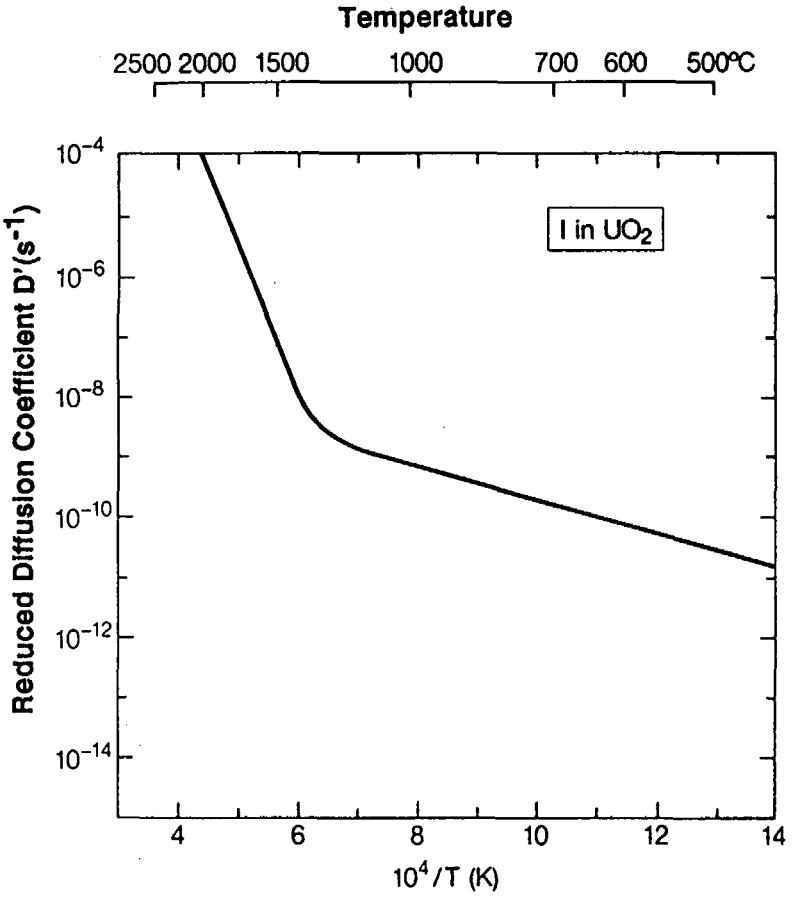

Fig. 59: Diffusion coefficient of iodine in UO_2 as function of temperature

Differing from the classical diffusion model, the Myers trap model /42/ was used for iodine release from UO_2 /43/. A formula is used here, which is limited to the release by recoil emission within the short periods of the existing transients and which treats the diffusion part as negligible.

The description of this "burst" type of process can be approximated by solving the diffusion equation with traps with the above boundary condition for a step increase in temperature by the following expression for the relative proportion of release:

$$F(T,t) = \sqrt{1 - e^{-\frac{t}{\tau}}} \cdot f_{burst}$$

t ... *time*,

T ... *temperature*,

F ... *fractional release*,

τ ... *temperature dependent time parameter for emission from traps*,

f_{burst} ... *temperature dependent fraction of iodine release from traps* .

Extension to transients with any temperature profile is done as follows:

Neither the number nor the energy distribution of the traps (and therefore the emission rates) are known for the material. In order to extend to temperature transients, the given function $F(T,t)$ is made into a sum of the releases for small temperature intervals, for which Δf_{burst} is formed for each ΔT, i.e. a released fission product amount corresponding to this ΔT interval, which can originate from different types of traps with different numbers occupying them. This is done for a given time interval by summation over support positions, where the release rate (total differential of the function $F(T,t)$) is formed. Gauss integration was selected in Code TRAGAS as an effective integration process, i.e. the time position of the supports and the weight function for the release rate must be matched to the integration problem. This depends on the shape of function $\tau(T)$ or $f_{burst}(T)$ here, which must be determined from experimental data for the two sources of release

- recoil part (2,3 %)
- kernel part (97,7 %)

$f_{burst}(T)$ is assumed as temperature activated for both sources with an activation energy which is estimated separately for experiments with burnt-up fuel kernels (Fig. 60) and for unirradiated UO_2.

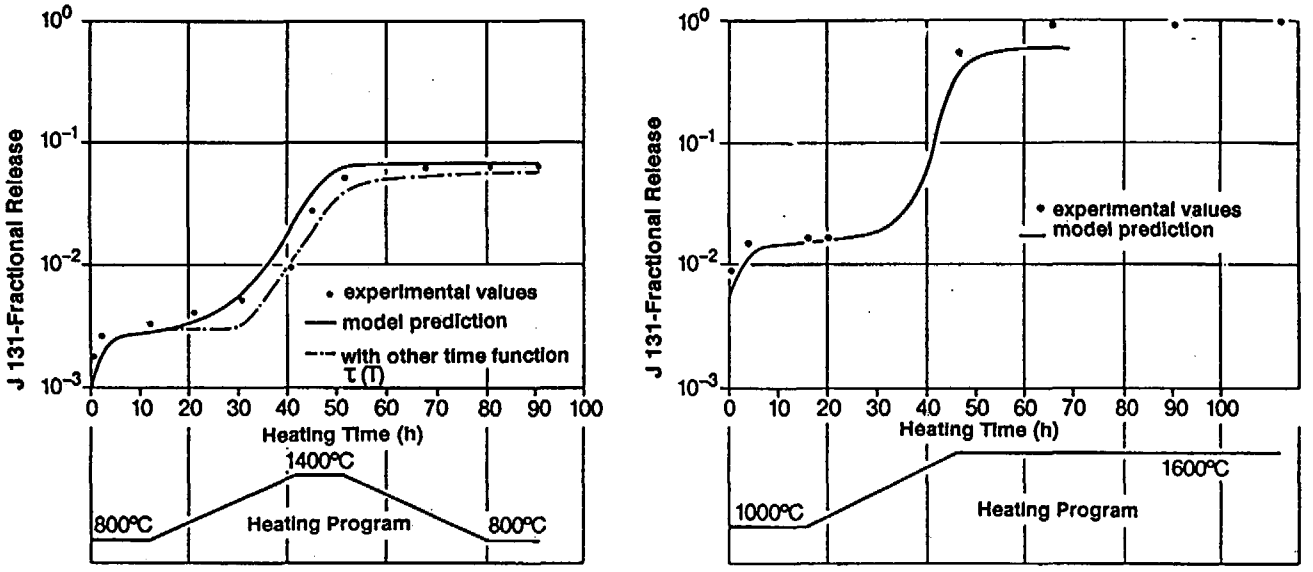

Fig. 60: Description of transient iodine release from UO_2 by the Christ formula for temperature-dependent re-emission from traps /42,43/

There is a standard activation energy of 300 kJ/Mol for the kernel part. This is consistent with experiments on UO_2 pellets, which also only show release above 1300 °C. The activation energy shows a release mechanism, which is called "thermal resolution" of inter-granular bubbles in the literature. In the recoil part, 25 kJ/Mol is found for unirradiated kernels (0,5 % FIMA) and 100 kJ/Mol for kernels with a burnup of 8 % FIMA. This means an increase in activation energy of $f_{burst}(T)$ with burnup and corresponds to the results for irradiation /44/.

4.3 Pressure vessel failure

The CONVOL /45/ calculates the failure rate of fuel particles in isothermal irradiation conditions. It determines the tangential stresses in the SiC layer of a particle taking into account three contributions:

- Pressure from the fission gases Xe, Kr and the reaction gas CO released from the particle kernel

- Stresses caused by swelling of the UO_2 kernel and which are transferred elastically to the comparatively rigid SiC layer

- Stresses which occur due to the PyC layers shrinking under the effect of neutron flux.

The criterion for a failed particle is met, when the tangential stress is at least equal to the shear strength of the SiC layer. The probability of the shear strength distributed according to a Weibull statistical distribution is combined with the cumulative probability of tangential stress.

Table 24 contains the data used by the CONVOL program to calculate the failure rate in irradiation experiments. On the assumption that the PyC and SiC material constants for strength, shrinkage and creep do not change during heating, CONVOL was tested for recalculating from KÜFA experiments /46/. Utilizing the pressure vessel model, the calculated failure rate was compared with the release of gaseous fission products in heating experiments. Fig. 61 shows this comparison for the Kr 85 release of R2-K13/1. The corrosion rate (modelled by the SiC becoming thinner) was adjusted to the experimental result.

Input parameter		Value	Standard deviation
Ratio of actual density to theoretical density of kernel		0,986	1,5
Ratio of actual density to theoretical density of buffer		0,44	11
Theoretical density of kernel	(g/cm^3)	11,0	-
Molecular weight of fuel	(g/Mol)	270	-
Kernel diameter	(µm)	497	3
Thickness of buffer layer	(µm)	94	11
Thickness of inner PyC layer	(µm)	41	10
Thickness of SiC layer	(µm)	36	5
Thickness of outer PyC layer	(µm)	40	6
Transverse contraction of PyC layer			
in elasticity		0,3	-
in creep		0,5	-
Modulus of elasticity of buffer layer	(MPa)	0,106	-
Modulus of elasticity of PyC layer	(MPa)	0,286	-
Modulus of elasticity of SiC layer	(MPa)	0,386	-
Creep constant of PyC	(m^4/N)	4,79 E+5	-
Shrinkage of buffer layer		0,4	-
Mean shear strength of SiC layer	(MPa)	660	-
Weibull parameter of SiC strength distribution		6,0	-
Kernel swelling constant (% / % FIMA)		1,1	-

Table 24: CONVOL input data for calculation of failure rate in irradiation experiments

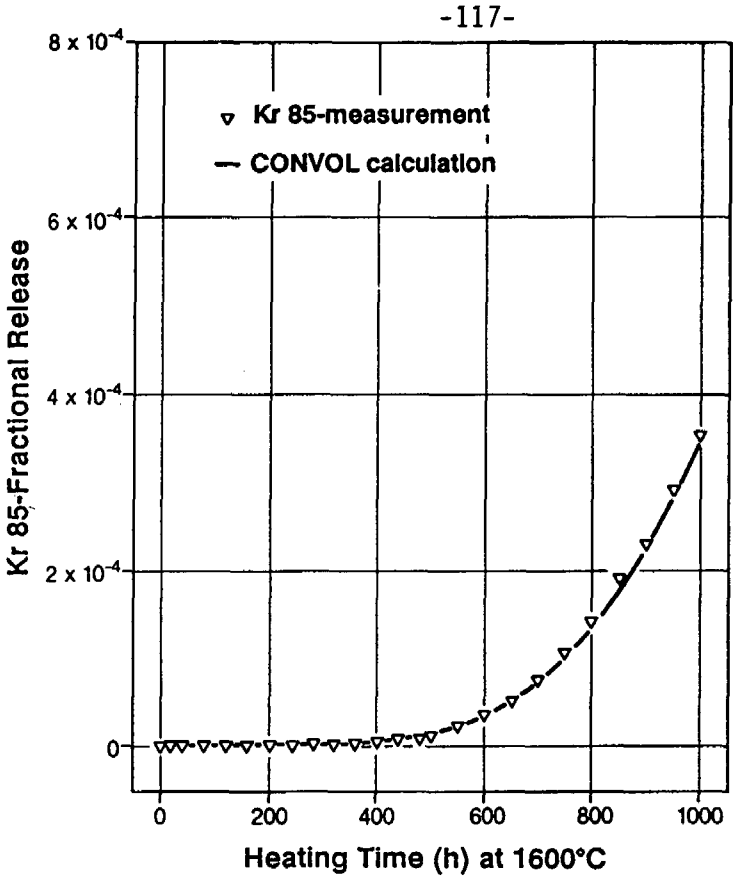

Fig. 61: Krypton release as a function of the heating time at 1600 °C. The results of experiment R2-K13/1 with $(Th,U)O_2$ TRISO particles (triangles) and the calculated failure rate from the CONVOL code (line drawn according to /46/) are shown.

4.4 Integrated failure and release model

A study was performed jointly by KFA and GA to find a new formulation for the model required for reactor design regarding the behaviour of fuel in an accident /47/. The following aspects were particularly stressed here:

- All annealing experiments which could be evaluated should be taken into consideration

- The behaviour of all measured fission products should be followed up

- Laboratory experiments should be integrated in the model whereever possible

After examining the recorded results, the following heating experiments were included in the quantitative evaluation:

Temperature	*Unirradiated Fuel Elements*	*Irradiated Particles*	*Irradiated Fuel Elements*	*Sum*
2100–2600°C	8	28	3	39
1500–2000°C	0	8	6	14
Total	8	36	9	53

After the observation that the fission products are released in the sequence silver, caesium, strontium and fission gases, the following conclusions were drawn:

1. Particle fracture is best defined as damage to the SiC. Because of the permeability of the PyC, the caesium release shows particle fracture directly, just as in the burn-leach process on unirradiated fuel.

2. Existing laboratory results can be used for the SiC failure. These are the table compiled by Montgomery in 1982 on SiC corrosion /33/ and the results found by Benz in 1982 on SiC decomposition.

3. The release of the fission gases is also delayed by the outer PyC. This is described by a diffusion coefficient of krypton through PyC, which is derived from heating experiments with BISO particles. In heating experiments with particles without outer pyrocarbon the caesium and krypton release is identical.

4. In the part played by silver it is not clear whether the release is determined by an independent diffusion process or whether silver and palladium first widen the SiC grain boundaries and can be regarded as precursors of SiC damage.

5. Obviously, irradiation affects the high temperature behaviour. As the available sample material does not cover all the parameters systematically, it is an open question whether high irradiation temperature, high values of burnup or neutron dose must be regarded as the primary cause of increased fission product release in accident simulation tests. The formula below can be used for the quantitative prediction of Cs 137 and Kr 85 release /31,47,48/:

The dependence of SiC failure on the temperature, the corrosion rate and the decomposition rate are determined by an Arrhenius formula. The corrosion rate $k(s^{-1})$ standardized for the usual thickness of the SiC of 35 µm is given by

$$k = k_o \cdot e^{-\frac{Q}{RT}} \quad .$$

where Q is the activation energy, R the universal gas constant and $T(K)$the heating temperature (see Fig. 47). Caesium is only released if SiC layers fail. The occurrence of SiC failures is a statistical phenomenon, which is more likely for thin SiC layers and high corrosion rates. The SiC thickness distribution is based on a normal distribution of 5 % (HOBEG particles) or 10 % (GA particles) variation. A log normal distribution is assumed for the corrosion rate, as is usual for thermally activated processes. The combination of the two distributions gives a complicated mathematical expression (formula on page 67 of /47/), which can be approximated by the Weibull distribution

$$\Phi = 1 - 2^{-(kt)^m} \quad .$$

The model function $\Phi(t)$ for the occurrence of SiC failure is compared with the kinetic caesium release curve from the KÜFA experiments (Fig. 62).

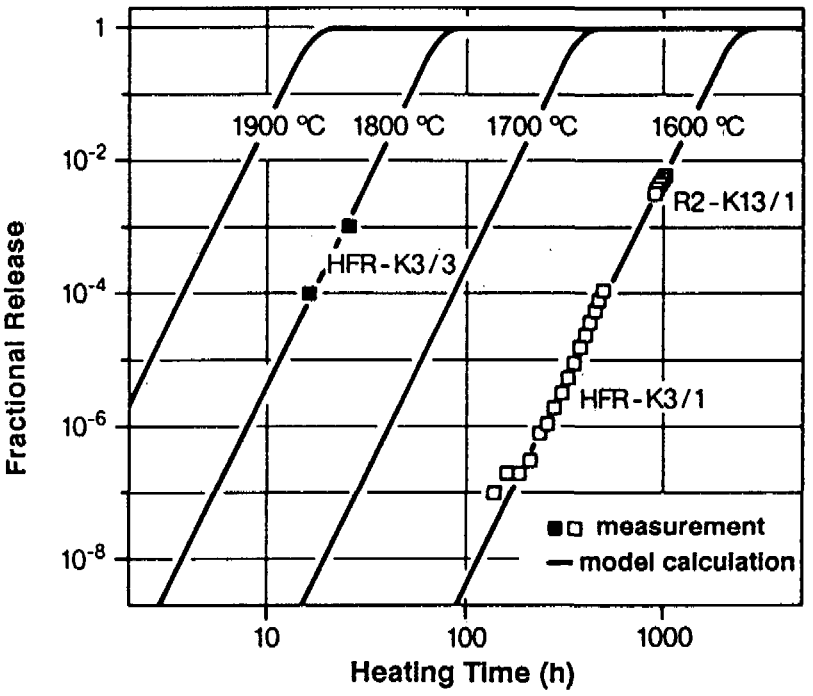

Fig. 62: Caesium release in the 1600 and 1800 °C heating tests on HFR-K3 fuel elements with UO_2 TRISO particles and R2-K13/1 with $(Th,U)O_2$ TRISO particles. The initial value (contamination) are subtracted from the results.

The corrosion rate $k(s^{-1})$ multiplied by the heating time $t(s)$ gives a dimensionless "ageing parameter" in the Weibull model. With changing heating temperature, the integral of the corrosion rate must be plotted against time. The form of the relese profile is determined by the Weibull parameter m. A small value of m corresponds to slow increase in release, and a large value of m to a steep increase. In the model, m is obtained from the variation of the SiC thickness and the scatter of the corrosion rate.

The krypton release profile is obtained by adding the SiC failure rate to the diffusion through the pyrocarbon. The SiC defect rate is given as a function of time by

$$\frac{d\Phi}{dt} \cdot$$

The part of the krypton inventory, which is released after time t from the particle due to diffusion through the pyrocarbon is written as

$$F_{PyC}(t) \quad .$$

The diffusion process may only occur after the SiC layer has failed. This situation is calculated in the integral:

$$F_{Kr}(t) = \int_0^t \frac{d\Phi(t')}{dt} F_{PyC}(t - t')\, dt' \quad .$$

In Fig. 63, F_{Kr} is compared with the measured krypton release rates.

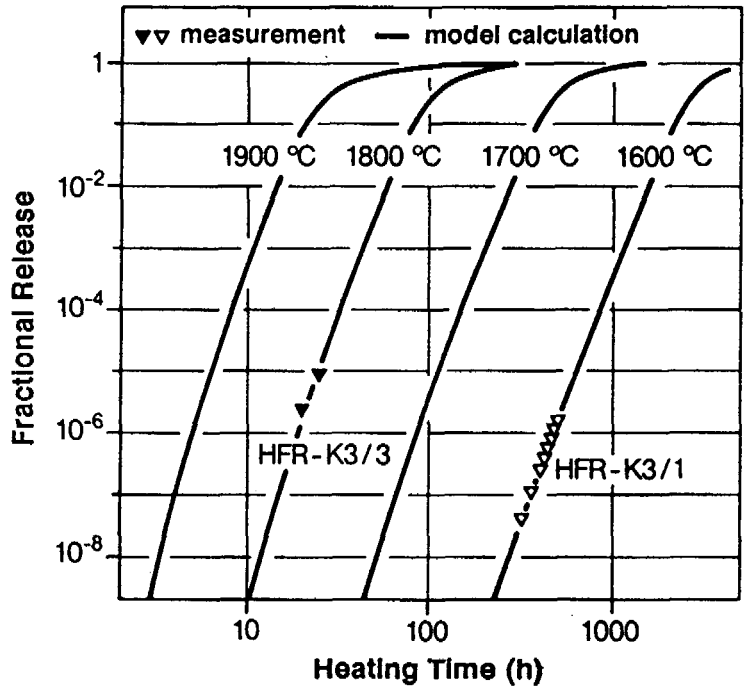

Fig. 63: Krypton release in 1600 and 1800 °C heating tests on HFR-K3 fuel elements with UO_2 TRISO particles. The initial values are subtracted. Using the SiC defect rate shown in Fig. 62, the measured krypton release is well reproduced.

The numerical values for the corrosion rate and for the diffusion coefficients of krypton in PyC used in the formula for F_{PyC} depend on fuel composition and on irradiation conditions. While the measured release curves for two fuel elements can be obtained from the same irradiation experiment by the model (Figs. 62 and 63), the calculation of the small release rates from spheres which were irradiated in the AVR and FRJ2 and then heated still presents difficulties. The development of the model can only be continued if it has been found qualitatively whether the degree of fission product release in the accident simulation depends primarily on irradiation temperature, burnup, irradiation period and/or fast neutron fluence.

The measured values and model calculations in Figs. 62 and 63 can be used as a conservative upper limit, as the irradiation parameters in the HFR-K3 experiment are greatly above the values expected for small HTR's. If, in addition, one takes into account that in an accident of the Module HTR or HTR 100 the temperature will rise to a maximum of about 1600 °C in 20 to 30 hours, and then drop to about 1000 °C in 1000 hours, the additional release of caesium and krypton (and iodine) must be regarded as negligibly small.

5. Literature

/1/ W. Jahn, M. Haben, W. Rehm
Sicherheitstechnische Untersuchungen zum Störfallverhalten des HTR-500, Corethermodynamik
KFA-Report, Jül-Spez-240, S. 53, Jan. 1984

/2/ W. Kröger, H. Nickel, R. Schulten
Safety Characteristics of Modern High-Temperature Reactors
IAEA-Conference, Scientific Programme for Nuclear Safety, Sept. 1985

/3/ W. Schenk, A. Naoumidis, H. Nickel
The Behaviour of Spherical HTR Fuel Elements under Accident Conditions
Journal of Nucl. Mat. 124, p. 25, 1984

/4/ K. Petersen, H. Barthels, H.E. Drescher, C.B. von der Decken, N. Iniotakis, W. Schenk, R. Schulten
The Fission Product Retention of Pebble-Bed Reactors in Ultimate Accidents
Nuclear Technology Vol. 46, p. 306, Dec. 1979

/5/ W. Schenk
Störfallsimulation an bestrahlten Kugelbrennelementen bei Temperaturen von 1400 bis 2500 °C
KFA-Report, Jül-1883, Dez. 1983

/6/ H. Reutler, G.H. Lohnert
Advantages of Going Modular in HTR
Nuclear Engineering and Design, Vol. 78, No. 2, April 1984

/7/ H. Nabielek, G. Kaiser, H. Huschka, H. Ragoß, M. Wimmers, W. Theymann
Fuel for Pebble-Bed HTRs
Nuclear Engineering and Design 78, p. 155, April 1984

/8/ W. Kröger, R. Moormann, K. Verfondern, N. Iniotakis
Festlegung prioritärer Arbeiten zum Spaltproduktverhalten mit Hilfe von Risiko-Trendanalysen
Jahrestagung Kerntechnik '85, München, Tagungsbericht S. 159, Mai 1985

/9/ W. Amian, u.a.
Neuere Arbeitsergebnisse aus dem Vorhaben "Diffusionsdaten und Spaltproduktfreisetzung"
KFA-Report, Jül-1421, Juni 1977

/10/ D.T. Goodin
Accident Condition Performance of High Temperature Gas-Cooled Reactor Fuels
DOE-Report, GA-A16508, Oct. 1983

/11/ G. Reitsamer, A. Strigl, J. Zeger
Spaltproduktfreisetzung aus TRISO-beschichteten Brennstoffteilchen des Experiments FRJ2-K11 unter Störfallbedingungen
ÖFZS Ber. 0474 u. 0475, Dez. 1983

/12/ R. Förthmann
Untersuchung zur Getterung metallischer Spaltprodukte im Primärkreislauf eines Hochtemperaturreaktors
KFA-Report, Jül-1670, Aug. 1980

/13/ W. Amian, D. Stöver
Private Communication (Rückhaltung der Schlüsselspaltprodukte)
Vorlage zum SiC-Workshop am 27. u. 28.11.1980 in der KFA

/14/ W. Schenk
Untersuchungen zum Verhalten von beschichteten Brennstoffteilchen und Kugelbrennelementen bei Störfalltemperaturen
KFA-Report, Jül-1490, Mai 1978

/15/ E. Groos, W. Schenk
Apparatur for Fission Gas Release Measurements from HTR Fuel Elements at Very High Temperatures
Conf. on Post-Irradiation Examination, BNES, Proc. p. 248

/16/ W. Schenk
Störfallsimulationstest an Kugelbrennelementen
aus KFA-Report, Jül-Conf.-53, S. 123, Juni 1985

/17/ S.A. Sterling
Cesium Release from Various Advanced HTGR Fertile Particle Designs
GA-Report, GA-A 15230, Feb. 1979

/18/ W. Schenk
Nachbestrahlungsausheizverfahren für Kugelbrennelemente und andere Brennstoffproben
KFA-Report, Jül-1454, Sept. 1977

/19/ D.T. Goodin, H. Nabielek, W. Schenk
Accident Condition Testing of US and FRG High-Temperature Gas-Cooled Reactor Fuels
KFA/GA-Report, Jül-Spez.-286, GA-A 17820, Jan. 1985

/20/ H.F. Krohn
Freisetzung von Spaltprodukten aus dem Core eines Kugelhaufenreaktors bei Störfällen mit Core-Aufheizung
KFA-Report, Jül-1791, 1982

/21/ Yosen Liu
Zur Behandlung der Spaltprodukte in Abbrandrechnungen unter Berücksichtigung neuer nuklearer Daten angewandt auf Grafitreaktoren
KFA-Report, Jül-678-RG, Juli 1970

/22/ W. Kühnlein, R. Schröder
Private Communication
KFA-IRW-TN-56/83
KFA-HBK-Quartalsberichte IV/84, IV/85

/23/ R. Duwe, W. Kühnlein, R. Schröder
Gamma-spektrometrische Abbrandmessungen an kugelförmigen Brennelementen
KFA-Report, Jül-1428, Juni 1977

/24/ M. Wimmers
Das Verhalten kugelförmiger Brennelemente bei der Massenerprobung
im AVR-Reaktor
Diss. RWTH Aachen, Januar 1977

/25/ H. Werner
Private Communication v. 01.01.1985

/26/ E. Groos, Ch. Bauer, G. Behrens
Private Communication
März 1986 (IRW-TN-27/82)

/27/ P.E. Brown, A.J. Inns
Post-Irradiation Examination on AVR Spherical Fuels
AERE-G. 2237, May 1982

/28/ H. Derz, A. Floßdorf
Private Communication, Juli 1986

/29/ W. Hei, H. Huschka, G. Kaiser, W. Rind
Status of Qualification of High-Temperature Reactor Fuel
Element Spheres
Nuclear Technology, Vol. 69, p. 44, April 1985

/30/ P.E. Brown, A.J. Inns
Post-Irradiation Examination of Spherical Fuel Elements from
Irradiation Experiments FRJ2-K10 and -K11
AERE-G. 2240, March 1982

/31/ H. Nabielek, W. Schenk, D.T. Goodin
HTR Fuel Behaviour in Accidents
ENC '86, Geneva, 1-6 June 1986

/32/ A. Naoumidis, R. Benz, H. Grübmeier
Behaviour of Fission Products in TRISO coated UO_2-Particles with Simulated High Burnup
High-Temp.-High Pressures, 1982, Vol. 14, p. 489

/33/ F.C. Montgomery
Final FY-82 Report on Fission Product-SiC Reactions
GA-Report 906641/1, Sept. 1982

/34/ A. Naoumidis
Zum Verhalten von beschichteten Brennstoffteilchen bei sehr hohen Temperaturen
KFA-Report, Jül-1465, Nov. 1977

/35/ W. Schenk, A. Naoumidis
Failure Mechanisms and Fission Product Release in High-Temperature Gas-Cooled Reactor Fuel under Conditions of Unrestricted Core Heatup Events
Nuclear Technology, Vol. 46, p. 228, Dec. 1979

/36/ R. Benz - Veröffentlichung in Vorbereitung
("Kinetics of Decomposition of CVD SiC in Modified TRISO-Coated Fuel Particles at Temperature of 1600° to 2200°C",
KFA Document IRW-TN-124/82, October 1982, GA Technologies Document 908378/0)

/37/ H. Grübmeier, A. Naoumidis, B.A. Thiele
Silicon Carbide Corrosion in High-Temperature Gas-Cooled Reactor Fuel Particles
Nuclear Technology, Vol. 35, p. 413, Sept. 1977

/38/ H. Nabielek, B.F. Myers
Fission Product Retention in HTR Fuel
BNES Conf. Gas Cooled Reactors Today, Bristol 1982

/39/ J. Thiel
Gasfreisetzung aus Defektpartikeln im Experiment FRJ2-P25
Private Communication, HRB Mannheim, 1982

/40/ U. Quade
Absicherung des Diffusionskoeffizienten für Jod in UO_2 durch Nachrechnung von Glühexperimenten mit nur pufferbeschichteten UO_2 Kernen (FRJ2-P28)
Private Communication, IA Bensberg, Sept. 1985

/41/ K. Verfondern
Nachrechnung des Ausheizexperiments FRJ2-P28 für die Spaltproduktnuklide J-131, Cs-137, Sr-90 und Ag-110m
Private Communication in HBK Vierteljahresbericht, I. Quartal 1986

/42/ B.F. Myers, R.E. Morrissey
The Measurement and Modelling of Time-Dependent Fission Product Release from Failed HTGR Fuel Particles under Accident Conditions
GA Bericht GA-A15439, San Diego, April 1980

/43/ A. Christ, A.-W. Mehner, W. Schenk
The Release of Iodine from HTR Fuel under Steady-State and Transient Conditions
IAEA Specialists Meeting, Gloucester, October 1985

/44/ A. Christ
Transiente Gasfreisetzung aus Defektpartikeln
Private Communication, HRB Mannheim, Juli 1984

/45/ K. Bongartz
Status of the Fuel Stress and Failure Rate Calculations at KFA
KFA Bericht Jül-1686, November 1980

/46/ G. Muncke
Partikelbruch bei Bestrahlungs- und Ausheizexperimenten
Private Communication, HRB Mannheim, August 1985

/47/ D.T. Goodin, H. Nabielek
The Performance of HTR Fuel in Accidents
KFA Technische Notiz HBK-TN-19/85 und GA Documents No. 908293, Dez. 85

/48/ H. Nabielek, K. Verfondern
Prediction of Fission Product Release in Accidents
IAEA Specialists Meeting, Gloucester, October 1985

This work was done in the context of the HBK Project, in which the partners GHT, HOBEG, HRB, KFA, NUKEM and SIGRI/RW participated, and which was supported by the West German Ministry of Research and Technology and the Land North Rhine Westphalia.

Thanks

We would like to express our thanks to Mr. G. Brunkowski for the execution of the accident simulation experiments in the A Test apparatus. Many workers in the Hot Cells took part in the work described and in compiling the report, and we would like to thank them for this.

In the chapter and model calculations, unpublished contributions were made available to us by Messrs Christ, Muncke and Thiel from HRB, Mr. Quade from Interatom and Mr. Verfondern from KFA. This made it possible to complete the paper.